



**KAUNAS UNIVERSITY OF TECHNOLOGY
MECHANICAL ENGINEERING AND DESIGN FACULTY**

Antony Francis Jayaraj

**DESIGN AND FABRICATION OF PERIODIC
MICROSTRUCTURES FOR TESTING OF HOT IMPRINT
PROCESS**

Master's Degree Final Project

Supervisor

Assoc. prof. dr. Giedrius Janušas

KAUNAS, 2017

**KAUNAS UNIVERSITY OF TECHNOLOGY
MECHANICAL ENGINEERING AND DESIGN FACULTY**

**DESIGN AND FABRICATION OF PERIODIC
MICROSTRUCTURES FOR TESTING OF HOT IMPRINT
PROCESS**

Master's Degree Final Project
Industrial Engineering and Management (code 621H77003)

Supervisor

Assoc. Prof. Dr. Giedrius Janušas
(date)

Reviewer

Prof. Dr. Habil Arvydas Palevičius
(date)

Project made by

(signature) Antony Francis Jayaraj
(date)

KAUNAS, 2017



KAUNAS UNIVERSITY OF TECHNOLOGY

MECHANICAL ENGINEERING AND DESIGN

(Faculty)

ANTONY FRANCIS JAYARAJ

(Student's name, surname)

INDUSTRIAL ENGINEERING AND MANAGEMENT, 621H77003

(Title and code of study programme)

" DESIGN AND FABRICATION OF PERIODIC MICROSTRUCTURE FOR TESTING OF
HOT IMPRINT PROCESS "

DECLARATION OF ACADEMIC INTEGRITY

_____ 220 _____
Kaunas

I confirm that the final project of mine, ANTONY FRANCIS JAYARAJ, on the subject "Design and fabrication of periodic microstructures for testing of hot imprint process" is written completely by myself; all the provided data and research results are correct and have been obtained honestly. None of the parts of this thesis have been plagiarized from any printed, Internet-based or otherwise recorded sources. All direct and indirect quotations from external resources are indicated in the list of references. No monetary funds (unless required by law) have been paid to anyone for any contribution to this thesis.

I fully and completely understand that any discovery of any manifestations/case/facts of dishonesty inevitably results in me incurring a penalty according to the procedure(s) effective at Kaunas University of Technology.

(name and surname filled in by hand)

(signature)

**KAUNAS UNIVERSITY OF TECHNOLOGY
FACULTY OF MECHANICAL ENGINEERING AND DESIGN**

Approved:

Head of
Production engineering
Department

(Signature, date)

Kazimieras Juzėnas

(Name, Surname)

**MASTER STUDIES FINAL PROJECT TASK ASSIGNMENT
Study programme INDUSTRIAL ENGINEERING AND MANAGEMENT**

The final project of Master studies to gain the master qualification degree, is research or applied type project, for completion and defence of which 30 credits are assigned. The final project of the student must demonstrate the deepened and enlarged knowledge acquired in the main studies, also gained skills to formulate and solve an actual problem having limited and (or) contradictory information, independently conduct scientific or applied analysis and properly interpret data. By completing and defending the final project Master studies student must demonstrate the creativity, ability to apply fundamental knowledge, understanding of social and commercial environment, Legal Acts, and financial possibilities, show the information search skills, ability to carry out the qualified analysis, use numerical methods, applied software, common information technologies and correct language, ability to formulate proper conclusions.

1. Title of the Project

Design and fabrication of periodic microstructures for testing of hot imprint process

Approved by the Dean Order No. V25-11-8, 21 April 2017

2. Aim of the project

To Design and to fabricate the Periodic Microstructure for testing of Hot Imprint Process

3. Structure of the project

- Literature review
- Simulation software
- Theoretical calculations
- Manufacturing of periodic microstructure

4. Requirements and conditions

- The designed periodic microstructure has the highest diffraction efficiency in the first order maxima.
- The selected manufacturing process could be used for fabrication of the master periodic microstructure.

5. This task assignment is an integral part of the final project

6. Project submission deadline:

Student

Antony Francis Jayaraj

(Name, Surname of the Student)

(Signature, date)

Supervisor

Assoc. Prof. dr. Giedrius Januřas

(Position, Name, Surname)

(Signature, date)

Antony Francis Jayaraj. DESIGN AND FABRICATION OF PERIODIC MICROSTRUCTURES FOR TESTING OF HOT IMPRINT PROCESS. *Master's* Final Project / supervisor assoc. prof. dr. Giedrius Janušas; Faculty of Mechanical Engineering and Design, Kaunas University of Technology.

Research field and area: Technological Science, Production Engineering

Keywords: *Periodical Microstructure, Thermal replication, Diffraction efficiency, Diffraction grating*

Kaunas, 2017, 71 p

SUMMARY

The main aim of the project is to design the periodical microstructure with the theoretical calculation by executing and analysing the Red, Green, and Blue laser of wavelength $\lambda=0.633\text{nm}$, $\lambda=0.532\text{nm}$, $\lambda=0.441\text{nm}$ of period, $4\mu\text{m}$, $5.6\mu\text{m}$, $10\mu\text{m}$ with the highest depth for the respective periods thus giving the highest Diffraction Efficiency for the 1st order maxima. The results are further compared and analysed further, after the theoretical calculation the periodical microstructure is manufactured by Contact lithography, Ion etching, UV Replication, and Electroplating process to produce the Nickel structure, this Ni structure is analysed with the help of Atomic microscopic producing 2D, 3D and the profile is generated. The fabricated Ni structure is thermal replicated on the Polycarbonate surface with many Imprints on it. From the analysis, we see there are two defects that occur while manufacturing the periodical microstructure and measurement defect that happens during the analysis in Atomic force microscopy for the Red laser.

Antony Francis Jayaraj, Periodinių mikrostruktūrų naudojamų terminio antrinimo tyrimuose kūrimas ir gamyba. *Magistro* galutinis projektas / vadovas doc. dr. Giedrius Janušas; Mechanikos inžinerijos ir dizaino fakultetas, Kauno technologijos universitetas.

Mokslo kryptis ir sritis: Technologijos mokslai, gamybos inžinerija

Reikšminiai žodžiai: Periodinės mikrostruktūros, terminis antrinimas, difrakcinis efektyvumas, difrakcinės gardelės

Kaunas, 2017, 71 p.

SANTRAUKA

Pagrindinis projekto tikslas yra suprojektuoti ir pagaminti periodinę mikrostruktūrą pasižyminčią didžiausiu difrakciniu efektyvumu pirmos eilės difrakciniuose maksimumuose apšviečiant $\lambda = 633\text{nm}$ bangos ilgio lazeriu. Darbe nustatytas optimalūs $4\mu\text{m}$, $5,6\mu\text{m}$ ir $10\mu\text{m}$ periodo stačiakampių periodinių mikrostruktūrų gyliai, siekiant maksimizuoti pirmos eilės difrakcinius maksimumus. Teoriniai rezultatai palyginti naudojant $\lambda = 532\text{nm}$ ir $\lambda = 441\text{nm}$ bangos ilgio lazerius. Suprojektuotų periodinių struktūrų gamybai parinktas technologinis maršrutas apimantis kontaktinę litografiją, reaktyvųjį joninį ėsdinimą, UV polimerinės replikos gamybą bei elektrocheminį Ni galvanizavimą. Matavimai atlikti atominės jėgos mikroskopu parodė, kad pagamintų periodinių mikrostruktūrų periodai 2,5% tikslumu atitinka užsiduotus, o gylio paklaidos neviršija 8,5%.

ACKNOWLEDGEMENT

I would like to thank my supervisor Assoc. Prof. Dr. Giedrius Janušas for giving me this opportunity, who helped and guided me in completing the project successfully, and giving immense knowledge about major concepts, and I sincerely thank our Assoc. Prof, Dr. Jolanta Baskutienė, for providing me this opportunity.

I would like to express my gratitude to my parents for giving me this opportunity and supported me from the start to the end, and helped me financially to achieve things.

I am Grateful for this wonderful Institution for giving me this opportunity and knowledge to stand on my chance and opportunity. I am very thankful to my friends and colleagues for helping me in need and supported me to the best of my abilities.

Table of Contents

Introduction	1
1. Literature Review	2
1.1 Periodic Microstructure.....	2
1.2 Microstructure Defects.....	2
1.3 Thermal Replication.....	4
1.4 Mechanical Hot Print Process	5
1.5 Master periodical structure.....	7
1.6 Polycarbonate for thermal replication of periodic Replication	8
1.7 Vibroactive pad and Replication process	10
2. Simulation of G-solver	11
2.1 Introduction	11
2.2 Procedures	12
2.2.1 Parameters	12
2.2.2 Graphical Editor	13
2.2.3 Listing/Run	15
2.2.4 Genetic Algorithm (GA).....	16
2.2.5 Execution or Run.....	18
2.2.6 1 st order Littrow	18
2.2.7 Diffraction Efficiency.....	19
2.2.8 Graphing	20
3. Theoretical Calculation	21
3.1 Red laser or He-Ne laser	21
3.1.1 G-solver results and charts For Period 4 μm	21
3.1.2 G-solver results and charts For Period 5.6 μm	22
3.1.3 G-solver results and charts for period 10 μm	23
3.2 Blue Laser or Helium-Cadmium Lasers.....	24

3.2.1 G-solver results and charts For Period 4 μm	25
3.2.2 G-solver results and charts For Period 5.6 μm	26
3.2.3 G-solver results and charts For Period 10 μm	27
3.3 Green laser or Nd-YAG laser.....	28
3.3.1 G-solver Results and chart for period 4 μm	28
3.3.2 G-solver results and charts for period 5.6 μm	29
3.3.3 G-Solver results and charts for period 10 μm	30
3.4 Comparison	31
4. Manufacturing of periodical microstructure	36
4.1 Introduction	36
4.2 Contact Lithography Process	36
4.3 Reactive Ion Etching Process.....	36
4.4 UV Replicated Process.....	37
4.5 Electroplating Process	37
4.6 Surface Explorer software analysis for Fabrication process	39
4.6.1 AFM results for Period 4nm.....	40
4.6.2 AFM results for Period 5.6nm.....	41
4.6.3 AFM Results for Period 10nm.....	42
4.7. Thermal Replication process or Hot imprint process.....	43
Conclusion	45
References.....	46
Appendix.....	47

LIST OF FIGURES

Figure 1 Hot imprint device for Ni stamping on grating structure (Polycarbonate), moving plate (1), master mold (2). Nickel plate imprints on polycarbonate (3), vibroactive pad (4), base of the instrument (5), Dynamometer (6), Control block of Temperature, Pressure, and time	5
Figure 2 Standard periodic microstructure of Lamellar or lamella Diffraction grating	7
Figure 3 Sample AFM (Atomic Force Microscopy) image of Master Nickel Periodic Microstructure of the surface	7
Figure 4 Chemical formula of Monolithic Polycarbonate known as Ketoprofen.....	8
Figure 5 Application of diffraction grating with lasers to observe the characteristics and properties of the object using Diffraction gratings and mirrors.....	10
Figure 6 Default parameter tab generates the number of maxima orders and materials for each period say 4 μ m, 5.6 μ m, and 10 μ m in G-solver.	12
Figure 7 Grating Editor is used to design the grating Canvas structure including both the substrate and Superstrate for 1period.....	14
Figure 8 Canvas of master periodical microstructure comprising both substrate and superstrate	15
Figure 9 Listings/Run tab generated to show parameters such as block, width, and material of usage as highlighted.....	16
Figure 10 GA Grating Definition listing tab shows the real parameters of min and max value generated.....	17
Figure 11 Defining the total depth range with specific increment and Diffraction orders in Run Parameters tab in G-solver.....	18
Figure 12 Results of the diffraction efficiency for maxima orders and total depths are generated from the Result tab in G-solver.....	19
Figure 13 one of generated Graphs defining the total depths vs Diffraction efficiency, maxima orders showing the peak value as the highest diffraction efficiency from final results.....	20
Figure 14 Total depth Verses Diffraction Efficiency of period 4 μ m, Red laser of wavelength $\lambda=0.633\text{nm}$ producing Highest D.E of depth 0.55nm in the First order (-1T, +1T) maxima among the other orders (3T, 4T, 5T).....	22

Figure 15 Total depth Verses Diffraction Efficiency of period 5.6 μm , Red laser of wavelength $\lambda=0.633\text{nm}$ producing Highest D.E of depth 0.55nm in the First order (-1T, +1T) maxima among the other orders (3T, 5T)	23
Figure 16 Total depth Verses Diffraction Efficiency of period 10 μm , Red laser of wavelength $\lambda=0.633\text{nm}$ producing Highest D.E of depth 0.55nm in the First order (-1T, +1T) maxima among the other orders (2T, 3T, 4T, 5T)	24
Figure 17 Total depth Verses Diffraction Efficiency of period 4 μm , Blue laser of wavelength $\lambda=0.441\text{nm}$ producing Highest D.E of depth 0.40nm in the First order (-1T, +1T) maxima among the other orders (2T, 3T, 4T, 5T)	25
Figure 18 Total depth Verses Diffraction Efficiency of period 5.6 μm , Blue laser of wavelength $\lambda=0.441\text{nm}$ producing Highest D.E of depth 0.40nm in the First order (-1T, +1T) maxima among the other orders (2T, 3T, 4T, 5T)	26
Figure 19 Total depth Verses Diffraction Efficiency of period 10 μm , Blue laser of wavelength $\lambda=0.441\text{nm}$ producing Highest D.E of depth 0.40nm in the First order (-1T, +1T) maxima among the other orders (2T, 3T, 4T, 5T)	27
Figure 20 Total depth Verses Diffraction Efficiency of period 4 μm , Green laser of wavelength $\lambda=0.532\text{nm}$ producing Highest D.E of depth 0.45nm in the First order (-1T, +1T) maxima among the other orders (3T, 5T)	28
Figure 21 Total depth Verses Diffraction Efficiency of period 5.6 μm , Green laser of wavelength $\lambda=0.532\text{nm}$ producing Highest D.E of depth 0.45nm in the First order (-1T, +1T) maxima among the other orders (2T, 3T, 4T, 5T).	29
Figure 22 Total depth Verses Diffraction Efficiency of period 10 μm , Green laser of wavelength $\lambda=0.532\text{nm}$ producing Highest D.E of depth 0.45nm in the First order (-1T, +1T) maxima among the other orders (2T, 3T, 4T, 5T).	30
Figure 23 Comparison chart of Maxima orders verses Diffraction efficiency of three lasers for period 4 μm of same depth 0.55nm defining the highest diffraction efficiency.....	31
Figure 24 Comparison chart of Maxima orders vs Diffraction efficiency of three lasers for period 4 μm of different depth 0.55nm, 0.45nm, 0.40nm defining the highest diffraction efficiency.....	32
Figure 25 Comparison chart of Maxima orders vs Diffraction efficiency of three lasers for period 5.6 μm of same depth 0.55nm defining the highest diffraction efficiency.....	32

Figure 26 Comparison chart of Maxima orders verses Diffraction efficiency of three lasers for period 10 μ m of same depth 0.55nm defining the highest diffraction efficiency.....	33
Figure 27 Periodical microstructure of Nickle before fabrication	37
Figure 28 Fabrication Process of Nickel Periodical microstructure: Silicon(a), photo resist coated silicon slab (b), Contact lithographic process(c), post contact lithography process (d), Reactive Ion Etching process(e), UV Replication process(f) Polymer extraction(g), Electroplating process of Ni(h), Nickel mold(i), Extraction of Ni periodical microstructure(j).	38
Figure 29 Final Nickel structure obtained after fabrication silicon mold to lamella shaped Nickel periodical microstructure.....	39
Figure 30 AFM images of Nickel periodic microstructure for period 4 μ m using Surface Explorer; 2D image of Ni(a) and 3D image of Ni(b). With generated results of X;11.7 μ m, Y:10.3 μ m, Z:572.7nm with Ra: 196.2nm and Rq: 216.3nm.	40
Figure 31 Profile of the Nickel periodical microstructure for the period 3.9 μ m with the depth of 572.7 nm, comprising a graph of Length(μ m) vs Depth (CS-1, crop, nm)	41
Figure 32 AFM images of Nickel periodic microstructure for period 5.6 μ m using Surface Explorer; 2D image of Ni(a) and 3D image of Ni(b). With generated results of X: 11.3 μ m and Y: 10.3 μ m and Z: 597.0nm, with Ra: 213.8nm and Rq: 230.1nm	41
Figure 33 Profile of the Nickel periodical microstructure for the period 5.7 μ m with the depth of 597.6nm, comprising a graph of Length(μ m) vs Depth (CS-1, crop, nm)	42
Figure 34 AFM images of Nickel periodical microstructure for period 10 μ m using Surface Explorer; 2D image of Ni(a) and 3D image of Ni(b). With generated results of X:11.3 μ m, Y:10.3 μ , Z:597.0nm and R _a (Average roughness):213.8nm, R _q (Mean square roughness):230.1nm.....	42
Figure 35 Profile of the Nickel periodical microstructure for the period 10.1 μ m with the depth of 582.7nm, comprising a graph of Length(μ m) vs Depth (CS-1, crop, nm)	43
Figure 36. Thermal replication process of Polycarbonate(a), Thermal replicated Nickel imprints on the polycarbonate surface(b).....	44

Introduction

Periodical microstructure is composed of silicon material, produced with the numerous process including Contact Lithography, Ion etching process, UV replication and electroplating process, this microstructure is mainly used for Thermal Replication processes and many processes including Hot embossing and Hot imprint process, this periodical microstructure is used for defining and analysing Diffraction efficiency for any replica. The periodical microstructure is used vast in fields including Optics, Electronics, Microfluidic devices, and laser industry.

The aim of this project is to Design and to Fabricate a Periodical Microstructure for Testing of Hot imprint process. To achieve this, aim the following set of tasks are done.

1. To determine the depth of the periodical microstructure using G-solver software in which the periodical microstructure for the period $4\mu\text{m}$, $5.6\mu\text{m}$, $10\mu\text{m}$, under Red laser which gives the highest Diffraction Efficiency in the first order maxima.
2. To Define manufacturing process of Master (Ni) periodic Microstructure imprint from Silicon material mold as described in flow diagram, selecting, and stating the process and procedures to obtain a thermoplastic polymer grating under thermal replication process with (Ni) imprints on it. The grating structure made is lamellar or lamella shaped Microstructure.
3. To evaluate the quality of the fabricated periodic microstructure, and comparison of theoretical result and manufacturing result is done.

1. Literature Review

1.1 Periodic Microstructure

The first periodic microstructure was founded by an American astronaut David Rittenhouse in the year 1785. From that year, the microstructure changed in sizes and shapes and even the manufacturing techniques were modified, but the concept remained the same. The microstructure is composed of narrow grooves with spaces in between them for propagating lights wavelength. As we see the technology is getting advanced day by day, the products are shrinking into Micro and Nanoparticles, whereas the Periodic microstructure is used in lasers, Sensors, and Holography [1]. The Periodic microstructure is manufactured with the total background of Microstructure Technology say Microfabrication in which most of them are manufacturers of mechanical and electro-mechanical elements. The periodic microstructure is measured experimentally with the following manufacturing regimes such as Time, Pressure, Temperature, and Vibrations are considered as the major factors [2] which give the positive or the better diffraction efficiency, those are obtained from the theoretical calculations simulated from the G-solver software. There are certain fabrication techniques like Ionic and chemical etching, Molding, Imprinting, Lithography, and holographic interferometry to produce a microstructure. There is some standard process such as UV embossing, ultrasonic embossing, and injection molding. For manufacturing small or micro components, Thermal embossing is a perfect technology for Micro and Nano components. Hot embossing has benefits such as high aspect ratio and low cost.

1.2 Microstructure Defects

Microstructure produced from the process such as hot embossing has some risks that leads defects while melting material and release of mold from the polymer surface such as

- Material Shrinkage,
- bubbles of residual gas

inside the polymer after the process, the insufficient filling ratio of the master mold shape, high surface roughness, non-uniform mold imprint, cracks produced between the mold and polymer. [3] Therefore from the views it seems that if the master mold is not manufactured precisely according to its shape then it may cause low Diffraction Efficiency. Ultrasonic excitations are mainly used for purposes like welding, Replicating and joining of thermoplastic materials with low soft temperature. From the process, the Ultrasonic waves are generated which gets converted into heat energy thus melts the thermoplastics thus causes the melt flow

between the master mold and polymer surface. With this procedure, a high-frequency technique is used to overcome the flow to the central part of the mold by filling the empty cavities of the mold, this helps to avoid defects such as bubble of residual gas effect. From the journals, we see the authors use sonotrode to apply excitation from the bottom side of the polymer using vibroactive pad which has a single layer piezoceramic as the actuator to produce good quality microstructure. The vibro-active pad designed to generate two vibration modes, first vibration mode at 5.2 kHz and second vibration mode at 8.8kHz [4] with the vibrations there are some disadvantages which occur due to the usage of high-frequency excitation and optimization were flaws include

1. Single layer vibroactivepad is not ready to produce huge displacements, what thusly dimin-ishes the impact of high frequency excitation, be-cause bring down drive strengths polymer to stream.
2. Indentation of vibroactivepad (particularly it's middle), under the activity of mechanical load. This causes bring down filling of the shape in the focal point of microstructure, hence staying void holes.

In addition, beforehand microstructures were made by utilizing second vibration mode at recurrence of 8.8 kHz. This causes uneven contact between surfaces of vibrating vibro-active pad and polymer, subsequently lessening the impact of high recurrence excitation amid the procedure, to take care of already specified issues vibro-active pad, considering the multilayer actuator is proposed. This sort of actuator is situated in the focal point of vibro-active pad, this blocks spaces, which rise under the activity of mechanical load.

As indicated by hypothesis multilayer, in view of a few layers of piezoceramic added to each other can gen-erate greater displacements and force, than single layer can do [5]. Along these lines, it powers preheated polymer to stream even more quickly and better fill purge cavities of master mold. the first vibration mode will be connected during the time spent mechanical hot imprint. This mode demonstrations to the surface of polymer symmetrically, in this manner creating better and more symmetric stream of polymer. The objective of the work is to enhance the nature of periodic microstructures, by utilizing vibroactive pad, considering multilayer actuator. here vibroactive pad, which depends on multilayer actuator, to-gether with its application during the time spent mechanical hot imprint are introduced. Finally, investigation of results is presented and results are talked about. The design of the vibroactive pad is mainly redeemed to improve the periodic microstructure. The stack type actuator is

composed from the multiple layers of piezo-ceramic which generates higher displacements than the single layer Total Energy $E=\Delta F \Delta l$, [6]

1.3 Thermal Replication

Microsystem building is an innovation that in its most broad shape can be characterized as scaled down mechanical and electro-mechanical components that are made utilizing the methods of microfabrication. Different creation systems are utilized to make a small scale or nanostructures. Ionic and chemical etching, molding, imprinting, lithography, and holographic interferometry are the driving innovations used to make Periodic microstructures. However, to decrease the time and costs, replication methods have been utilized.

- innovative procedures, such as
- ultrasonic thermal embossing,
- ultraviolet embossing, and
- injection molding

have been utilized for quite a while presently in microreplication. The thermal embossing procedure is appropriate for assembling little and medium arrangement of micro components. With the expansion of low expenses of replication, hot embossing is a standout amongst the most utilized replication methods in today's microstructures fabrication. Although, it has a few downsides. scientific specialists underline a few thermal embossing issues such as low example constancy, filling proportion, surface inconsistencies, and adhesion between the polymer and the form while demolding. These angles can be controlled and their effect on the last item can be lessened by choosing exact manufacturing techniques comprising of pressure, temperature, and squeezing time. Also, including high-frequency vibrations can give a probability to expand the quality and exactness of the Replica. various replication forms are thought about by computing the coefficient of the assurance keeping in mind the end goal to locate the most productive parameters of periodical microstructure replication.

The replicated profile of periodical microstructure is the principle of all replication innovative procedures. It is examined by contrasting optical results about with hypothetical qualities to comprehend whether the replication procedure was effective. The necessity for the mass production of periodical microstructures incorporates determination, overlay, and economy. Enhancing the nature of reproduction by high-frequency excitation makes conceivable to make the complex Micro or Nano level optical components (Diffractive Optical

Element) with better optical properties and higher determination. It empowers to utilize them in bio-therapeutic, microscale optics, microfluidic devices, electronics, etc. The most vital point which decides optical nature of the grating is +1 and -1 maxima. This property is unequivocally attractive in different applications. To enhance this part of periodical microstructure first the entire replication prepare must be contemplated. As expressed beforehand, it will be exhibited how the parameters impact the nature of periodical microstructure [7].

1.4 Mechanical Hot Print Process

The mechanical hot imprint procedure is a complex innovative operation, in view of materials state changes. It is performed with a hydraulic press. It comprises of hydraulic hold, a gauge of weight, mold horn, controlled stage, thermometer, dynamometer, and control block of temperature, time, and pressure as mentioned in figure 1. Its fundamental parameters are Range of temperature 20–200°C, range of pressure 0–106 N/m², Horn measurements 20mm×20mm to expand the nature of replicated microstructure, high-frequency oscillations are added to the replication procedure.

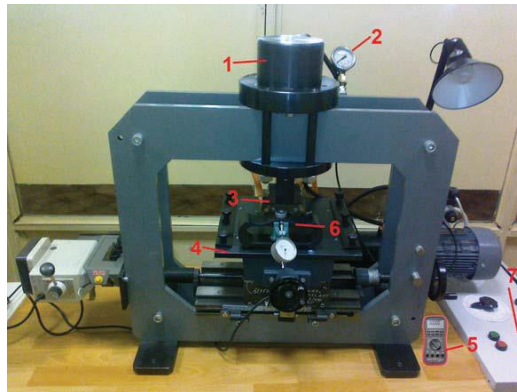


Figure 1 Hot imprint device for Ni stamping on grating structure (Polycarbonate), moving plate (1), master mold (2). Nickel plate imprints on polycarbonate (3), vibroactive pad (4), base of the instrument (5), Dynamometer (6), Control block of Temperature, Pressure, and time. [7]

The schematic drawing of ultrasonic thermal embossing is introduced in Figure 1. As a matter of first importance, the moving plate (1) with the master mold (2) is preheated and persistently kept up to have the assigned temperature. The warmed plate then is moved to the polycarbonate (3). By squeezing the inflexible mold with the required example, a negative example is accomplished. At a similar minute, the vibroactive pad (4), which depends on the base of the instrument (5) begins to produce high-frequency excitations. The heating plate (1) presses the

polycarbonate down for 0.5 s until the pressure achieves nominal value (0.1, 0.2, 0.3, 0.4, or 0.5 Mpa) and later nominal pressure is held for assigned time (5, 10, or 15 s). At last, the form is discharged. The replication procedure is completed at standard ambient temperature and pressure (25°C, 101.325 Pa). The piezoelectric material (PZT-4) energizes high-recurrence vibrations, which with the assistance of aluminium vibrating stage are being transmitted to the polycarbonate. The piezoelectric material and vibrating stage make one component—vibroactive pad. dissimilar procedures of warmth exchange can happen amid a replication procedure. There is extra heat loss on top of the material and form surfaces to the earth because of radiation and convection, heat loss by conduction to the shape, and temperature change in hot imprint process. The formula depicts heat transfer conductivity

$$\rho(T) C_p(T) \frac{\partial T}{\partial t} + \nabla(-k \nabla T) = q \quad (1)$$

where k is thermal conductivity, ρ is density, C_p is heat capacity, T is temperature, and q is the rate of the heat generation. The hot imprint process has the three-major process where they are Heating, imprinting, and demolding.

Heating: The underlying temperature of the form and polycarbonate is 293 K, the same as the temperature of the condition. In this progression, when the stamp touches polycarbonate, amid their underlying contact, the warming of the shape starts up to 421 K temperature. Amid the heating procedure of the mold, the warmth is conveyed to the polycarbonate and it begins to twist against of the impact of the warmth. The heating stride takes brief time about $t = 2.10^{-7}$ s.

Imprinting: In the procedure, the shape goes down and presses polycarbonate, in the meantime the contact is made between the mold and polycarbonate increments. Polycarbonate makes the distortion and Plastic Deformation shows up.

Demolding: During progression, the hot shape ($T = 421$ K) is demolded lastly polycarbonate is cooled. Polycarbonate appears as the shape occasional microstructure.

Hot imprint process is used mainly for the reproduction of Microstructure, because this process has many advantages than the other replication process. the benefits include better quality of the microstructure to attain this factors like temperature, pressure, time is considered and other factors such as high-frequency excitation should be considered to enhance the quality periodical microstructure

1.5 Master periodical structure

The reproductions of periodical microstructures will be investigated. To manufacture these copies, the ace periodical microstructure is required. By utilizing the ace periodical microstructure, it is conceivable to manufacture every one of the reproductions with the coveted procedure regimes. The ace microstructure utilized as a part of this work was made of Nickel. It had a $4\mu\text{m}$ period, the land and the edge is equivalent – $2\mu\text{m}$ and $300\mu\text{m}$ profundity. The practical perspective of an ace microstructure can be found in Figure 2 Standard periodic microstructure of Lamellar or lamella Diffraction grating The photo was made with AFM (Atomic force microscope).

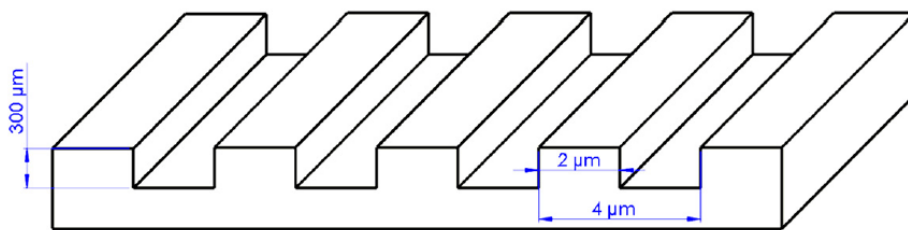


Figure 2 Standard periodic microstructure of Lamellar or lamella Diffraction grating [1].

The periodic microstructure was utilized for production of microstructure copies as well as for breaking down what diffraction efficiencies could be acquired having a perfect reproduction as shown in Figure 3 Sample AFM (Atomic Force Microscopy) image of Master Nickel Periodic Microstructure of the surface [1] With the assistance of G-Solver programming, the perfect copy was demonstrated and every manufactured reproduction were contrasted with these outcomes.

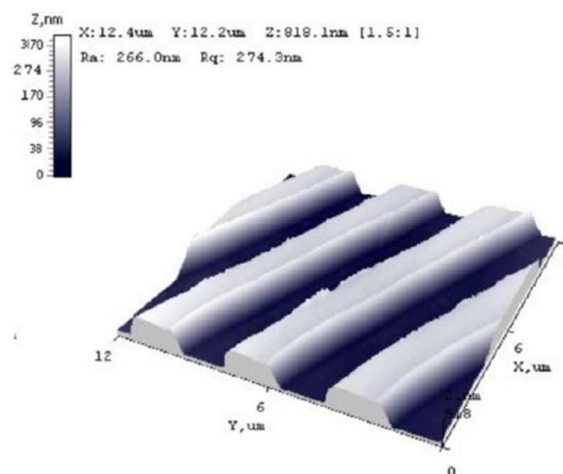


Figure 3 Sample AFM (Atomic Force Microscopy) image of Master Nickel Periodic Microstructure of the surface [1]

1.6 Polycarbonate for thermal replication of periodic Replication

The use of polycarbonate (Fig. 1) in replication of Periodical Microstructures was investigated by Janušas G, Narijauskaitė B. in 2013. It is expressed that Polycarbonate is an appropriate material for periodical microstructure's replication due to its physical properties, for example, [1]

- Quality
- Capacity to withstand scratches
- Effortlessly cleaned
- Ease of use in high temperatures.

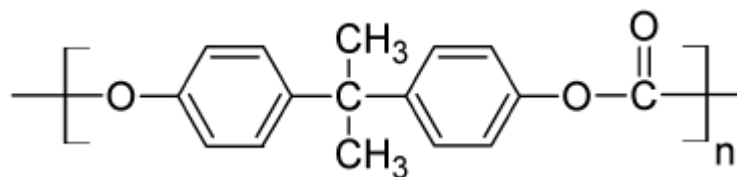


Figure 4 Chemical formula of Monolithic Polycarbonate known as Ketoprofen

The type of polycarbonate we use has a good refractive index with the best properties, the name of the replica is Monolithic polycarbonate known as Ketoprofen, as shown in Figure (4) the physical, chemical, and thermal properties are mentioned in below tables 1,2,3.

Table 1 Thermal properties Polycarbonate [1]

Melting temperature (T_m)	267°C
Glass transition temperature (T_g)	150°C
Heat deflection temperature – 10 kN	145°C
Heat deflection temperature 0.45 Mpa	140°C
Heat deflection temperature – 1.8 Mpa	128-138°C
Upper working temperature	115-130°C
Lower working temperature	40°C
Linear thermal expansion coefficient	65-70×10 ⁻⁶ /K
Specific heat capacity	1.2-1.3 kJ/(kg·K)
Thermal conductivity	23°C 0.19-0.22 W/(m·K)

Table 2 Chemical properties of polycarbonate [1]

Young's modulus	2.0-2.4 Gpa
Tensile strength	55-75 Mpa
Compressive strength	>80 Mpa
Poisson's ratio	0.37
Coefficient of friction	0.31

Table 3 Physical properties of polycarbonate [1]

Density	1.20-1.22 g/cm ³
Refractive index	1.584-1.586
Water absorption - Equilibrium	0.16-0.35 %
Water absorption – over 24 hours 0.1 %	0.1 %
Light transmittance	88 %

Monolithic Polycarbonate is a material that can be used for diffraction grating, mechanical hot imprint process is done on this material with nickel imprinting because of its good impact strength say 20-21kg/m², which absorbs UV rays. This type of polycarbonate has physical properties such as good strength, flexibility, transparency, and relatively low flammability, which is more suitable for periodical microstructure replication.

The main benefits of this polymer is

- the highest strength of industrial transparent materials (250 times stronger than glass)
- a relatively small weight (1.2 g / cm³, 2 times lighter than glass)
- The sufficiently high degree of transparency (88%)
- Protective properties: resistance to environmental influences, high resistance to chemical agents [12].

Monolithic Polycarbonate is used in applications such as construction, automotive, furniture, medical, electrical and electronics, microfluidic devices, music, optics, and surveillance systems because of its practical application: ease of processing, flexibility, flexibility, ease of cleaning [8].

1.7 Vibroactive pad and Replication process

From the above discussions, we see the production process of the periodic microstructure through Thermal replication process otherwise known as hot embossing produces some quality microstructure with manufacturing defects like during UV replication process, electroplating and measurement defects in analysis process to overcome these defects and to produce a good quality microstructure, to overcome the main factors as mentioned above, a vibroactive pad is used to energize the high-frequency vibrations to the polycarbonate with a specific end goal to build the good quality periodical microstructures. The vibrating pad is made of an aluminium barrel and a ring of piezoelectric material. The piezoelectric component chose was PZT-4 developed by Kaunas University of Technology group in 2012[1], from the theoretical aspect calculation, the analysis is done to produce a better diffraction efficiency to improve the lamellar grating structure quality. The Diffraction grating have used for many applications in which a small example of usage procedure is mentioned below in figure 4

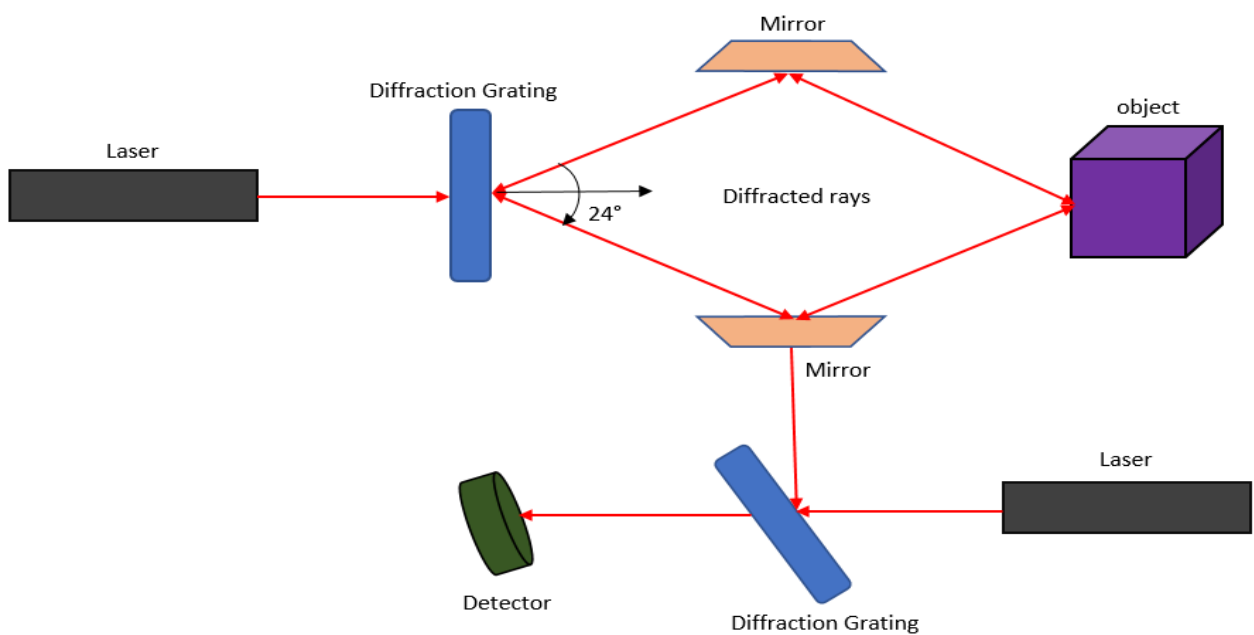


Figure 5 Application of diffraction grating with lasers to observe the characteristics and properties of the object using Diffraction gratings and mirrors.

The Diffraction grating is designed and fabricated in this project were the gratings can be used for many purposes by the scientists of Kaunas University of Technology and can be used for many other sources like Telecommunication modules, and other industrial sectors including Optical communication, Photovoltaics, catalysis, structural biology, Electronic and magnetic materials

2. Simulation of G-solver

2.1 Introduction

G-Solver is a software composed of full vector implementation which executes results and comprises of calculations called Rigorous Coupled Wave (RCW) Analysis. These calculations give a numerical package of Maxwell's conditions for the grating structure that lies at the limit between two homogeneous direct isotropic characteristics and properties which is the superstrate and substrate [9]. The course of action is careful, as in the full plan of vector Maxwell's conditions are clarified and stated as below:

- 1) a piecewise-direct estimation to the grating development, and
- 2) A truncation parameter for the Fourier series portrayal of the permittivity and im-
permittivity inside each grating layer. G-Solver is set up to work with linear isotropic
homogeneous materials.

The latest G-solver V25 has lot of upgraded features which could help us to develop a grating and further simulations are generated, following is a list of the principal features

- 1) Graphical Grating Editor
- 2) Automatic piecewise approximation construction
- 3) Significantly extended hereditary calculation for automatic design
- 4) General algebraic constraints and equation editor
- 5) enhanced graphing
- 6) Object linking and embedding
- 7) Adjusted interface with autonomous gliding G-Solver windows
- 8) The materials record (Gsolver.ini) is currently composed to the root directory (location
of the GsolverV51.exe file)
- 9) More predictable utilization of units. All structures now expect the contribution to the
client Units determination on the Parameters tab.
- 10) The genetic algorithm merit function has been expanded to allow for summing a result
over a set of angles or wavelengths. This allows for optimization over certain parameter
ranges
- 11) The consequences of a Grating Listing run or a GA run can now be replicated to the
interior piecewise grating structure taking into consideration the aftereffects of (say) a
GA run to then be utilized straightforwardly in a Grating Listing run or from Run [9].

Material library is available, were suitable material are chosen for gratings are selected and further simulated therefore the material list are mentioned below.

This identifies three materials of the following constant refractive indices:

1.0, 1.25, and 1.5. Besides the CONSTANTS section, V5.1 INI files contain the following sections: DRUDE, SELLMEIER, HERZBERGER, SCHOTT, POLYNOMIAL, TABLE with at least one entry in for each type [9]

2.2 Procedures

The procedure includes many steps that are followed to execute the result and the chart is generated finally.

2.2.1 Parameters

The parameter tab is the initial and the main step to initiate the diffraction grating figure 1 shows the characteristics and features of the software.

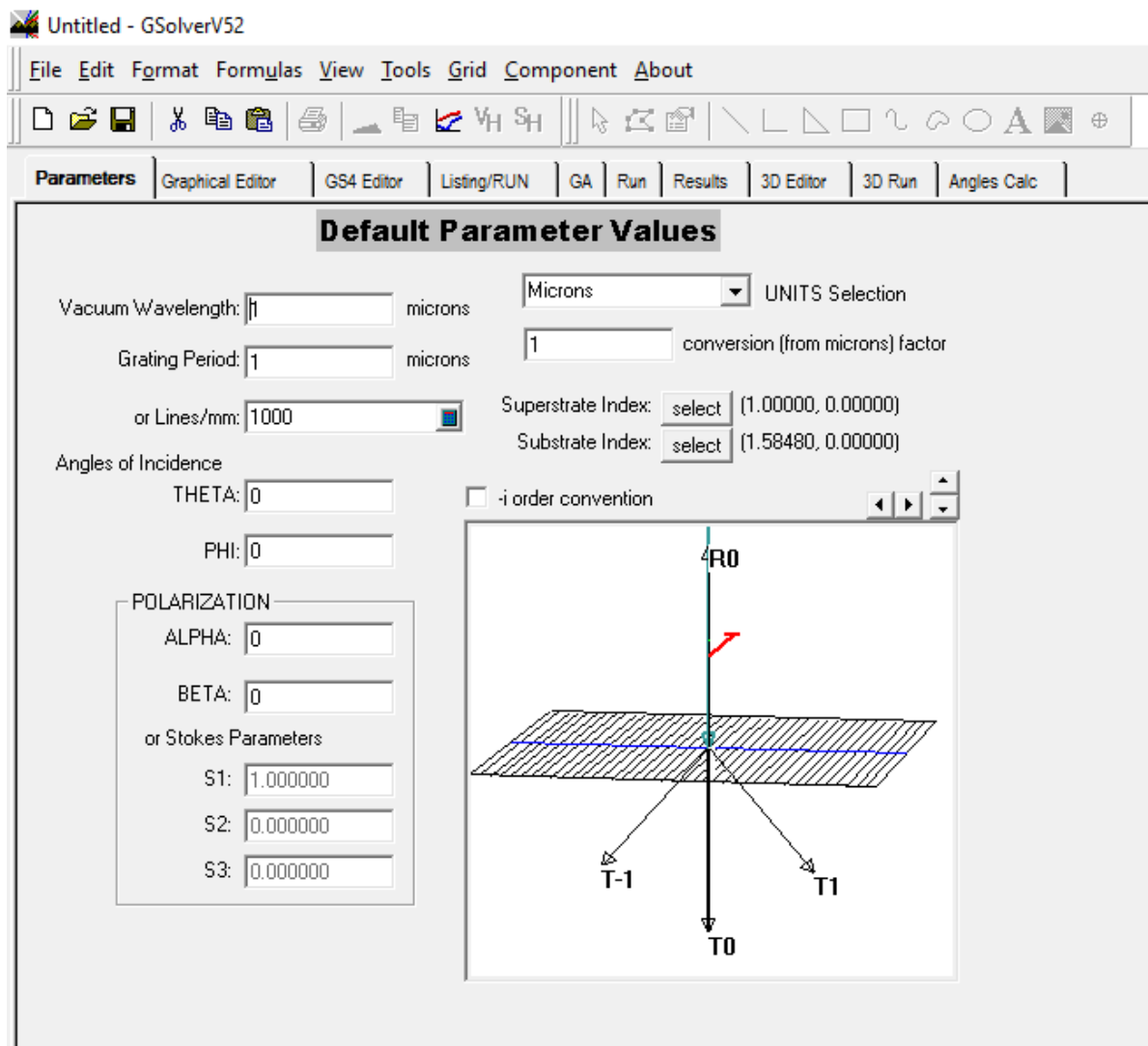


Figure 6 Default parameter tab generates the number of maxima orders and materials for each period say $4\mu\text{m}$, $5.6\mu\text{m}$, and $10\mu\text{m}$ in G-solver.

The Vacuum wavelength is the wavelength of the laser used, say Red, Green, or Blue is here we use He-Ne laser as the main source for diffraction patterns that occurs when impacts on the surface or canvas of the grating structure. The Wavelength or the Refractive Index for Red=0.633 μm , Green=0.532 μm , Blue=0.441 μm , the grating period is taken in 3 parameters, they are 4 μm ,5.6 μm , and 10 μm which are simulated for the 3 lasers.

- The Superstrate index indicates the material or the surrounding of the grating structure or canvas. In the option, we select material like Nickel or even Air.
- The substrate index indicates main structure or canvas property or material, here we select material such as Polycarbonate or another polymer material
- The angle is the main phenomena were for period 4 μm , 5.6 μm , 10 μm the incident angle is 90 degrees perpendicular to the grating structure. The lasers get diffracted, producing numbers of Diffraction orders or maxima
- For period 4 μm Red and green laser = 11 Diffraction orders or maxima is produced and for blue= 15 Diffraction orders or maxima is produced
- For period 5.6 μm , Red laser = 15 Diffraction orders or maxima is produced and for green = 17 Diffraction orders or maxima are produced and for blue = 21Diffraction orders or maxima is produced.
- For Period 10 μm , Red laser= 26 diffraction orders or maxima are produced and for green laser = 30 Diffraction orders or maxima are produced and for Blur laser = 36 Diffraction orders or maxima is produced.
- From the Diffraction Orders, the best Maxima or the order is selected. The simulated result shows that the 1st order maxima were the angle for period 4 μm is 10 degrees and for period 5.6 μm is 6 degrees and for period 10 μm is 4 degrees. The best suitable orders with the respective angles are selected and simulated.

2.2.2 Graphical Editor

Graphical editor is the primary tool for defining a linear grating structure. The crossed gratings are handled separately for both editing and calculation, and are discussed in the 3DEditor and 3DRun.

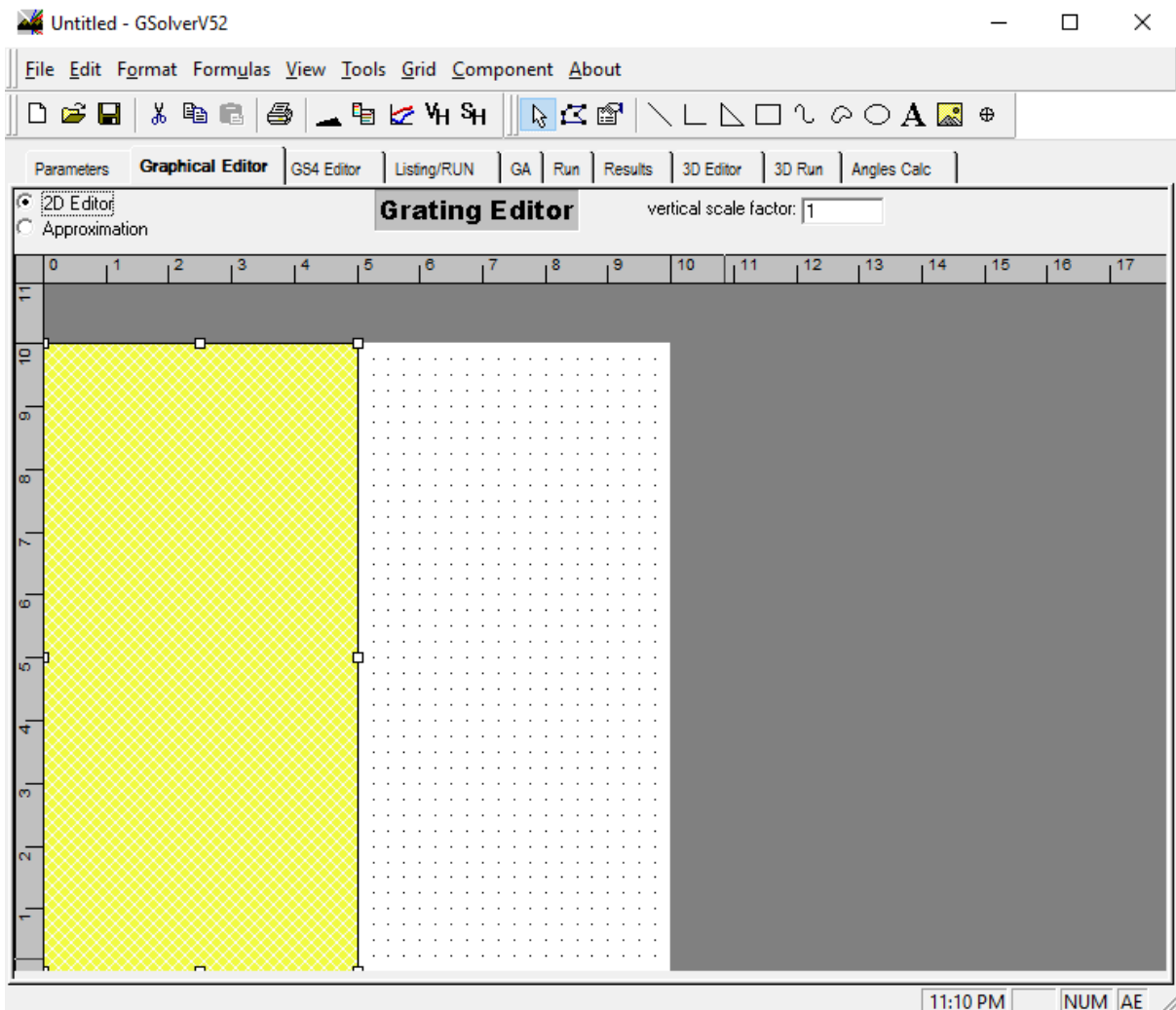


Figure 7 Grating Editor is used to design the grating Canvas structure including both the substrate and Superstrate for 1 period.

The highlighted area is called the ‘canvas’ where all drawing takes place. The canvas serves as an edge-on view of the grating structure. The region that exists below the canvas is the substrate and the area above the substrate is the superstrate. The canvas is the ‘modulation region’ where the grating exists. This is illustrated in the following Figure 6.

With the software tool utilizing the primitive shapes and programmed profile, required figure is drawn, selecting "Estimation" radio option which intimates the constant approximation schedule from the upper left corner summons the structure. The internal functions which is generated by the schedule that inspects the canvas grid points and generates the constant approximation which develops the grating structure. The 2D editor option can be used to specify the 2D structure of the canvas and the grating structure with its geometrical properties and material properties.

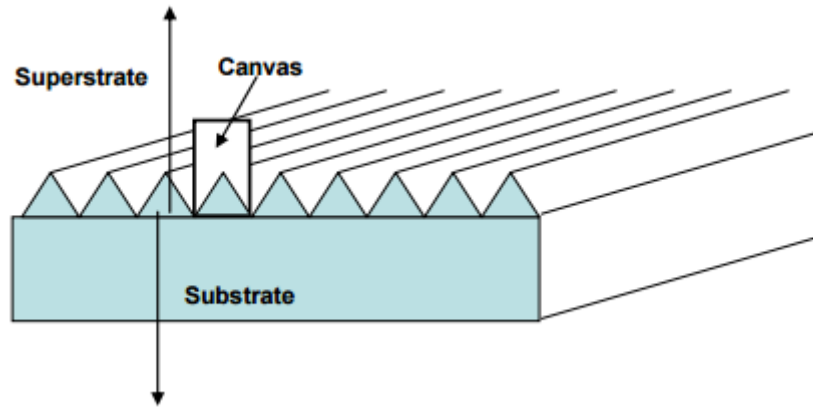


Figure 8 Canvas of master periodical microstructure compromising both substrate and superstrate. [9]

The canvas width is equal to 1 grating period for every unit configurations (ie. 10 units on the ruler). There are two dialog options that defines how the canvas can be displayed, which states Canvas Properties, Measurements, and Size dialogs.

G-Solver has the standard coordinate mapping format to MM_LOMETRIC which is interpreted or considered as one logical unit that equals 0.1 mm as internal calculation. The actual dimensions depend on the type of configurations used were, the other screen modes are as follows [9]

- MM_HIENGLISH one logical unit is 0.001 inch
- MM_HIMETIRIC one logical unit is 0.01mm
- MM_ISOTROPIC one logical unit is 1 pixel in both X and Y
- MM_LOENGLISH one logical unit is 0.01 inch
- MM_TEXT one logical unit is one pixel
- MM_TWIPS one logical unit is 1/1440 inch [9]

The drawing is made with 1 grating period selecting superstrate material as air and substrate material as polycarbonate moved to next step of Listings/run.

2.2.3 Listing/Run

The Listing/RUN tab is considered the main interface in the G-solver schedule. The internal piecewise constant grating approximation is listed on the grid, and furthermore, the different sections can be adjusted and obliged with user-defined algebraic constraints. The listing tab is comprised of Grating definition listing in which the required parameters is entered and generated automatically.

	A	B	C	D	E	F	G	H
1	Grating Definition Listing							
2	Theta:	0						
3	Phi:	0						
4	Alpha:	0						
5	Beta:	0		0	1	100		
6	wavelength:	0.633						
7	Period:	4						
8	uperstrate:	Air						
9	Substrate:	PC						
10	Orders:	5						
11	LAYER:	1						
12	Thickness:	1	1					
13	Block:	1						
14	Width:	0.5	0.5					
15	Material:	PC						
16	Block:	2						
17	Width:	0.5	1					
18	Material:	Air						

Figure 9 Listings/Run tab generated to show parameters such as block, width, and material of usage as highlighted.

The grating structure is found in segment B together with the grating parameters. Segment A is utilized to mark the section B options and to set free parameters, a group of controls are used from the right side of the grid. Segment C shows the total thickness at each layer, for data usage.

Layer 1 consists of primary layer composed of parameters such as block 1 and block 2 were the thickness, width and material of both substrate and superstrate is executed and generated. The material of block 1 is considered as Polycarbonate and for block 2 is Air, both width of the block is given 0.5mm as shown in Figure 8. The primary thing to do is to populate the matrix with the grating definition structure made on the Editor utilizing the Approximation activity, any unfilled framework cell can be utilized to hold middle outcomes. Lattice option are assembled under Format, Formulas, View, and Grid. A hefty portion of the controls work on components of the network. In those cases, the component must be chosen before the controls are actuated. After giving the inputs to the specified fields the populate button is clicked which gets generated automatically thus giving the values of the width and block area.

2.2.4 Genetic Algorithm (GA)

A Genetic calculation has been fundamentally upgraded. It depends on Differential Evolution (DE) Differential Evolution became out of Ken Price's endeavours to determine the Chebyshev Polynomial Fitting Problem that had been postured to him by Rainer Storm. A leap forward happened when Ken thought of utilizing vector contrasts for differentiating the vector

populace. Since this fundamental thought, a great discussion amongst Ken and Rainer and unlimited ruminations and PC simulation on both parts yielded numerous considerable enhancements which make Diffraction Efficiency the adaptable and vigorous tools. [9]

	A	B	C	D	E	F	G	H
1	GA Grating Definition Listing							
2	Theta:	0						
3	Phi:	0			Real Parameters			
4	Alpha:	0		Min Value	Max Value			
5	Beta:	0		0	1	0.3586425781		
6	wavelength:	0.633		0	1	0.6758422852		
7	Period:	4		0	1	0.5240478516		
8	uperstrate:	Air						
9	Substrate:	PC		Weight: 0.700				
10	Orders:	5		CrossOver: 0.				
11	LAYER	1		Population: 25				
12	Thickness	1	1	MaxIterations:				
13	Block:	1		Method: Rand				
14	Width:	0.5	0.5					
15	Material:	PC		RUN GA	Populate	Copy/Update		
16	Block:	2				Update Parms		
17	Width:	0.5	1	Abort	GA test	Options		
18	Material:	Air						
19								

Figure 10 GA Grating Definition listing tab shows the real parameters of min and max value generated.

The G-Solver Diffraction Efficiency usage considers a self-assertive number of actual parameters and all the well-known advancement methodologies. therefore, skill and intelligence is much needed to solve or execute the Grating efficiency. On the off chance that the arrangement requirements are too far away from home of any physical arrangement, the calculation is probably going to just meander around in parameter space and never creates an expected result. For optimization, a very powerful tool of diffraction efficiency to grating design is used in case of applications. The procedure followed are all the same, were the required parameters are entered and the results are generated by selecting the populate option which gives result as shown in figure 9, for example, min value and max value with the weight, crossover, and populace.

2.2.5 Execution or Run

RUN tab provides immediate access to several key grating parameters which helps in generating the result and the chart for the periods and wavelength thus giving a wide range of values indicating the diffraction efficiencies.

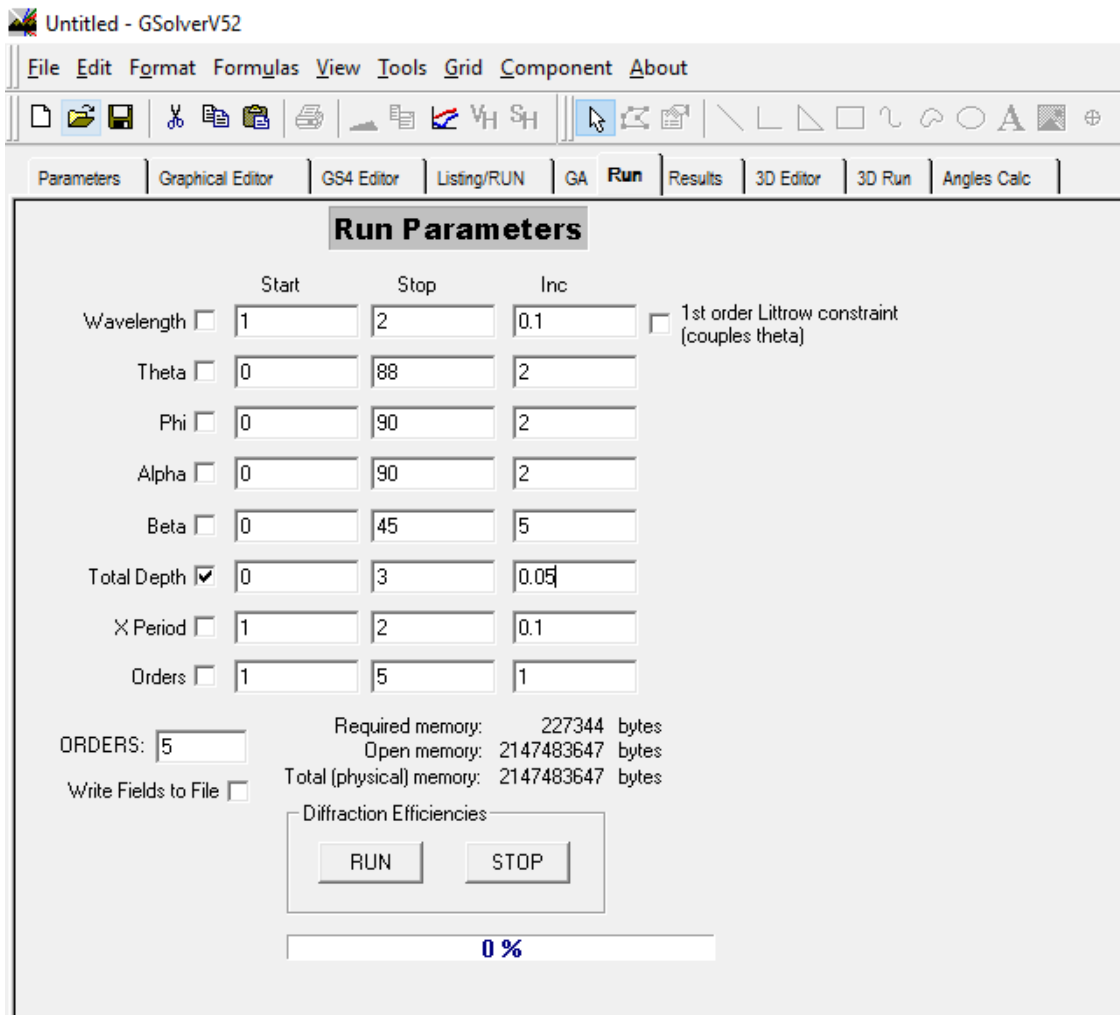


Figure 11 Defining the total depth range with specific increment and Diffraction orders in Run Parameters tab in G-solver.

The values of the wavelength, incident, and diffracted angles are automatically generated with the values given in the first tab, parameter tab. In execution tab, we give inputs for total depths and changes in increment value.

2.2.6 1st order Littrow

The 1st order Littrow check box invokes a simple Littrow condition. As the wavelength changes, Theta is altered so that the first-order Littrow condition (in reflection) is satisfied. A Littrow constraint is generally run as a function of wavelength only.

After giving the input parameters with required order numbers, the run option is clicked to view the results to select the best diffraction efficiency [9].

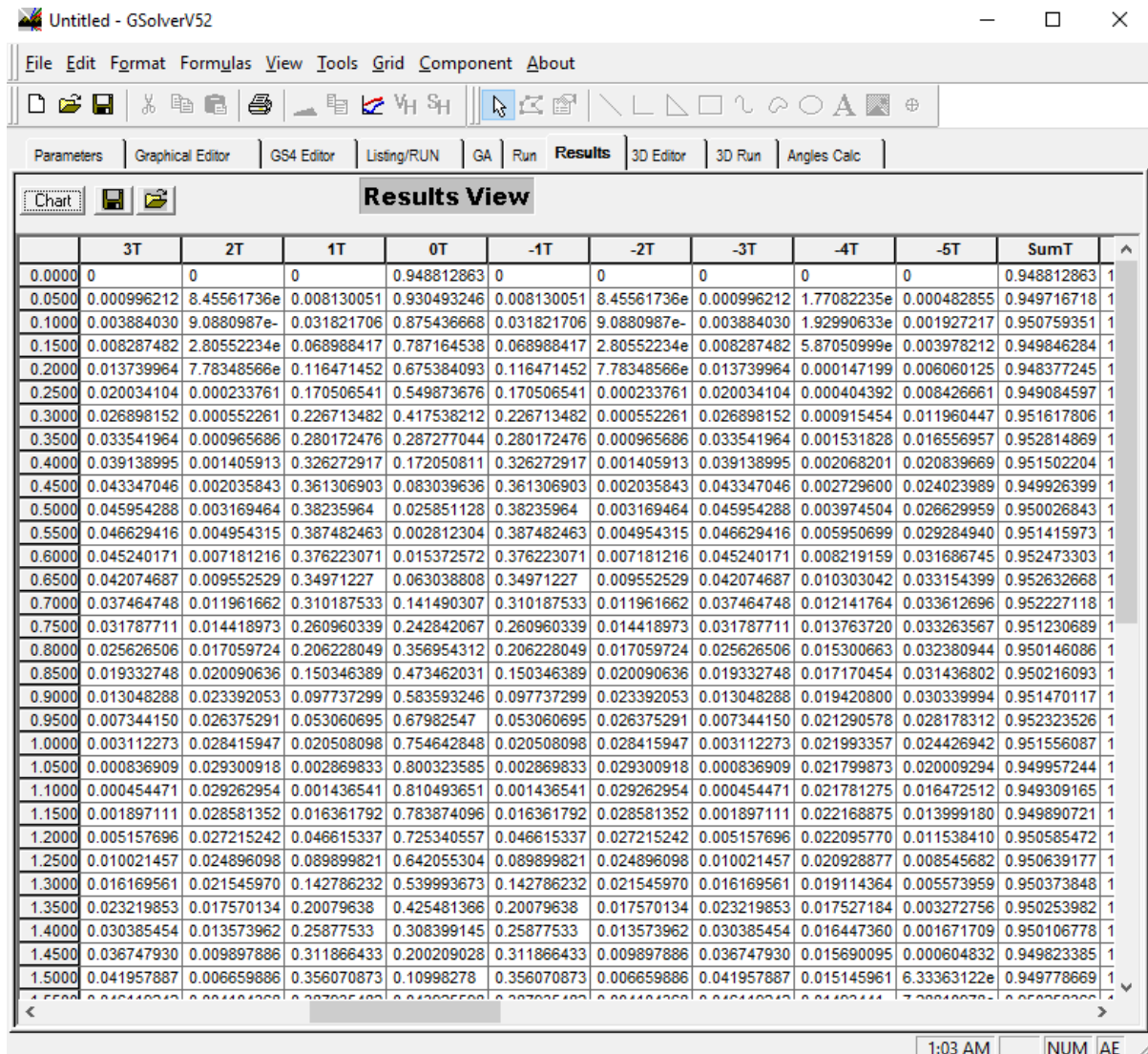


Figure 12 Results of the diffraction efficiency for maxima orders and total depths are generated from the Result tab in G-solver.

The results are generated by from the result tab therefore differentiating the best depths and maxima's thus creating the highest diffraction efficiency from the results tab using G-solver as shown in figure 11.

2.2.7 Diffraction Efficiency

The diffraction efficiency is defined as follows:

$$DE_k = [(E_x \text{conj}(E_x))_k + (E_y \text{conj}(E_y))_k + (E_z \text{conj}(E_z))_k] * re(k_{zRk})/k_{zinc} \quad (2)$$

where subscript k = diffraction order, k_{zRk} is the z -component of the K th diffraction order (as defined by the grating equation), and R is the reflection. R gets changed to T for the transmitted orders. Since all orders are represented as plane waves, if the z -component of the diffracted k -vector is 0 (or pure imaginary), then DE is identically 0 for that order [9].

2.2.8 Graphing

The graph is generated by selecting a single column or even multiple columns, after selecting the chart button in the top of the Run tab.

The initial chart uses defaults on all settings. To modify any component of the chart, tap on the different devices. The properties dialogue box of the item is selected for execution for instance, to change x -axis properties, for example, like Image, limits, and numerical data's. G-Solver's graphing tool has a strong base that provides graphing results perfectly by selectin the required columns or rows for execution and includes many display and customization properties. Required information for many features are explained in the graphing chapter [9].

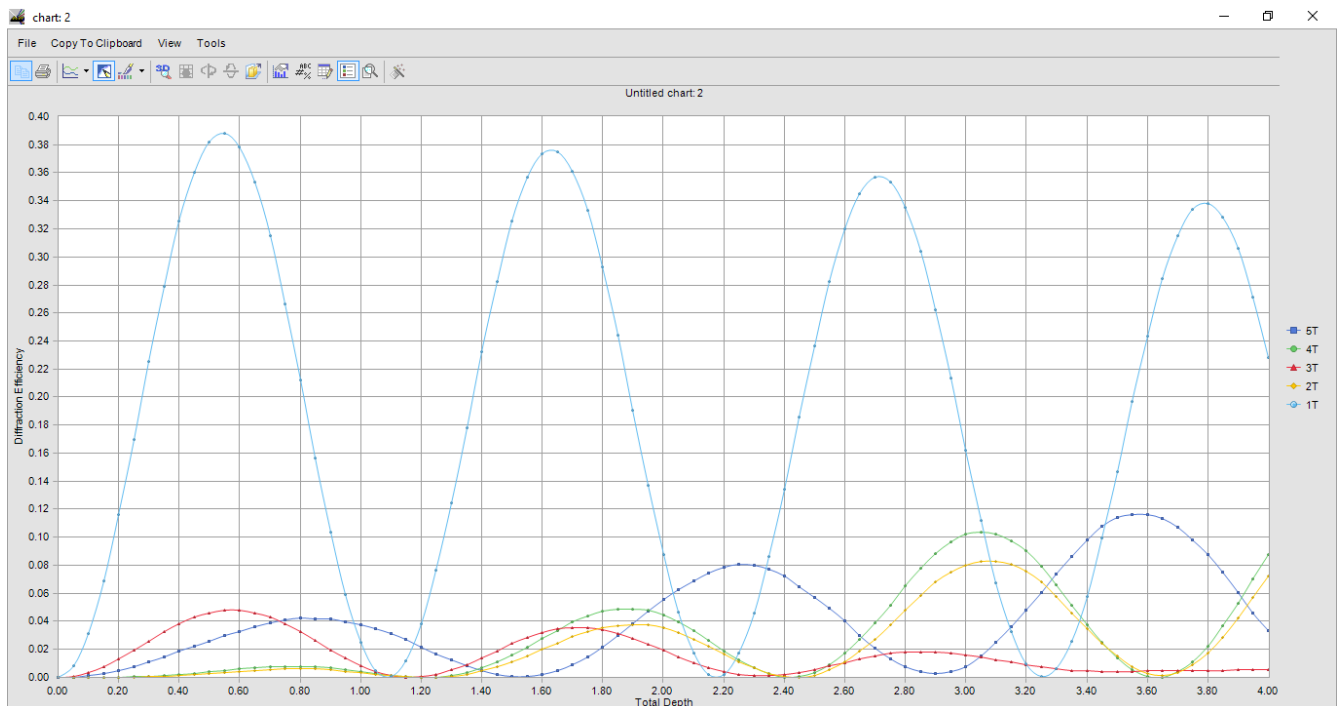


Figure 13 one of generated Graphs defining the total depths vs Diffraction efficiency, maxima orders showing the peak value as the highest diffraction efficiency from final results. The Graphing option gives a perfect result for a required period and Laser section through which the highest Diffraction Efficiency is produced were the best results are compared and selected for execution.

3. Theoretical Calculation

The total functional features and procedures about G-solver is discussed above, as this software can be used to simulate and generate certain results that should come up with the practical aspects, we simulate the diffraction orders of certain lasers like RED, BLUE, GREEN with their respective wavelengths or bandwidths to give possible results to find out the better or the greatest diffraction efficiency by comparing the numbers in the result tables and the waves that are created from the chart. Therefore, the best number is considered as the great or highest diffraction efficiency and further moved onto simulation.

3.1 Red laser or He-Ne laser

He-ne laser is otherwise known as the Red laser is used for many applications such as alignment of high power CO₂ and YAG treatment lasers and pointing beams, Medical uses. The wavelength of the Red laser is 0.633nm the super-substrate material is Air and the substrate material is taken as polycarbonate, the canvas is drawn and the required norms are entered and generated. The input parameters are implied and further procedures are done to obtain results and charts, the generated results are screened below.

3.1.1 G-solver results and charts For Period 4μm

The results thus obtained are elaborated Specifically where the best Diffraction orders and their depths are selected, highlighted to intimate the best diffraction efficiency after then the chart is generated with the selected Rows and columns which represent sinusoidal waves were the peak points are the greatest or highest diffraction efficiency. The chart defines about Diffraction efficiency verses total depth producing the highest diffraction efficiency in the 1st order maxima -1T and +1T generating the highest peak value of depth 0.55nm as shown in the figure 13. The graph shows the waves of both positive and negative diffraction orders of 1T, 3T, 4T and 5T of total depth from 0 to 4.

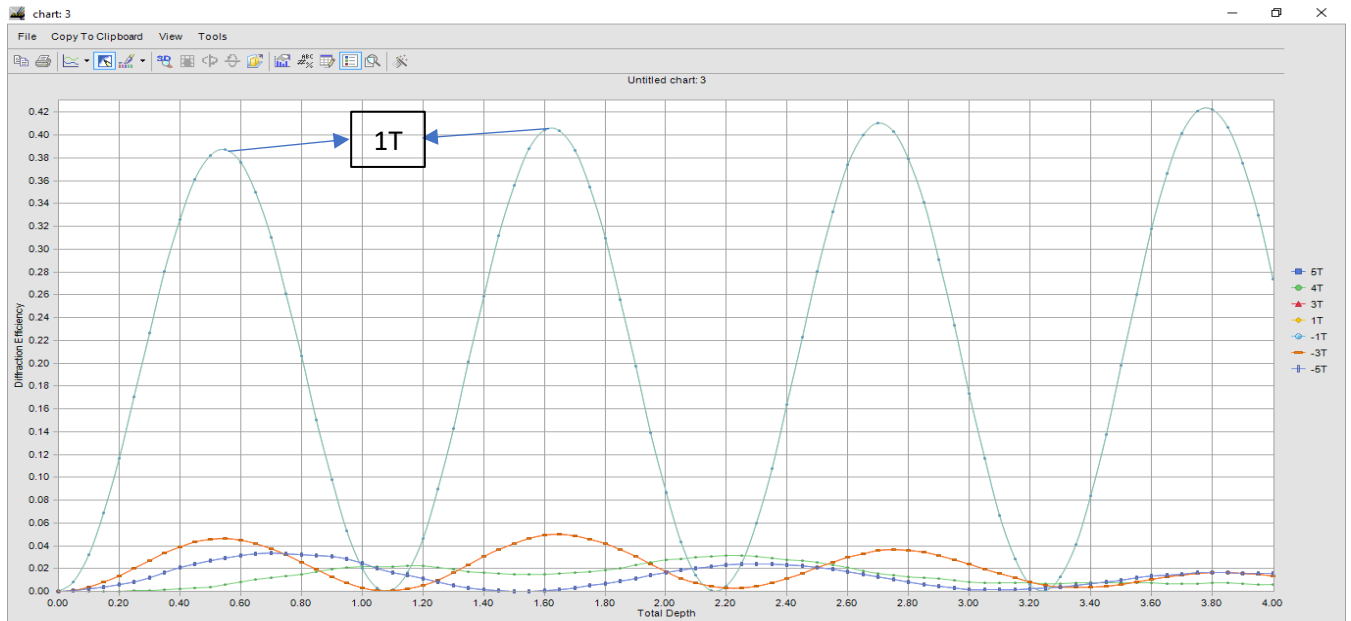


Figure 14 Total depth Verses Diffraction Efficiency of period $4\mu\text{m}$, Red laser of wavelength $\lambda=0.633\text{nm}$ producing Highest D.E of depth 0.55nm in the First order (-1T, +1T) maxima among the other orders (3T, 4T, 5T).

The values of the results, Diffraction orders generated from the G-solver software is used to obtain the graph. The values of the diffraction orders are recalculated using Excel to neglect the material properties as from the early researchers we see that geometrical properties are more important than the material properties therefore not analysing the material but the geometry. The values of the result and recalculation are attached in APPENDIX 1.

3.2.2 G-solver results and charts For Period $5.6\mu\text{m}$

The same wavelength 0.633nm is given for Red laser or He-Ne laser but the period is changed to $5.6\mu\text{m}$ and the super-substrate material is Air and the substrate material is taken as polycarbonate the canvas is drawn and the required norms are entered and generated by the following procedures, the results are generated and the required graph is made using the G-solver software. The results and charts are screened below.

the results are obtained and the best readings are highlighted thus indicating the best diffraction efficiency, the required reading such as the rows and columns are selected to obtain the graph to spot the peak or greater value for implementation which is the Diffraction efficiency. The chart describes about Diffraction efficiency verses total depth producing the highest diffraction efficiency in the 1st order maxima -1T and +1T generating the highest peak value of depth

0.55nm as shown in the figure 13. The graph shows the waves of both positive and negative diffraction orders of 3T, 5T of total depth from 0 to 4.

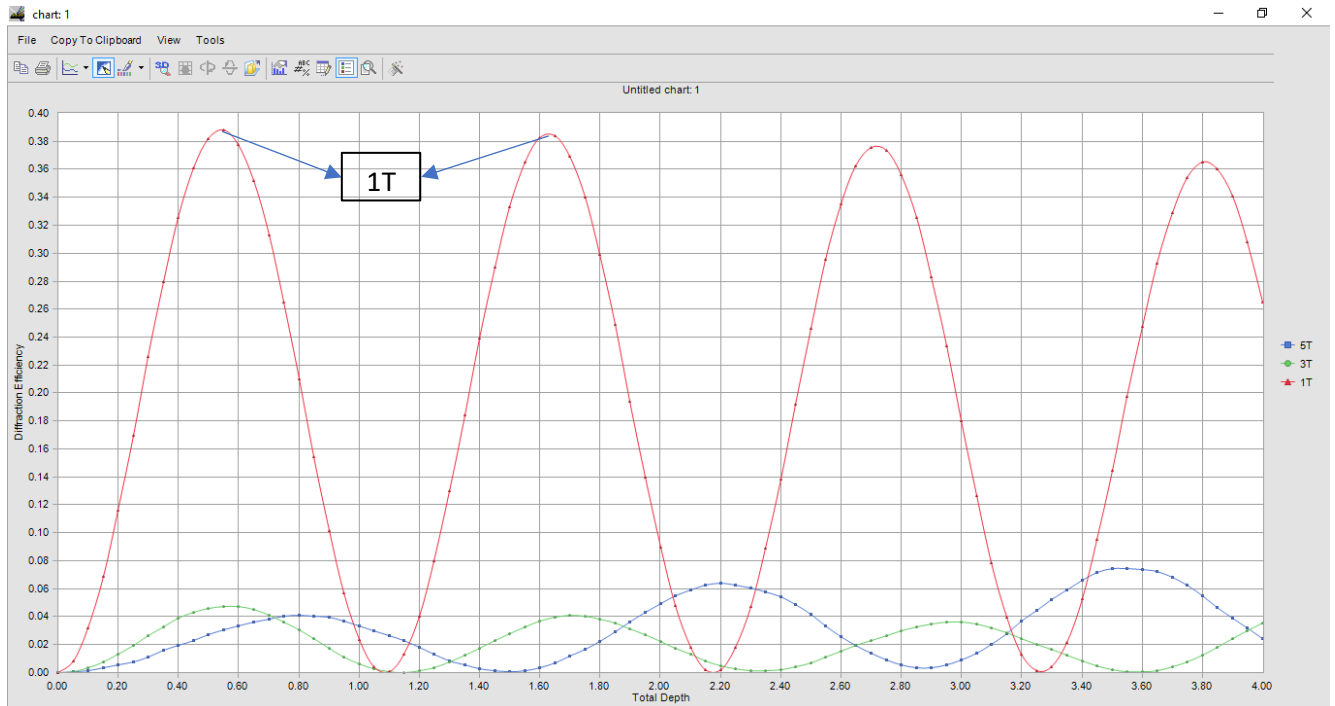


Figure 15 Total depth Verses Diffraction Efficiency of period $5.6\mu\text{m}$, Red laser of wavelength $\lambda=0.633\text{nm}$ producing Highest D.E of depth 0.55nm in the First order (-1T, +1T) maxima among the other orders (3T, 5T)

The values of the results, Diffraction orders generated from the G-solver software is used to obtain the graph. The values of the diffraction orders are recalculated using Excel to neglect the material properties as from the early researchers we see that geometrical properties are more important than the material properties therefore not analysing the material but the geometry. The result values and recalculation is attached in APPENDIX 2.

3.3.3 G-solver results and charts for period $10\mu\text{m}$

The values or parameters of Red laser or He-Ne laser are implied with the same wavelength of about 0.633nm is used, here the period is changed into $10\mu\text{m}$, the super-substrate material is Air and the substrate material is taken as polycarbonate the canvas is drawn and the required norms are entered and generated by the following procedures, thus the Results and Charts are further generated using the G-solver software. The chart shows Diffraction efficiency verses total depth producing the highest diffraction efficiency in the 1st order maxima -1T and +1T generating the highest peak value of depth 0.55nm as shown in the figure

13. The graph shows the waves of both positive and negative diffraction orders of 1T, 2T, 3T, 4T and 5T of total depth from 0 to 4.

From the generated Results, the peak value or the greatest values are selected, the greatest values in the Rows and Columns are selected, highlighted to draw a chart using the G-solver software.

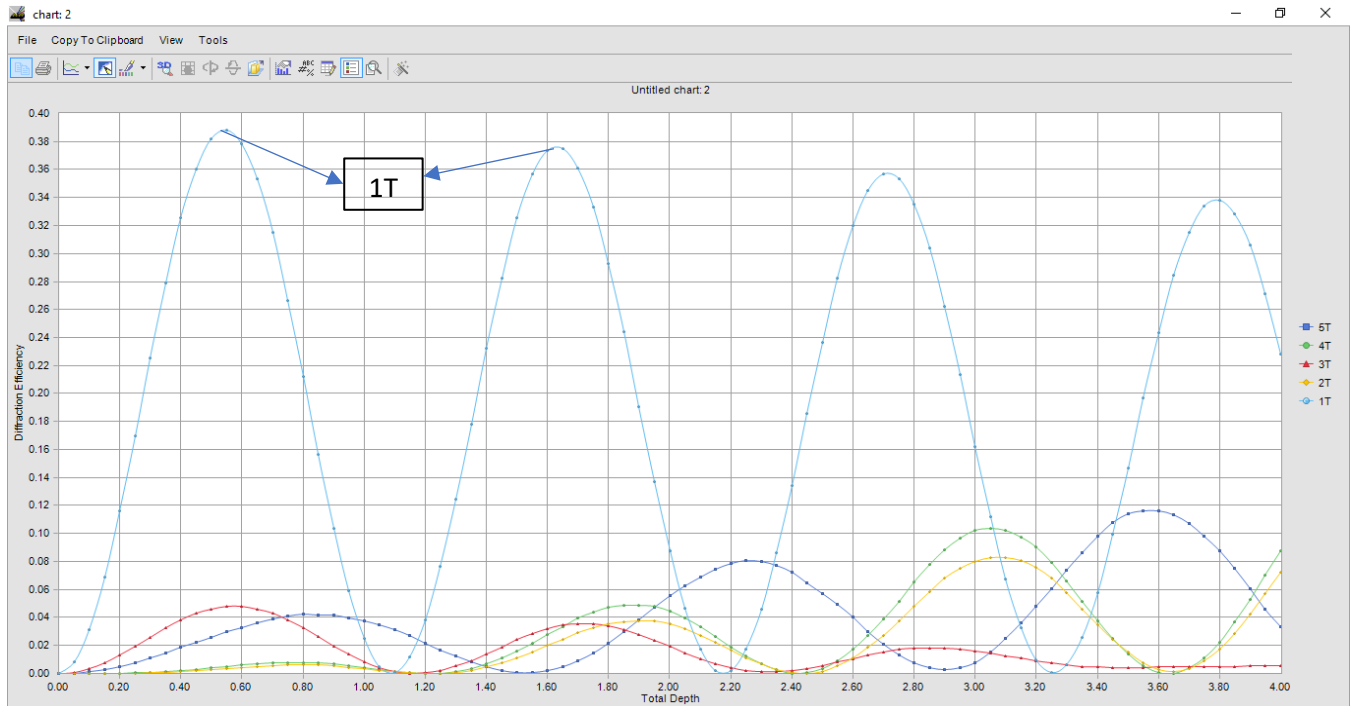


Figure 16 Total depth Verses Diffraction Efficiency of period $10\mu\text{m}$, Red laser of wavelength $\lambda=0.633\text{nm}$ producing Highest D.E of depth 0.55nm in the First order (-1T, +1T) maxima among the other orders (2T, 3T, 4T, 5T)

The values of the results, Diffraction orders generated from the G-solver software is used to obtain the graph. The values of the diffraction orders are recalculated using Excel to neglect the material properties as from the early researchers we see that geometrical properties are more important than the material properties therefore not analysing the material but the geometry. The value of the result and recalculation is attached in APPENDIX 3.

3.2 Blue Laser or Helium-Cadmium Lasers

Blue lasers are usually produced by Helium-Cadmium Lasers with the wavelength of 441nm and Argon-ion lasers with the wavelength of 458 to 488nm . Blue lasers emit electromagnetic radiations which are visible as Blue or violet to human eyes. Blues lasers are used in applications such as Medical Diagnostics, Telecommunication, and Information

technology. We impute 441 nm as the wavelength of Blue lasers in G-solver software with the respective period of 4 μm , 5.6 μm , and 10 μm .

The norms are implied in the G-solver software with the wavelength 0.441nm and **period 4 μm** . The super-substrate material is considered as Air and the substrate material is taken as Polycarbonate. The canvas is drawn for 1 period and the results are generated with the specific value of total depth given and the final chart is drawn with the maximum values of the result sheet, the results are obtained with the required parameters, where the highest value is highlighted, the chart is later generated by selecting the required Rows and Columns and the peak value is selected.

3.2.1 G-solver results and charts For Period 4 μm

From the results, the required values are selected; the highest values are highlighted and the graphs are obtained for the highest or peak values which intimate the greatest Diffraction efficiency.

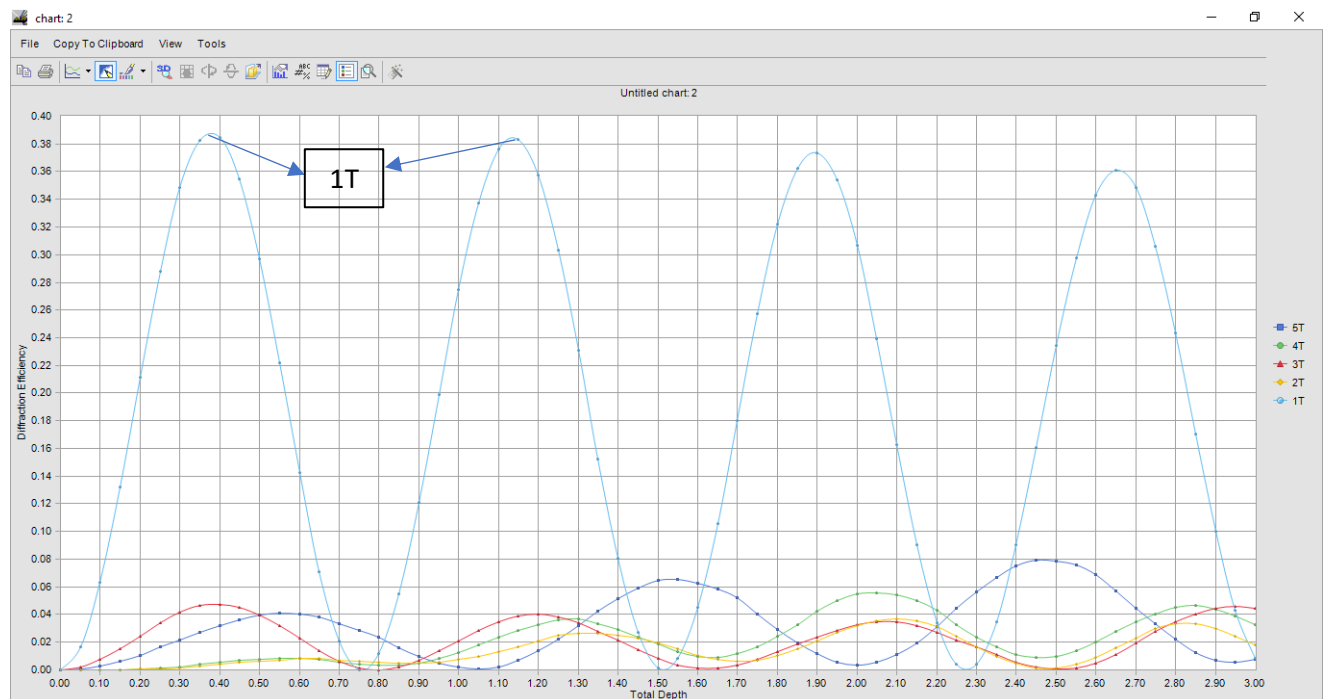


Figure 17 Total depth Verses Diffraction Efficiency of period 4 μm , Blue laser of wavelength $\lambda=0.441\text{nm}$ producing Highest D.E of depth 0.40nm in the First order (-1T, +1T) maxima among the other orders (2T, 3T, 4T, 5T).

The values of the results, Diffraction orders generated from the G-solver software is used to obtain the graph as shown in figure 16. The values of the diffraction orders are recalculated using Excel to neglect the material properties as from the early researchers we see that

geometrical properties are more important than the material properties therefore not analysing the material but the geometry. The values of the result and recalculation are attached in APPENDIX 4.

3.2.2 G-solver results and charts For Period 5.6 μm

The blue laser or Helium-Cadmium laser is generated in the G-solver software with the same wavelength 0.441nm with the Air as super-substrate and the substrate as Polycarbonate but the period changes to 5.6 μm the values of the diffraction orders from G-solver is implied in the excel and the values are Recalculated later, The input parameters such as wavelength, super-substrate, substrate, and period in entered in the following areas and the procedure is followed to obtain the results and charts. The results of period 5.6 μm are executed and its chart is screened below in fig 17. From the obtained results, the highlighted rows and columns are selected from which the peak or greater values are selected and the chart is generated using the G-solver software.

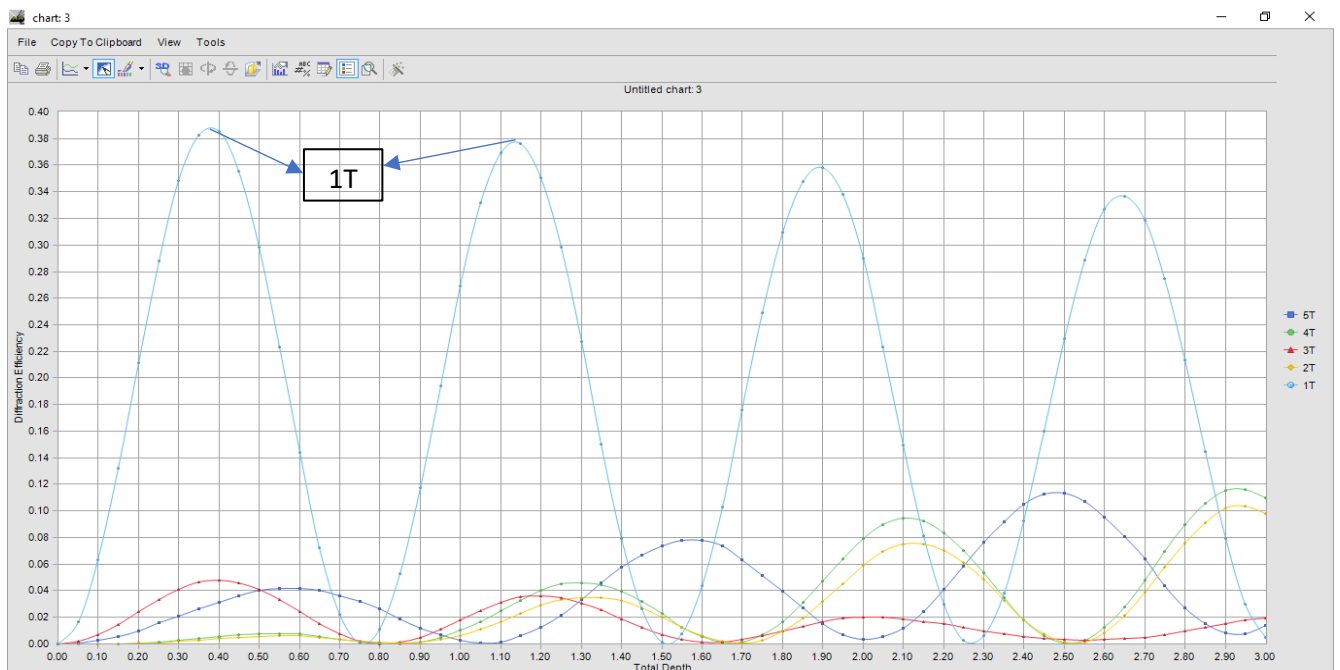


Figure 18 Total depth Verses Diffraction Efficiency of period 5.6 μm , Blue laser of wavelength $\lambda=0.441\text{nm}$ producing Highest D.E of depth 0.40nm in the First order (-1T, +1T) maxima among the other orders (2T, 3T, 4T, 5T).

The values of the results, Diffraction orders generated from the G-solver software is used to obtain the graph as shown in figure 17. The values of the diffraction orders are recalculated using Excel to neglect the material properties as from the early researchers we see that geometrical properties are more important than the material properties therefore not analysing

the material but the geometry. The values of the result and recalculation are attached in APPENDIX 5.

3.2.3 G-solver results and charts For Period 10 μm

The wavelength of the Blue laser or Helium- Cadmium Laser say 0.441nm is implied the default parameter value area, Air is considered as the Super-substrate material and Polycarbonate as Substrate. The incident angle is all given according to their diffraction orders. The whole process is carried out in G-Solver software. The following results are obtained from the software by implying the parameters in the following areas where the procedures are done as mentioned in the Simulation of G-solver software for the **period 10 μm** , the results are executed where the charts are mentioned below in figure 18.

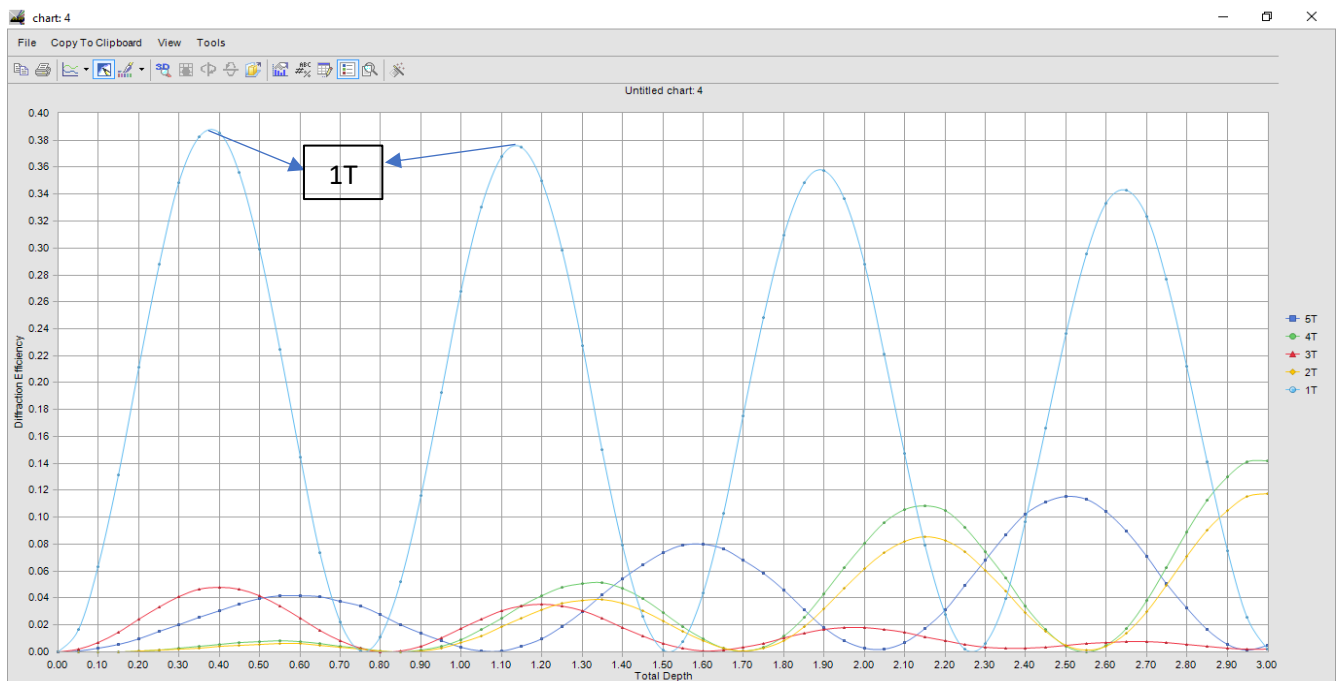


Figure 19 Total depth Verses Diffraction Efficiency of period 10 μm , Blue laser of wavelength $\lambda=0.441\text{nm}$ producing Highest D.E of depth 0.40nm in the First order (-1T, +1T) maxima among the other orders (2T, 3T, 4T, 5T).

From the obtained results, the chart is executed by selecting the required rows and columns. The greatest values of the results, the diffraction orders are selected and the chart is executed. Indicating the peak values as the greatest and best diffraction efficiency

The values of the results, Diffraction orders generated from the G-solver software is used to obtain the graph as shown in figure 18. The values of the diffraction orders are recalculated using Excel to neglect the material properties as from the early researchers we see that

geometrical properties are more important than the material properties therefore not analysing the material but the geometry. The values of the result and recalculation are attached in APPENDIX 6.

3.3 Green laser or Nd-YAG laser

The Green Laser or Nd-YAG laser mainly use Lithium triborate instead of KTP. These lasers are mostly used for pointing devices used for night vision rescue and pointers for guns. Here we use green lasers as the source with the wavelength 0.532nm used in G-solver software with the following periods 4 μ m, 5.6 μ m, 10 μ m. The super-substrate material is considered as Air and the substrate material as Polycarbonate. The canvas is drawn for 1 period in graphical editor phase with the respective materials and the result is obtained with the required depths. The charts are later drawn with the maximum or the greatest values.

3.3.1 G-solver Results and chart for period 4 μ m

From the results obtained the required diffraction orders and depths are selected. The greatest values are selected and highlighted to intimate the maximum values with this the chart is generated from which the peaks points are considered as the greatest diffraction efficiency points, the chart executed is shown in figure 19.

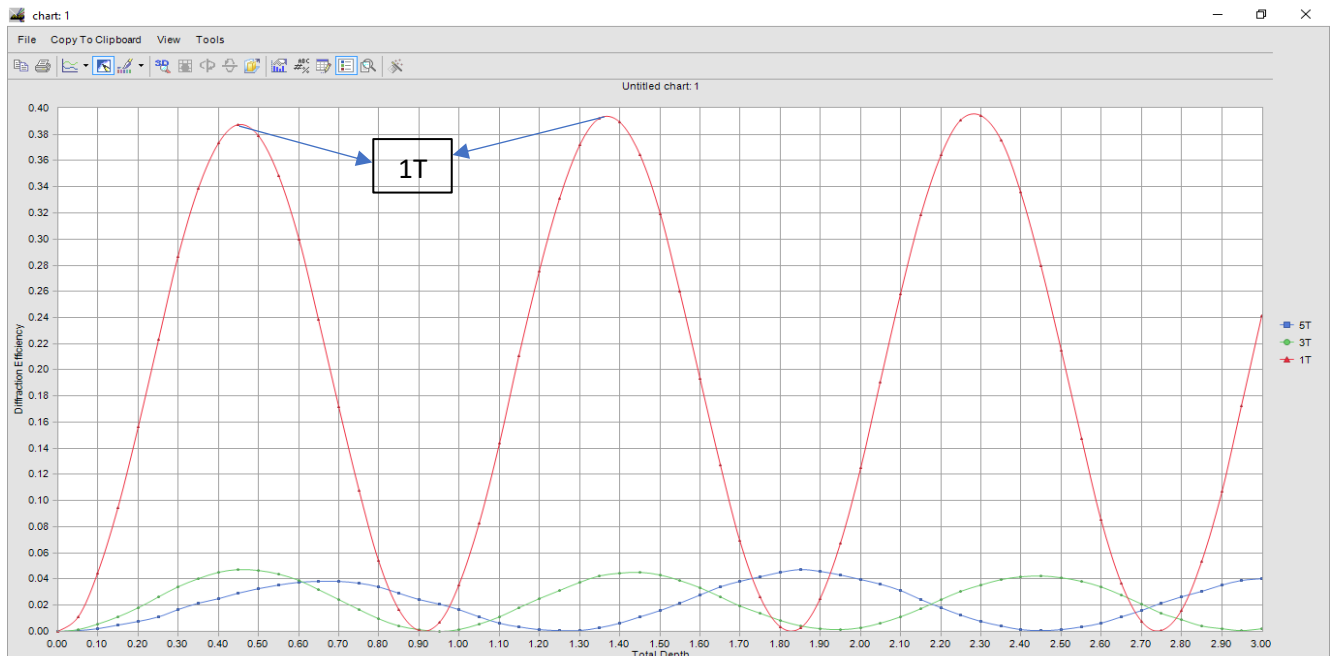


Figure 20 Total depth Verses Diffraction Efficiency of period 4 μ m, Green laser of wavelength $\lambda=0.532$ nm producing Highest D.E of depth 0.45nm in the First order (-1T, +1T) maxima among the other orders (3T, 5T).

The results and charts are generated or simulated from the G-solver software, from the values obtained the calculation as shown in figure 19, is done manually in the excel with the required values of Diffraction orders and the values later recalculated. The result values and records are attached in APPENDIX 7.

3.3.2 G-solver results and charts for period 5.6μm

The Green laser or Nd-YAG laser is tested for the best Diffraction efficiency by implying the Wavelength 0.532nm, for the period 5.6μm. the super-substrate material is selected as Air and the substrate as Polycarbonate which is obtained from **Thermal Replication** with Nickel. For this period, also the canvas is drawn for one period and the results are obtained for the required depths and generated.

From the results, the Diffraction orders and the depths are highlighted which mentions the greatest or the better values. The required values are selected where the chart is obtained by generating the selected values, the chart is shown in figure 20.

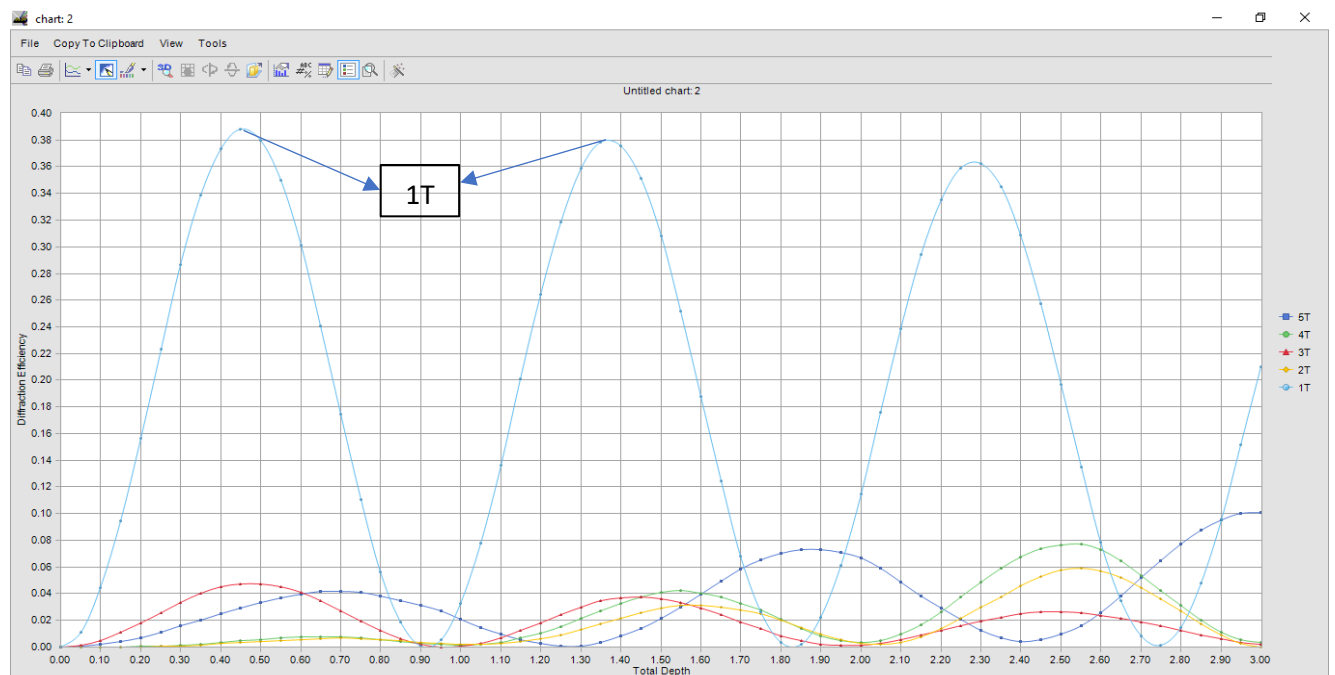


Figure 21 Total depth Verses Diffraction Efficiency of period 5.6μm, Green laser of wavelength $\lambda=0.532\text{nm}$ producing Highest D.E of depth 0.45nm in the First order (-1T, +1T) maxima among the other orders (2T, 3T, 4T, 5T).

Therefore, the results and charts are generated with the help of G-solver software for the green laser as shown in figure 20. From the values obtained the numbers are calculated manually in

the excel and later the values of diffraction orders are recalculated to find the greatest diffraction efficiency of period $5.6\mu\text{m}$, the calculations are attached in APPENDIX 8.

3.3.3 G-Solver results and charts for period $10\mu\text{m}$

The Green laser or Nd-YAG laser is tested for the best Diffraction efficiency by implying the Wavelength 0.532nm , for the period $10\mu\text{m}$. the super-substrate material is selected as Air and the substrate as Polycarbonate which is obtained from **Thermal Replication** with Nickel. For this period, also the canvas is drawn for one period and the results are obtained for the required depths and generated.

From the results, the Diffraction orders and the depths are highlighted which mentions the greatest or the better values. The required values are selected where the chart is obtained by generating the selected values, where the chart is shown in figure 21.

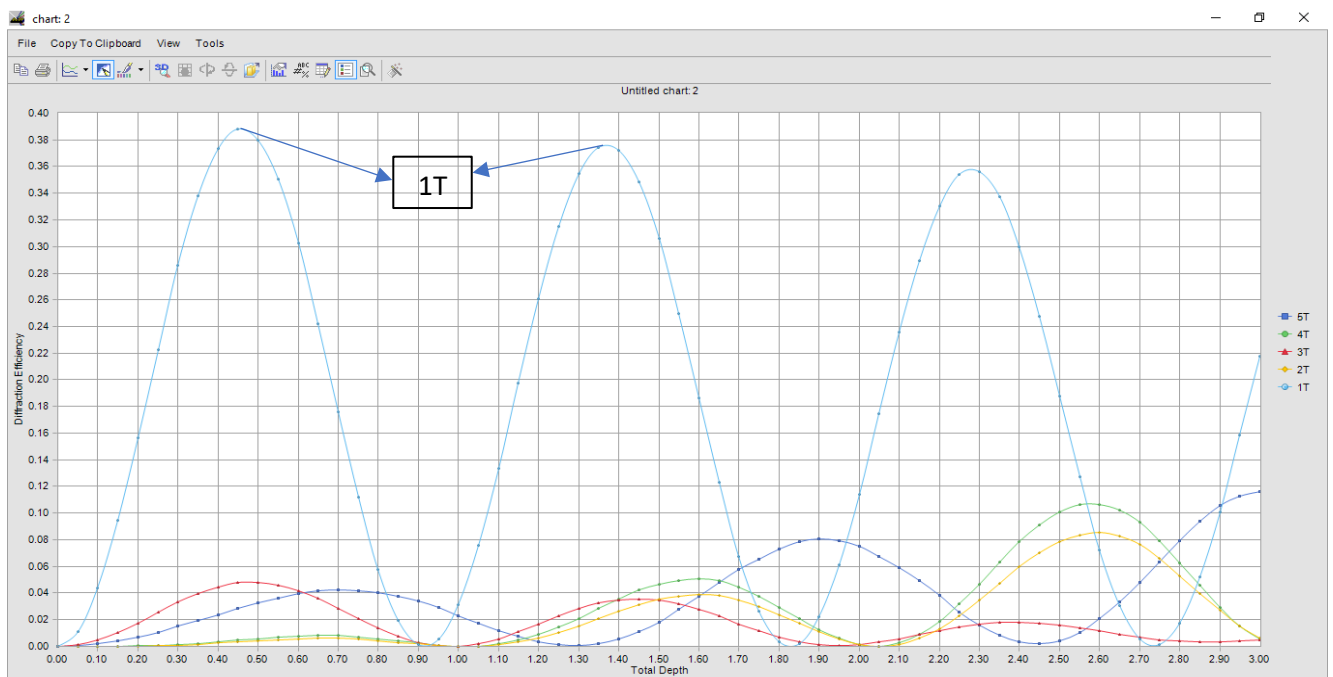


Figure 22 Total depth Verses Diffraction Efficiency of period $10\mu\text{m}$, Green laser of wavelength $\lambda=0.532\text{nm}$ producing Highest D.E of depth 0.45nm in the First order (-1T , $+1\text{T}$) maxima among the other orders (2T , 3T , 4T , 5T).

Therefore, the results and charts are generated with the help of G-solver software for the green laser. From the values obtained the numbers are calculated manually in the Excel and later the values of diffraction orders are recalculated to find the greatest diffraction efficiency of period 10nm , the calculation which is carried out in excel is attached in APPENDIX 9.

3.4 Comparison

The comparison is done using the pie chart for all the lasers say Red, Green, and Blue by relating the results. This process is done to prove the geometrical properties and characteristics to give the best Diffraction efficiency among all the three colours proving both with the same depth and with the different depths of the respective lasers with the period say $4\mu\text{m}$, $5.6\mu\text{m}$ and $10\mu\text{m}$ with the diffracted maxima of both positive and negative orders 5T,4T,3T,2T, 1T and 0T to show the difference between the lasers.

For period 4nm the pie-chart shows which have the best diffraction efficiency have the peak point with different depths and with the same depth of 0.55nm , the full descriptions of the comparison are stated below in tables, the chart consists of Maxima orders vs Depths.

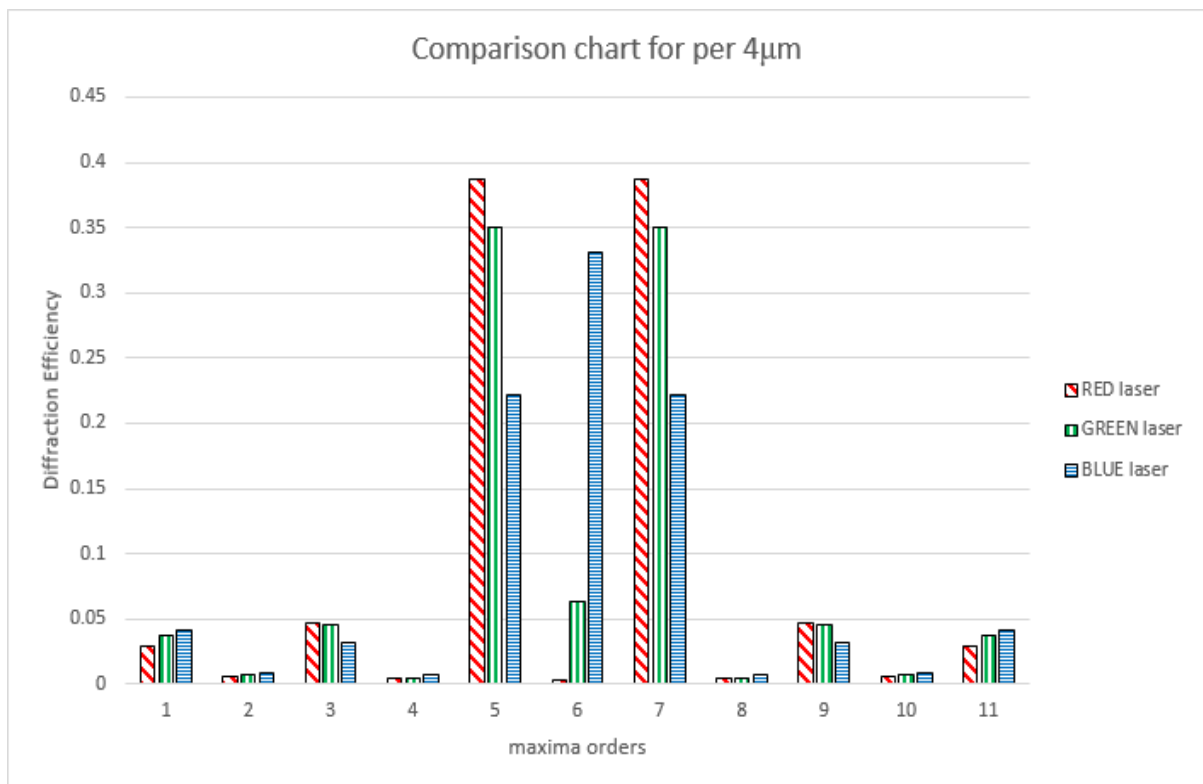


Figure 23 Comparison chart of Maxima orders verses Diffraction efficiency of three lasers for period $4\mu\text{m}$ of same depth 0.55nm defining the highest diffraction efficiency.

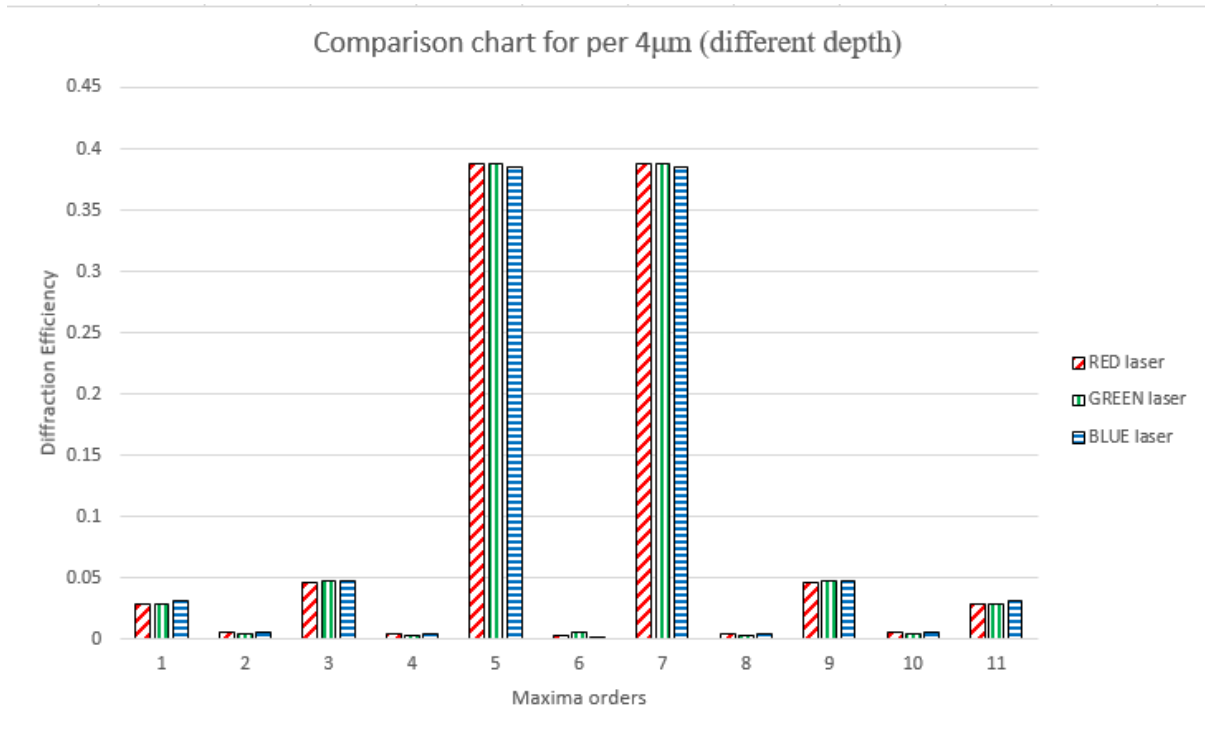


Figure 24 Comparison chart of Maxima orders vs Diffraction efficiency of three lasers for period 4µm of different depth 0.55nm, 0.45nm, 0.40nm defining the highest diffraction efficiency.

For Period 5.6nm the pie-chart is made to prove which has the better Diffraction efficiency the diagram shows which has the peak value comparing with the different depths and same width of 0.55nm

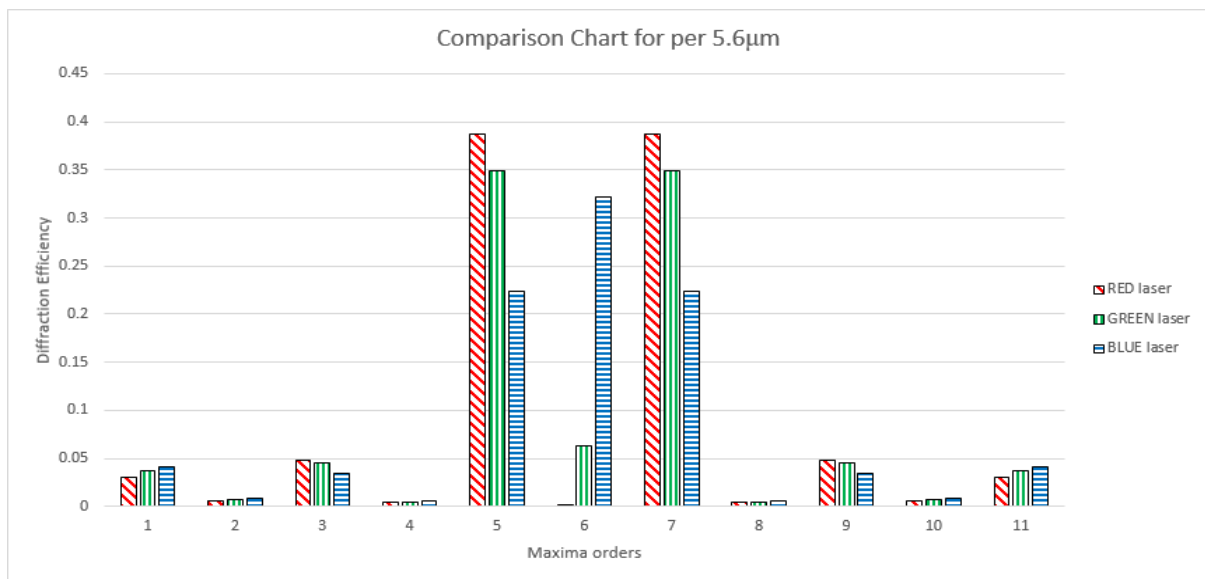


Figure 25 Comparison chart of Maxima orders vs Diffraction efficiency of three lasers for period 5.6µm of same depth 0.55nm defining the highest diffraction efficiency.

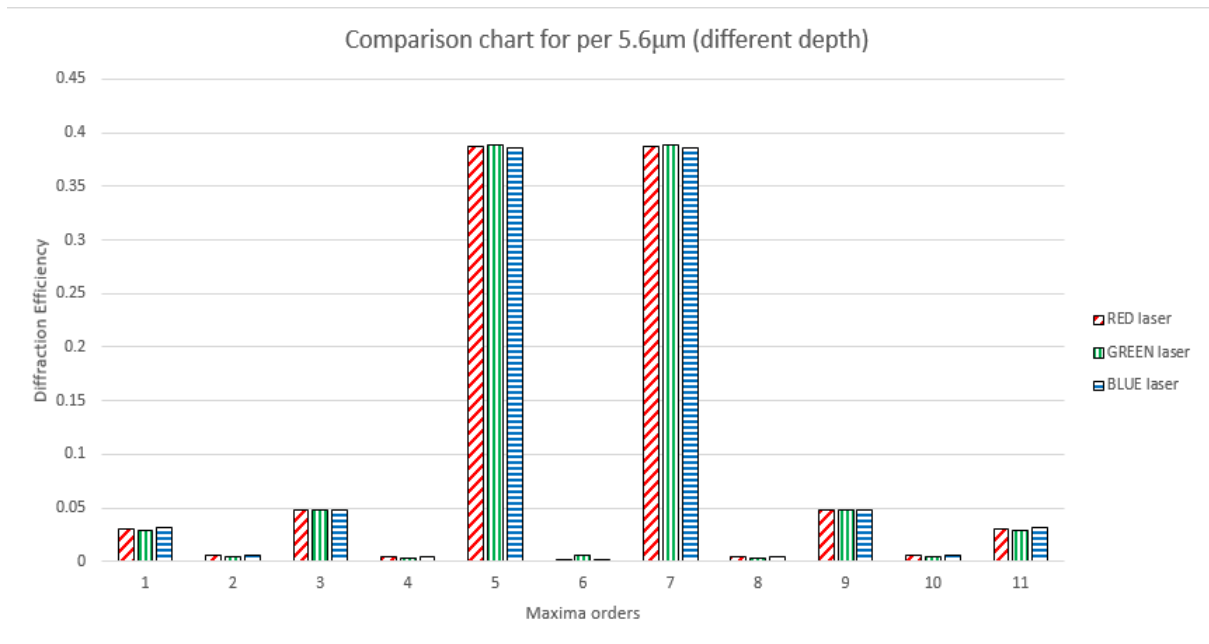


Figure 25 Comparison chart of Maxima orders vs Diffraction efficiency of three lasers for period 5.6µm of Different depth 0.55nm,0.45nm, and 0.40nm defining the highest diffraction efficiency.

For period 10µm the pie-chart is made to show which colour has the best Diffraction efficiency. Comparing both the chart with same depth 0.55nm and different depths the peak point is considered best laser.

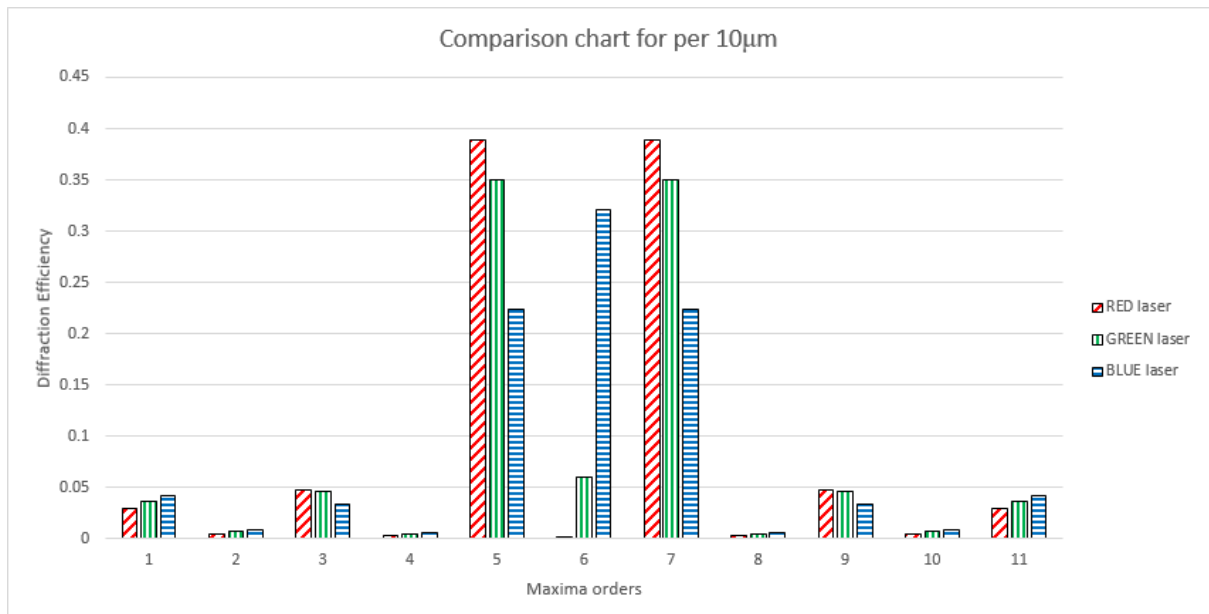


Figure 26 Comparison chart of Maxima orders verses Diffraction efficiency of three lasers for period 10µm of same depth 0.55nm defining the highest diffraction efficiency.

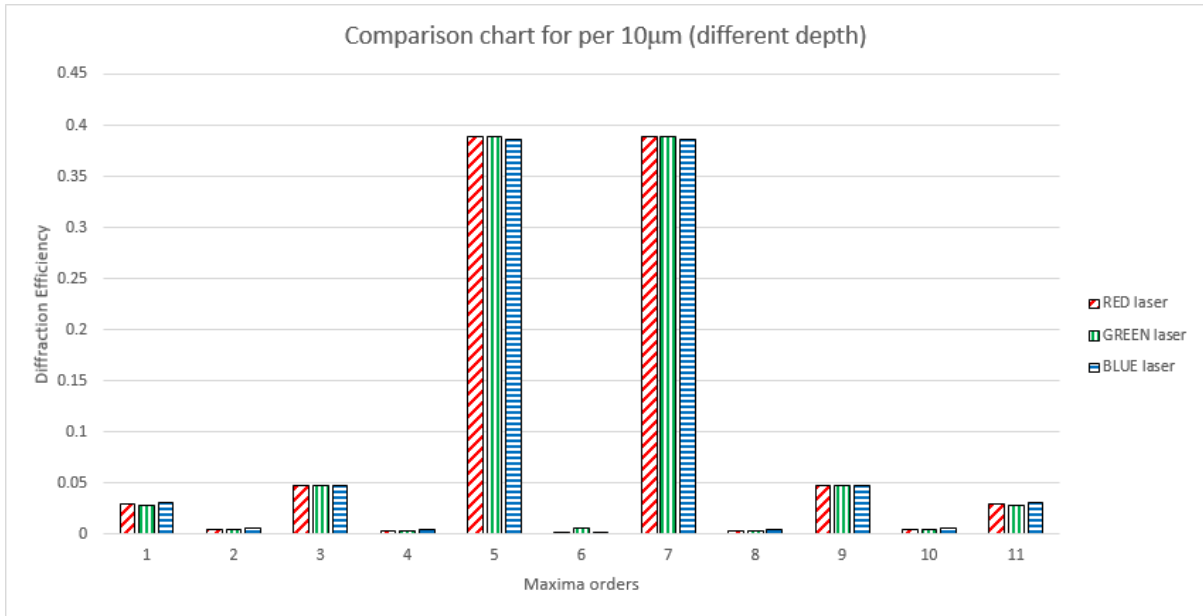


Figure 26 Comparison chart of Maxima orders verses Diffraction efficiency of three lasers for period 10µm of different depth 0.55nm, 0.45nm, and 0.40nm defining the highest diffraction efficiency.

Table 4 Comparison of three lasers with the Same depths

Lasers	Periods			Description
	4µm	5.6µm	10µm	
Depth of Red ($\lambda=0.633\text{nm}$)	0.55nm	0.55nm	0.55nm	Red helium laser with the highest peak of first maxima order -1T and +1T have better diffraction efficiency than the other two lasers
Depth of Blue ($\lambda=0.441\text{nm}$)	0.55nm	0.55nm	0.55nm	Blue laser with the lowest diffraction efficiency because of its lowest peak value of maxima -1T and +1T, when compared with the red and blue
Depth of Green ($\lambda=0.532\text{nm}$)	0.55nm	0.55nm	0.55nm	Green laser with the moderate peak level value of maxima -1T and +1T does not have the exact properties or diffraction efficiency of red but they do have a good Diffraction efficiency than blue

Table 5. comparison of three lasers with the different depths

Lasers	Periods			Description
	4 μ m	5.6 μ m	10 μ m	
Depth of Red ($\lambda=0.633$ nm)	0.55nm	0.55nm	0.55nm	Red laser has the peak value at this depth giving the best diffraction efficiency which is suitable for the polycarbonate material
Depth of Blue ($\lambda=0.441$ nm)	0.40nm	0.40nm	0.40nm	Blue laser has the highest peak at this depth which gives better diffraction efficiency but does not have same property of red laser which satisfies the polycarbonate material
Depth of Green ($\lambda=0.532$ nm)	0.45nm	0.45nm	0.45nm	Green laser has the lowest peak value than Red and Blue lasers, thus produce the lesser diffraction efficiency and lacking properties doesn't suit the polycarbonate material.

4. Manufacturing of periodical microstructure

4.1 Introduction

The fabrication part is a set of processes with various procedures involved. The Silicon material is structured into a periodic trapezoidal profile with the different periods like $4\mu\text{m}$, $5.6\mu\text{m}$, $10\mu\text{m}$ with respective depths from 0 to 2nm . Which further undergoes processes like Contact lithography process followed by Reactive ion etching in the SF_6/N_6 gas mixture plasma using Plasma etching equipment PK-2420RIE and UV Replicated process. At the end of the process, Electroplating is done to obtain the final product, the nickel structure.

4.2 Contact Lithography Process

Contact lithography process is a molding process where the trapezoidal Silicon material is covered with a thin film with which a Photoresist is placed, this photoresist helps the substrate to handle the physical parameters like Temperature, pressure, and time when the molding occurs. Imprinting or molding can be done in the form of UV rays, electrons, ions, and X-rays, thus forming the silicon and photoresist into rectangular groove called Lamella or laminar grating. The process is done with the help of Lloyd's mirror holographic lithography setup which is available in Kaunas university of technology. This machine can produce pattern structures with periods less than 500 nm, can be used for Diagnostic and measurement technologies, New materials for high-tech, Technologies for sustainable development and energy. The main usage of this equipment is for holographic lithography and microfabrication [7].

4.3 Reactive Ion Etching Process

Reactive ion etching process is an etching process which etches or removes the unwanted, deposited material from the substrate material silicon. Reactive ion etching (RIE) process will utilise mid-level RF power and mid-range pressure to connect both physical and chemical etching in this process, where the positive ions from plasma will bombard the wafer's surface where on the other side the radicals will get absorbed by the surface this produces high selectivity ratios and anisotropic profiles which is less than 3 microns wide (SF_6/N_6 gas mixture plasma). this plasma thus eliminates or etches the photoresist from the substrate, therefore, gives a final product of RIE with the help of RF reactive ion etching system with the technical specification of power 3kW, homogeneous etching area diameter 15 cm [6], as Lamella structured silicon which further undergoes UV Replication.

4.4 UV Replicated Process

UV light hardening Replication is done using a photopolymer called acrylic trimethylolpropane ethoxylate with a layer thickness of about $2\mu\text{m}$ and 3c m^2 of area, the test structure is produced because of UV replication by sandwiching the polymer replica material over silicon, UV-photopolymer stamping between the test structure and the substrate. After the UV exposure, the test structure was removed and the replica was left for post-polymerization, photopolymer for UV light hardening usually contains a mixture of binders, polymer, monomers, photo-initiators, and sensitizers. The polymer structure is finally removed and further used for electroplating process to obtain nickel.

4.5 Electroplating Process

In Electroplating the photopolymer was metallized with nickel where stamping is done using the electron beam evaporation with the substrate temperature as 20°C , residual gas pressure 10^{-4} Pa , deposition rate $v = 1\text{--}2\text{ nm/s}$, and finally nickel stamp was fabricated by using the electroplating process, electroplating based on nickel sulfonate ($\text{Ni}(\text{SO}_3\text{NH}_2)$) electrolyte and additives, following conditions with pH – 3.5-4.5, temperature 50°C , 23NHSONiOC , current density 4 mA/cm^2 . After electroplating process, the stamped nickel structure is removed from the photopolymer. The complete diagram of the Fabrication process of periodic microstructures, Nickel for testing of Hot imprint process is indicated below. The final nickel structure obtained from the process is shown below in fig 26.

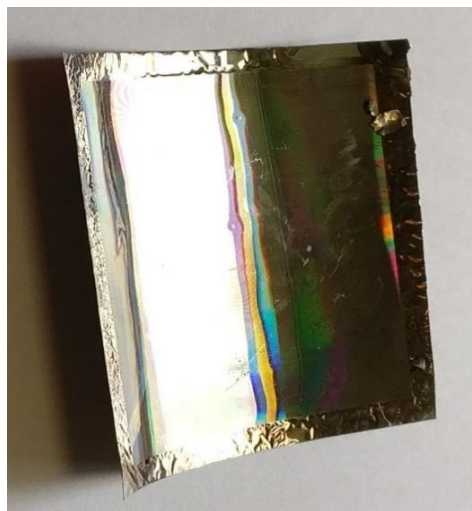


Figure 27 Periodical microstructure of Nickel before fabrication

This nickel is fabricated under silicon mold with the number of process that mold the nickel into lamellar shaped periodical microstructure further used for hot imprint process on the polycarbonate surface.

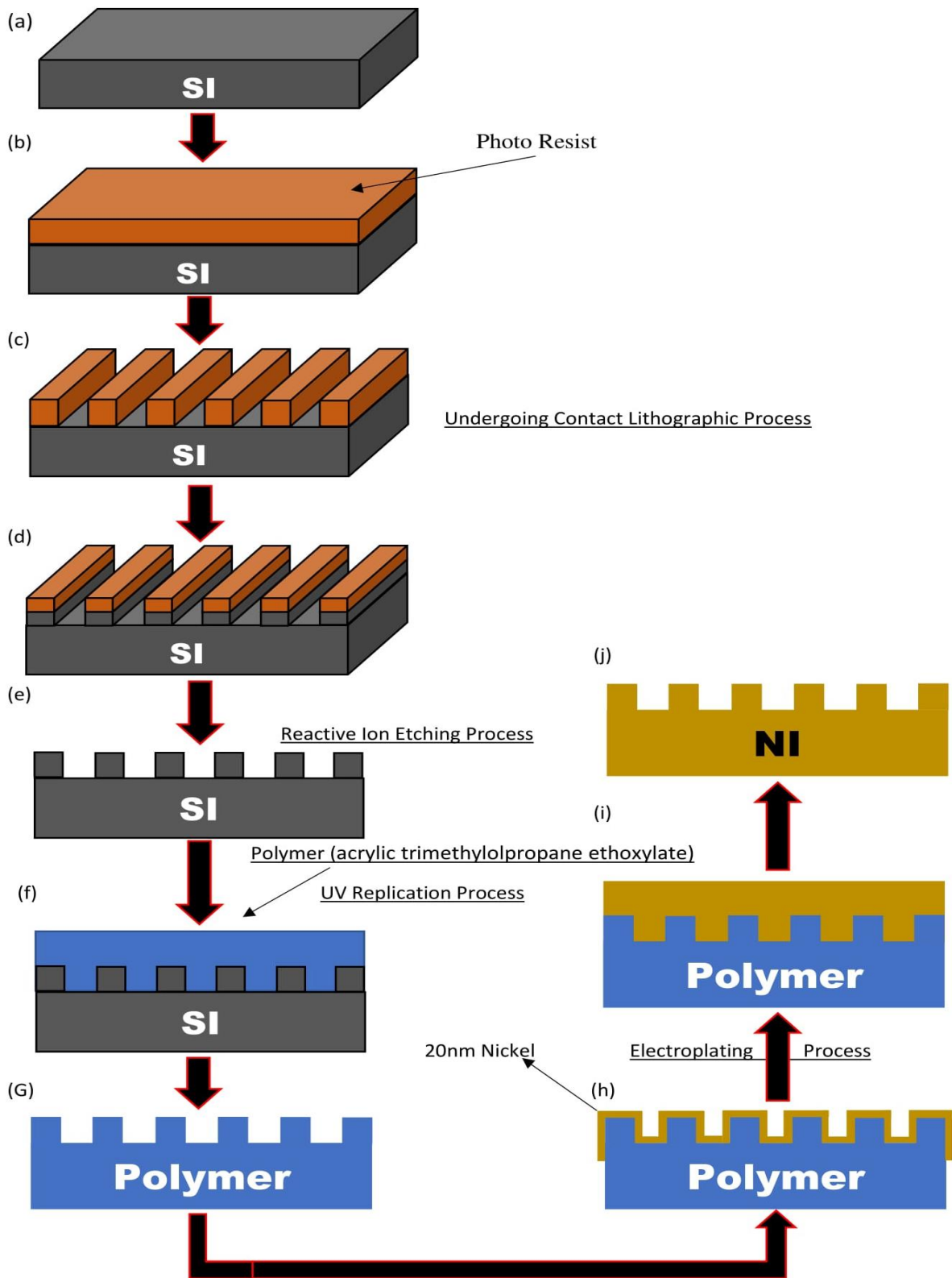


Figure 28 Fabrication Process of Nickel Periodical microstructure: Silicon(a), photo resist coated silicon slab (b), Contact lithographic process(c), post contact lithography process (d), Reactive Ion Etching process(e), UV Replication process(f) Polymer extraction(g), Electroplating process of Ni(h), Nickel mold(i), Extraction of Ni periodical microstructure(j).

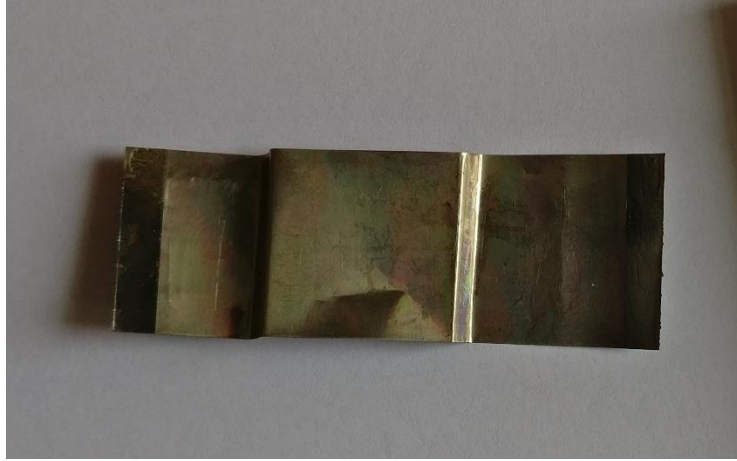


Figure 29 Final Nickel structure obtained after fabrication silicon mold to lamella shaped Nickel periodical microstructure.

4.6 Surface Explorer software analysis for Fabrication process

The fabrication process is done in AFM mode, Atomic Force of Microscopes are used for the analysis of the Materials, Analysis of polished fused silica substrates ruled gratings and Holographic gratings, they are usually used in the Photonics Industry. AFM otherwise known as Surface Explorer is used for measuring three dimension structures comprises depths and angle, image independent of optical properties, no samples such as coatings and cross sections, non-destructive in Atomic Force Microscopy

Holographic grating including heights is maintained to very high tolerances with high precision and accuracy. The results are generated into AFM with three different Periods and depths the fabrication results are generated for the period $4\mu\text{m}$, $5.6\mu\text{m}$, $10\mu\text{m}$. The 2D, 3D and the profile for the grating is as shown below with the following figures,

R_a is the average Roughness of the surface which is nothing but mean absolute profile seeing no difference amongst peaks and valleys. The average roughness can be the same for surfaces with roughness profile entirely unexpected because it depends just on the normal profile heights.

$$R_a = \frac{1}{L} \int_0^L |Z(x)| dx \quad (3)$$

Surfaces that have diverse undulations are not recognized and the points of interest include: simplicity of acquiring a similar average the roughness of less advanced instruments, for instance, a profilometer can give (R_a); the likelihood of a reiteration of the parameter, since it

seems exceptionally steady statistically, prescribed as a parameter for the portrayal of arbitrary surfaces, it is typically used to depict machined surfaces [13].

R_q is the root mean square of roughness (R_q) is a capacity that takes the square of the measures. The RMS roughness of a surface is like the roughness average, with the main contrast being the mean squared absolute values estimations of surface roughness profile.

$$R_q = \sqrt{\frac{1}{L} \int_0^L |Z^2(x)| dx} \quad (4)$$

The software does not need to be sophisticated to obtain R_q. For this reason, much of the surface analysis equipment (profilometer and SPMs) provides R_q. In SPM, the R_q depends on the swept area of the sample, the scan size. The R_q is more sensitive to peaks and valleys than the average roughness due to the squaring of the amplitude in its calculation [13].

4.6.1 AFM results for Period 4nm.

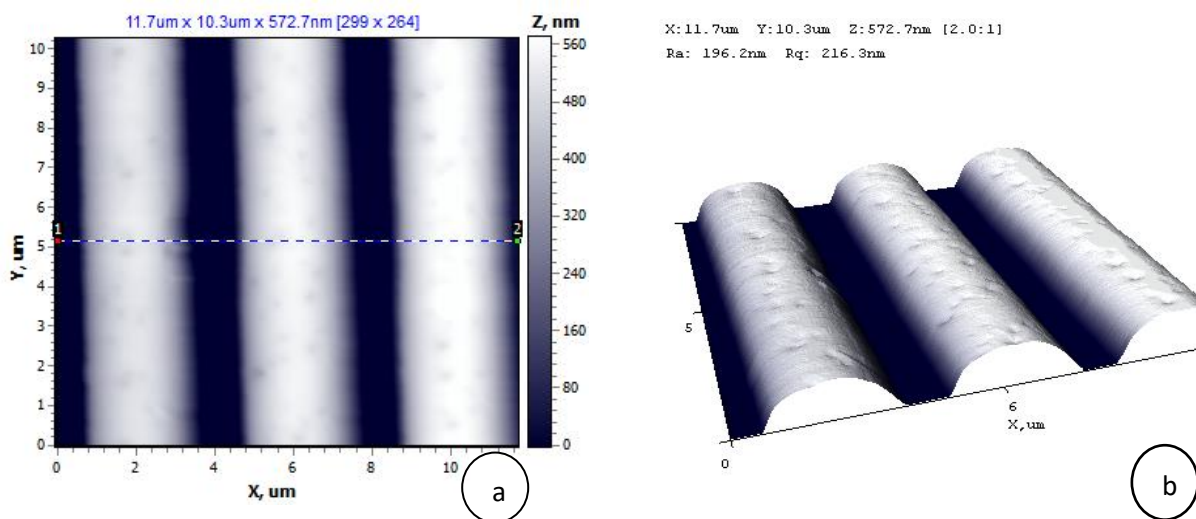


Figure 30 AFM images of Nickel periodic microstructure for period 4 μm using Surface Explorer; 2D image of Ni(a) and 3D image of Ni(b). With generated results of X; 11.7 μm, Y: 10.3 μm, Z: 572.7 nm with Ra: 196.2 nm and Rq: 216.3 nm.

The graph or the profile consists of the period 4 μm and depths of between 0 to 3 in which the best depths say 0.56 and parameters of X; 11.7 μm, Y: 10.3 μm, Z: 572.7 nm with R_a (Average roughness): 196.2 nm and R_q (Mean square roughness): 216.3 nm.

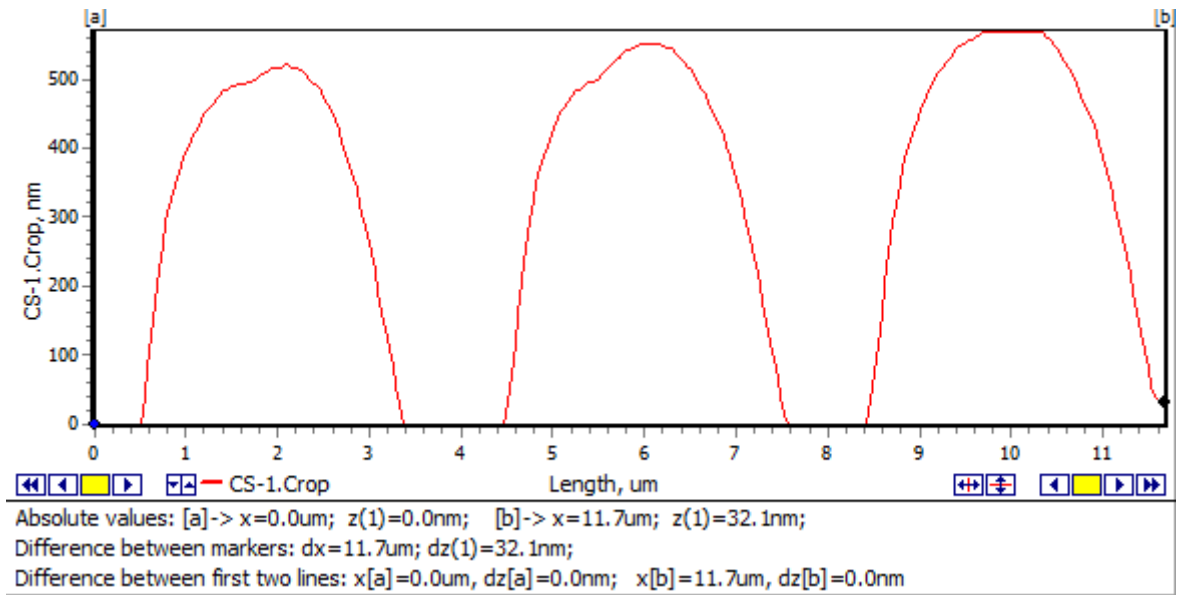


Figure 31 Profile of the Nickel periodical microstructure for the period $3.9\mu\text{m}$ with the depth of 572.7 nm , comprising a graph of Length(μm) vs Depth (CS-1, crop, nm)

4.6.2 AFM results for Period $5.6\mu\text{m}$

The AFM (Atomic Force Microscopy) image for the period $5.6\mu\text{m}$ is screened below the figure 2D, 3D image and the profile which is generated from the Surface Explorer with the X: $11.3\mu\text{m}$ and Y: $10.3\mu\text{m}$ and Z: 597.0nm , with R_a : 213.8nm and R_q : 230.1nm .

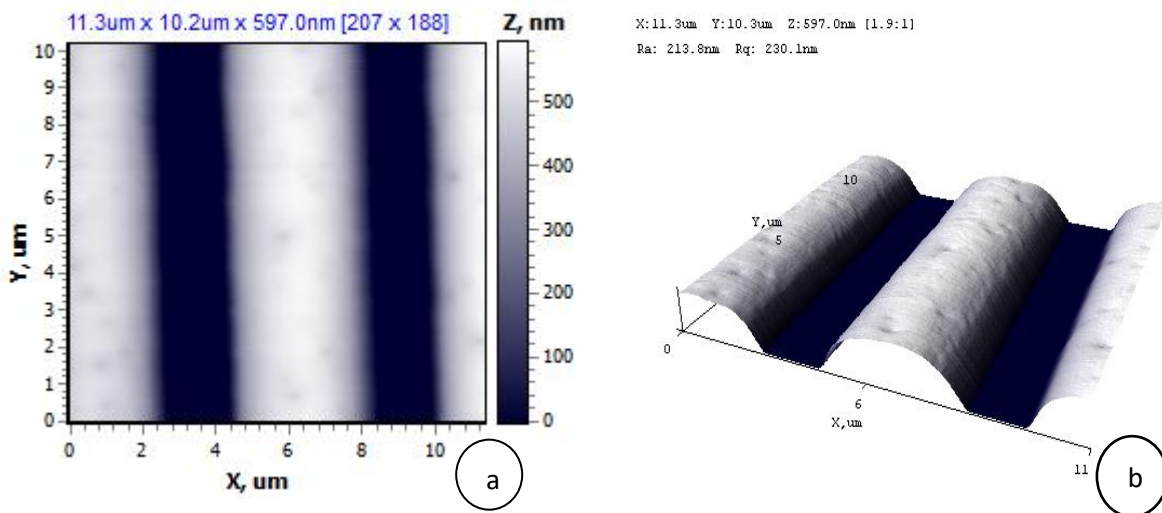


Figure 32 AFM images of Nickel periodic microstructure for period $5.6\mu\text{m}$ using Surface Explorer; 2D image of Ni(a) and 3D image of Ni(b). With generated results of X: $11.3\mu\text{m}$ and Y: $10.3\mu\text{m}$ and Z: 597.0nm , with R_a : 213.8nm and R_q : 230.1nm

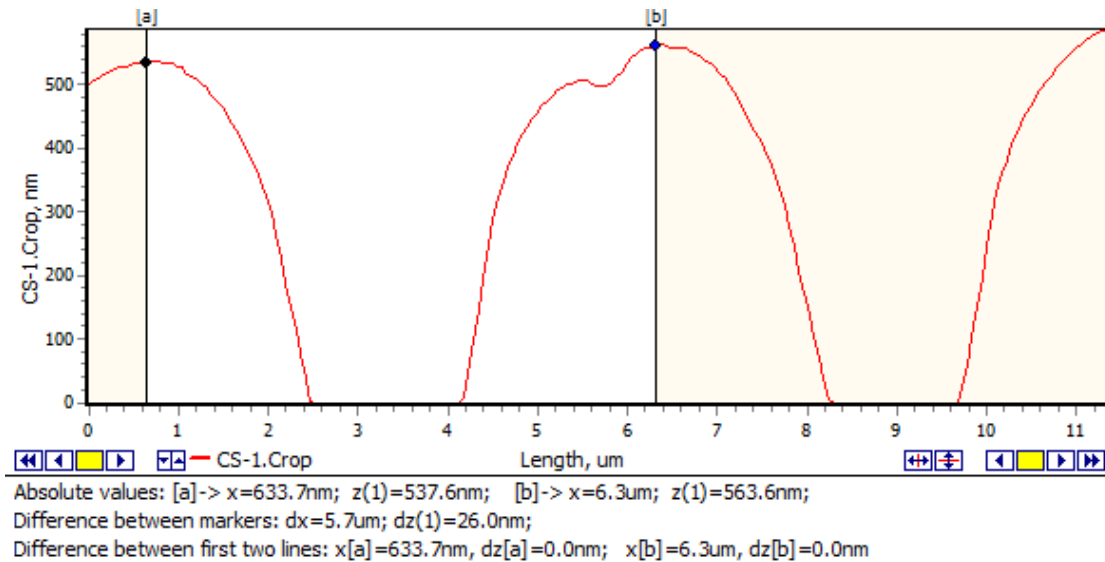


Figure 33 Profile of the Nickel periodical microstructure for the period $5.7\mu\text{m}$ with the depth of 597.6nm , comprising a graph of Length(μm) vs Depth (CS-1, crop, nm)

4.6.3 AFM Results for Period 10nm

The AFM image is for the period 10nm , 2D, 3D and profile image from the surface explorer is generated and shown in figure 8,9, and 10 below with the parameters X: $11.3\mu\text{m}$, Y: $10.3\mu\text{m}$, Z: 597.0nm and R_a (Average roughness): 213.8nm , R_q (Mean square roughness): 230.1nm

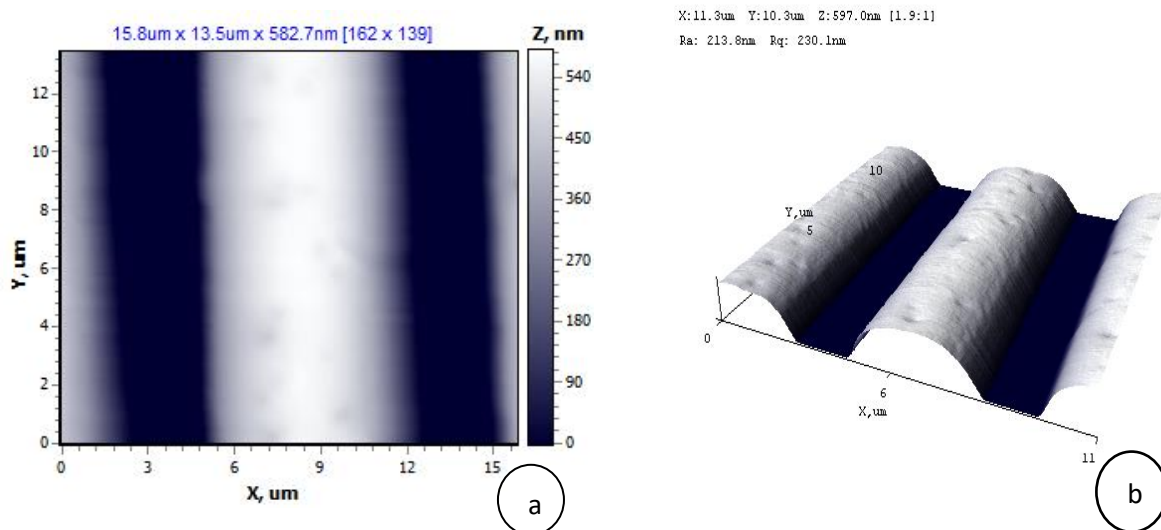


Figure 34 AFM images of Nickel periodical microstructure for period $10\mu\text{m}$ using Surface Explorer; 2D image of Ni(a) and 3D image of Ni(b). With generated results of X: $11.3\mu\text{m}$, Y: $10.3\mu\text{m}$, Z: 597.0nm and R_a (Average roughness): 213.8nm , R_q (Mean square roughness): 230.1nm

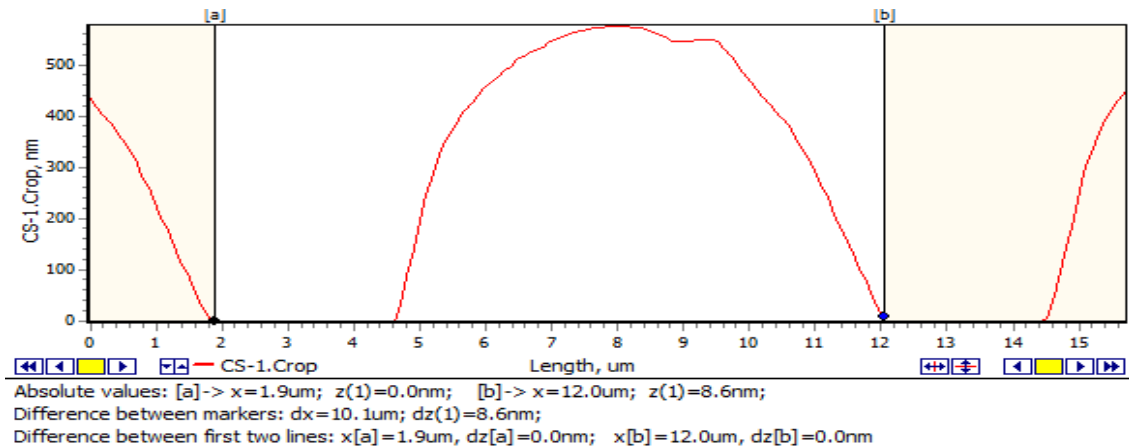


Figure 35 Profile of the Nickel periodical microstructure for the period $10.1\mu\text{m}$ with the depth of 582.7nm , comprising a graph of Length(μm) vs Depth (CS-1, crop, nm)

Therefore, the AFM results for the Nickel microstructure is analysed and further calculation is done to differentiate the errors between the theoretical measurements and Manufacturing measurements to spot the difference between them. The respective calculation is done using the percentage error formula between the theoretical measurements and Manufacturing measurements of the RED laser, depth error occurs because of the manufacturing defects including certain process and period error is caused by geometrical defects that happen in the G-solver analysis which is shown in Table 6.

Table 6 Percentage between Theoretical and Manufacturing Measurements

Theoretical Measurements (RED Laser)		Manufacturing Measurements (RED Laser)		Error Percentage	
Period	Depth	Period	Depth	% Error of Period	% Error of Depth
$4\mu\text{m}$	550nm	$3.9\mu\text{m}$	572.7nm	2.5%	4.1%
$5.6\mu\text{m}$	550nm	$5.7\mu\text{m}$	597.0nm	1.7%	8.5%
$10\mu\text{m}$	550nm	$10.1\mu\text{m}$	582.7nm	1%	5.9%

4.7. Thermal Replication process or Hot imprint process

The microstructure is created with few steps that are followed as mentioned above, final product Nickel is obtained from the fabrication process, the mechanical hot imprint

procedure is a complex innovative operation, considering materials state changes. The mechanical hot imprint procedure is performed with the help of a hydraulic press thus making Nickel imprints on the surface of the polycarbonate. Here high-frequency oscillations are used to increase the quality of the replicated microstructure. The schematic diagram of thermal replication or hot imprint process with the heating plate, Nickel master mold, polycarbonate structure and vibroactive pad is shown in figure 35.

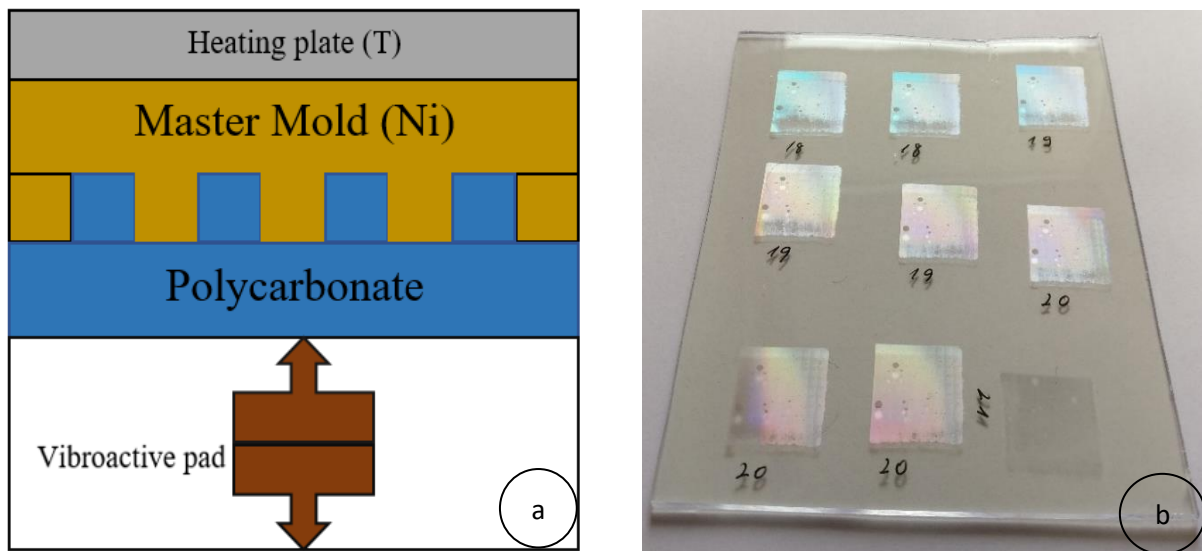


Figure 36. Thermal replication process of Polycarbonate(a), Thermal replicated Nickel imprints on the polycarbonate surface(b).

The heating process takes place in the heating plate (T) with the master mold. This master mold thus presses down the grating material making required patterns onto the softened material (polycarbonate) with the vibrating pad below. The heating plate presses the nickel mold on polycarbonate for time till 0.5s until the pressure touches nominal value and the nominal pressure attains the required time, were the piezoelectric material energizes high-frequency vibrations with the assistance of aluminium vibrating stage are being exchanged to the polycarbonate. The piezoelectric material and vibrating stage make one component called vibroactive pad. After making the imprints the mold is released. The fabricated material, Imprinted polycarbonate grating structure with the rainbow colours is shown in the above fig 35. The final grating structure, Polycarbonate with the Ni imprints can be used for many application, therefore its 1st order maxima are used with mirrors to excite the diffracted rays thus making more precise in properties and kind of usage. While using the periodic microstructure high amount of excitation produces the highest value of Diffraction Efficiency.

Conclusion

The Design and Fabrication of the periodic microstructure are done therefore with the set of procedures is followed to execute the prior conclusion of the project work.

1. The Depth of the periodical Microstructure of period $4\mu\text{m}$, $5.6\mu\text{m}$, $10\mu\text{m}$ for Red, blue, green lasers of corresponding wavelength $\lambda=0.633\text{nm}$, $\lambda=0.441\text{nm}$, $\lambda=0.532\text{nm}$ is generated using G-solver software, among which the Red laser produces the highest Diffraction Efficiency in depth of 550nm to 600nm in the First order maxima (-1T, 1T) having the highest peak value from the results and chart generated from the software.
2. The fabrication process of Periodical microstructure is executed with Contact Lithography, Ion etching process, UV replication process and Electroplating process. Master Nickel periodic microstructure analysis results are obtained through AFM images of 2D, 3D and profile of the Ni periodic microstructure is generated, finally Ni imprints are made on the surface of the Polycarbonate (Diffraction Grating).
3. Theoretical Measurements and obtained Manufacturing dimensions resulted a difference in corresponding period Error of 2.5%, 1.7%, 1% and Depth error of 4.1%, 8.5%, 5.9%. Manufacturing error from Contact lithographic process, Ion etching and UV replication process, and the Geometrical errors occur during obtained AFM (Atomic Force Microscopic) Image analysis. The grating improves the quality with reduced errors and obtain a higher Diffraction Efficiency. This grating structure can be used for research applications by the scientists of Kaunas University of technology and for furthermore applications apart.

References

1. Giedrius Janusas, E. C. (2015). Experimental and modeling means for analysis and replication periodical microstructures.
2. Li, J. L. (2008). Effect of Hot embossing process parameters on Hot polymer flow and micro channel accuracy produced without vacuum . *materials processing Technology*.
3. Yoshihiko, Y. n. (2003). Defect analysis in thermal nanoimprint Lithigraphy. *vacuum science technology* .
4. Narijauskaite, B., Palevicius, A., Janusas, G., & Sakalys, R. (2013). Numerical investigation of dynamical properties of vibroactive pad during hot imprint process,. *Vibroengineering*.
5. Goldfarb, M., & Celanovic, N. (1997). Modeling piezoelectric stack actuators for control of micromanipulation. *Control Systems*.
6. Figura, J. (2013). Modeling and control of piezoelectric microactuators.
7. A. Palevicius, G. J. (2015). Analysis of the Influence of High-Frequency Excitation Into Quality of the Replicated Microstructure. *Periodical Microstructure, Ultrasonic Thermal*.
8. Giedrius Janusas, E. C. (2015). Replication of Periodic Microstructures. 23-33.
9. David Fluckiger, P. (2012). G Solver Version 5.2 User's Guide and product design .
10. Lloyd's mirror holographic lithography setup.
<https://apcis.ktu.edu/MMI/en/site/katalogas?more=6733>
11. RF reactive ion etching system.
<https://apcis.ktu.edu/MMI/en/site/katalogas?more=6767>.
12. <http://dospehi.com.ua/Poleznaya-informatsiya/2015-09-09-15-56-28.html>
13. R.R.L. De Oliveira, D. A. (2012). Measurement of the Nanoscale Roughness by Atomic Force Microscopy, Basic Principles and Applications.
14. Rokas Šakalys, G. J. (2014). Quality Analysis of Periodical Microstructures, Created By Using High Frequency Vibration Excitation .
15. Agyapong, P. (2005). Diffraction Gratings: Theory and Applications.
16. Palmer, C. (2004). DIFFRACTION GRATING HANDBOOK. New York, USA: Newport Corporation.

Appendix

1. Calculation of Red laser or He-Ne laser for Period 4 μ m with the Diffraction orders

Depth	5T	4T	3T	2T	1T	0T	Sum T
0	0	0	0	0	0	0.948813	0.948813
0.05	0.000483	1.77E-06	0.000996	8.46E-07	0.00813	0.930493	0.949717
0.1	0.001927	1.93E-05	0.003884	9.09E-06	0.031822	0.875437	0.950759
0.15	0.003978	5.87E-05	0.008287	2.81E-05	0.068988	0.787165	0.949846
0.2	0.00606	0.000147	0.01374	7.78E-05	0.116471	0.675384	0.948377
0.25	0.008427	0.000404	0.020034	0.000234	0.170507	0.549874	0.949085
0.3	0.01196	0.000915	0.026898	0.000552	0.226713	0.417538	0.951618
0.35	0.016557	0.001532	0.033542	0.000966	0.280172	0.287277	0.952815
0.4	0.02084	0.002068	0.039139	0.001406	0.326273	0.172051	0.951502
0.45	0.024024	0.00273	0.043347	0.002036	0.361307	0.08304	0.949926
0.5	0.02663	0.003975	0.045954	0.003169	0.38236	0.025851	0.950027
0.55	0.029285	0.005951	0.046629	0.004954	0.387482	0.002812	0.951416
0.6	0.031687	0.008219	0.04524	0.007181	0.376223	0.015373	0.952473
0.65	0.033154	0.010303	0.042075	0.009553	0.349712	0.063039	0.952633
0.7	0.033613	0.012142	0.037465	0.011962	0.310188	0.14149	0.952227
0.75	0.033264	0.013764	0.031788	0.014419	0.26096	0.242842	0.951231
0.8	0.032381	0.015301	0.025627	0.01706	0.206228	0.356954	0.950146
0.85	0.031437	0.01717	0.019333	0.020091	0.150346	0.473462	0.950216
0.9	0.03034	0.019421	0.013048	0.023392	0.097737	0.583593	0.95147
0.95	0.028178	0.021291	0.007344	0.026375	0.053061	0.679825	0.952324
1	0.024427	0.021993	0.003112	0.028416	0.020508	0.754643	0.951556
1.05	0.020009	0.0218	0.000837	0.029301	0.00287	0.800324	0.949957
1.1	0.016473	0.021781	0.000454	0.029263	0.001437	0.810494	0.949309
1.15	0.013999	0.022169	0.001897	0.028581	0.016362	0.783874	0.949891
1.2	0.011538	0.022096	0.005158	0.027215	0.046615	0.725341	0.950585
1.25	0.008546	0.020929	0.010021	0.024896	0.0899	0.642055	0.950639
1.3	0.005574	0.019114	0.01617	0.021546	0.142786	0.539994	0.950374
1.35	0.003273	0.017527	0.02322	0.01757	0.200796	0.425481	0.950254
1.4	0.001672	0.016447	0.030385	0.013574	0.258775	0.308399	0.950107
1.45	0.000605	0.01569	0.036748	0.009898	0.311866	0.200209	0.949823
1.5	6.33E-05	0.015146	0.041958	0.00666	0.356071	0.109983	0.949779
1.55	7.29E-05	0.014934	0.046119	0.004104	0.387935	0.043926	0.950258
1.6	0.000585	0.015188	0.048988	0.002648	0.404491	0.007084	0.950883
1.65	0.001583	0.015833	0.049927	0.002598	0.404081	0.002957	0.951001
1.7	0.003073	0.016661	0.048729	0.00405	0.386917	0.031645	0.950507
1.75	0.004919	0.017573	0.045885	0.007	0.354659	0.089877	0.949949
1.8	0.006918	0.018753	0.041917	0.011333	0.309828	0.172412	0.949909
1.85	0.009066	0.020504	0.036855	0.016746	0.255841	0.272386	0.95041
1.9	0.011513	0.022857	0.030634	0.022818	0.197185	0.380943	0.950957
1.95	0.014196	0.025359	0.023736	0.029196	0.139039	0.488006	0.951059
2	0.016649	0.027367	0.017119	0.035494	0.086425	0.584582	0.950687
2.05	0.018477	0.02867	0.011523	0.040936	0.043673	0.663661	0.950218
2.1	0.019870457	0.02960365	0.007215886	0.044617338	0.014298629	0.718846929	0.95005884
2.15	0.021351975	0.030561873	0.004277859	0.046180525	0.000764363	0.744089312	0.95036250
2.20	0.023000124	0.031432787	0.002821538	0.04603113	0.004244495	0.735878425	0.95093857
2.25	0.024125031	0.031598067	0.002949517	0.044443726	0.024583957	0.69587649	0.95127708
2.30	0.02423446	0.030778685	0.004612191	0.041024994	0.060177745	0.629377689	0.95103383
2.35	0.023646153	0.029373517	0.007566766	0.035592831	0.107925525	0.542269833	0.95047941
2.4	0.022899191	0.027928712	0.011471012	0.028709894	0.163683	0.4408376	0.95022121
2.45	0.022079808	0.026585911	0.016002919	0.021311175	0.222876918	0.332847815	0.95056127
2.5	0.020893212	0.025062393	0.020864704	0.014174294	0.280753331	0.227633428	0.95112929

Recalculated values

Depth	5T	4T	3T	2T	1T	0T
0	0.000000	0.000000	0.000000	0.000000	0.000000	1.000000
0.05	0.000508	0.000002	0.001049	0.000001	0.008561	0.979759

0.1	0.002027	0.000020	0.004085	0.000010	0.033470	0.920776
0.15	0.004188	0.000062	0.008725	0.000030	0.072631	0.828728
0.2	0.006390	0.000155	0.014488	0.000082	0.122811	0.712147
0.25	0.008879	0.000426	0.021109	0.000246	0.179654	0.579373
0.3	0.012569	0.000962	0.028266	0.000580	0.238240	0.438767
0.35	0.017377	0.001608	0.035203	0.001014	0.294047	0.301504
0.4	0.021902	0.002174	0.041134	0.001478	0.342903	0.180820
0.45	0.025290	0.002873	0.045632	0.002143	0.380353	0.087417
0.5	0.028031	0.004184	0.048372	0.003336	0.402472	0.027211
0.55	0.030780	0.006255	0.049011	0.005207	0.407269	0.002956
0.6	0.033268	0.008629	0.047498	0.007540	0.394996	0.016140
0.65	0.034803	0.010815	0.044167	0.010028	0.367101	0.066173
0.7	0.035299	0.012751	0.039344	0.012562	0.325750	0.148589
0.75	0.034969	0.014469	0.033417	0.015158	0.274340	0.255293
0.8	0.034080	0.016103	0.026971	0.017955	0.217049	0.375684
0.85	0.033084	0.018070	0.020346	0.021143	0.158223	0.498268
0.9	0.031887	0.020411	0.013714	0.024585	0.102722	0.613360
0.95	0.029589	0.022356	0.007712	0.027696	0.055717	0.713860
1	0.025671	0.023113	0.003271	0.029863	0.021552	0.793062
1.05	0.021063	0.022948	0.000881	0.030844	0.003021	0.842484
1.1	0.017352	0.022944	0.000479	0.030826	0.001513	0.853772
1.15	0.014738	0.023338	0.001997	0.030089	0.017225	0.825226
1.2	0.012138	0.023244	0.005426	0.028630	0.049039	0.763046
1.25	0.008989	0.022016	0.010542	0.026189	0.094568	0.675393
1.3	0.005865	0.020112	0.017014	0.022671	0.150242	0.568191
1.35	0.003444	0.018445	0.024435	0.018490	0.211308	0.447755
1.4	0.001759	0.017311	0.031981	0.014287	0.272364	0.324594
1.45	0.000637	0.016519	0.038689	0.010421	0.328341	0.210786
1.5	0.000067	0.015947	0.044176	0.007012	0.374899	0.115798
1.55	0.000077	0.015716	0.048533	0.004319	0.408242	0.046225
1.6	0.000615	0.015973	0.051518	0.002785	0.425385	0.007450
1.65	0.001665	0.016648	0.052500	0.002732	0.424901	0.003110
1.7	0.003233	0.017529	0.051266	0.004261	0.407064	0.033293
1.75	0.005178	0.018499	0.048302	0.007369	0.373345	0.094613
1.8	0.007283	0.019742	0.044127	0.011931	0.326166	0.181503
1.85	0.009539	0.021574	0.038778	0.017620	0.269190	0.286598
1.9	0.012107	0.024036	0.032213	0.023995	0.207354	0.400589
1.95	0.014927	0.026664	0.024957	0.030699	0.146194	0.513118
2	0.017512	0.028786	0.018007	0.037335	0.090907	0.614905
2.05	0.019445	0.030172	0.012127	0.043080	0.045961	0.698430
2.10	0.020915	0.031160	0.007595	0.046963	0.015050	0.756634
2.15	0.022467	0.032158	0.004501	0.048593	0.000804	0.782953
2.20	0.024187	0.033054	0.002967	0.048406	0.004463	0.773844
2.25	0.025361	0.033216	0.003101	0.046720	0.025843	0.731518
2.30	0.025482	0.032363	0.004850	0.043137	0.063276	0.661783
2.35	0.024878	0.030904	0.007961	0.037447	0.113549	0.570522
2.40	0.024099	0.029392	0.012072	0.030214	0.172258	0.463932
2.45	0.023228	0.027969	0.016835	0.022420	0.234469	0.350159
2.50	0.021967	0.026350	0.021937	0.014903	0.295179	0.239330

2. Red laser or He-Ne laser For Period 5.6µm

Depth	5T	4T	3T	2T	1T	0T	Sum T
0	0	0	0	0	0	0.948812863	0.948812863
0.05	0.000386519	2.23E-06	0.000943709	1.36E-06	0.008087644	0.931003729	0.94984666
0.1	0.001557197	2.57E-05	0.003697955	1.55E-05	0.031671442	0.877354915	0.951290518
0.15	0.003306041	8.49E-05	0.00795753	5.12E-05	0.068714377	0.790652086	0.950880196
0.2	0.005320875	0.000201723	0.013314346	0.000126352	0.116085777	0.679406699	0.949504844
0.25	0.007848453	0.000451503	0.019534857	0.000293559	0.170000015	0.553259732	0.949516506
0.3	0.011395841	0.000860677	0.026325148	0.000568151	0.226099302	0.42037058	0.95086882
0.35	0.015660712	0.001337912	0.03297958	0.000892663	0.279553718	0.290594586	0.951443757
0.4	0.019704588	0.001899832	0.038719623	0.00129365	0.325736971	0.176087347	0.950796675
0.45	0.023267922	0.002762035	0.043167258	0.00193011	0.360881876	0.086440591	0.950458993

0.5	0.026802386	0.003971285	0.046175741	0.002845701	0.382193836	0.026992155	0.950970051
0.55	0.030401991	0.005208369	0.047544992	0.003838217	0.387909268	0.001490739	0.95129641
0.6	0.033599234	0.006187556	0.047141222	0.004714735	0.377556747	0.012536371	0.950935359
0.65	0.036274139	0.006948945	0.045030256	0.005487233	0.352015586	0.059341405	0.950853723
0.7	0.038555962	0.007541708	0.041342066	0.00620277	0.313351985	0.137397299	0.951386279
0.75	0.04014588	0.007933448	0.036332715	0.006879628	0.26477651	0.239402834	0.951539195
0.8	0.040763005	0.008225507	0.030432968	0.007575598	0.210364824	0.356238317	0.950962119
0.85	0.040542168	0.008441685	0.024029116	0.008234507	0.15454886	0.479011101	0.950603775
0.9	0.039377593	0.00827678	0.017497386	0.008585533	0.101909984	0.599638304	0.950932855
0.95	0.036821319	0.007485293	0.011429272	0.008419456	0.056965656	0.708849054	0.951091045
1	0.033160072	0.006342425	0.006464263	0.00786656	0.023547133	0.795748534	0.95050944
1.05	0.029647288	0.005368977	0.002894539	0.007247108	0.004272096	0.851380764	0.95024078
1.1	0.026631439	0.004735661	0.000749707	0.006701872	0.000599143	0.872050304	0.950885947
1.15	0.022995999	0.004358666	0.000136799	0.006186894	0.012893818	0.858100565	0.951244916
1.2	0.018123633	0.004270697	0.00117844	0.005705463	0.040213535	0.811358973	0.95034251
1.25	0.012984679	0.00468807	0.00380553	0.005393138	0.080292317	0.734970413	0.94929788
1.3	0.008674126	0.005867862	0.007762845	0.005401926	0.129746723	0.634836931	0.949743894
1.35	0.005341291	0.007907229	0.012594379	0.005807157	0.184248336	0.519330639	0.951127424
1.4	0.002888964	0.010612895	0.017718483	0.006625844	0.239083447	0.397654768	0.951514033
1.45	0.001389459	0.013724203	0.022828702	0.007855348	0.289977451	0.278932011	0.950482337
1.5	0.000805734	0.017255886	0.027967967	0.009485528	0.333178046	0.172261885	0.949648205
1.55	0.001257984	0.021166964	0.032923803	0.011466293	0.365050799	0.086370855	0.95010254
1.6	0.003264689	0.02488585	0.03700617	0.013695733	0.382529747	0.028278019	0.951042397
1.65	0.006956425	0.027846533	0.039640892	0.016093031	0.384042531	0.002159936	0.951318759
1.7	0.011604128	0.030357754	0.040728787	0.018672298	0.369616109	0.009118735	0.951076888
1.75	0.016646816	0.03296795	0.040327708	0.021383093	0.340477728	0.047400907	0.951007497
1.8	0.022384612	0.035222357	0.038470404	0.023861122	0.299028657	0.113216575	0.951150879
1.85	0.0290871	0.035934374	0.035357324	0.025540724	0.24885635	0.201558244	0.951109988
1.9	0.036164627	0.034641769	0.031420389	0.026100519	0.194282725	0.305719806	0.950939862
1.95	0.042919485	0.031994297	0.027035664	0.025718971	0.139763225	0.416234267	0.951097548
2	0.04915368	0.028787947	0.022415082	0.024805054	0.089619428	0.521947095	0.951509476
2.05	0.054746944	0.025490953	0.017695585	0.02360429	0.047822805	0.61296008	0.951681231
2.1	0.059392438	0.022237338	0.013011062	0.022078001	0.017783045	0.68242276	0.951426527
2.15	0.062590862	0.01896393	0.00863896	0.020061809	0.002109055	0.726311115	0.951040347
2.2	0.063826034	0.015731009	0.005009666	0.017515618	0.002190083	0.742348057	0.950892875
2.25	0.062911432	0.012884865	0.002490439	0.0146144	0.017884987	0.729429107	0.951001352
2.3	0.060490298	0.010963343	0.001196744	0.011724422	0.047635542	0.687178478	0.951199174
2.35	0.057638291	0.010411504	0.001053858	0.009320099	0.088863805	0.616810788	0.951385903
2.4	0.054194916	0.01138473	0.001992712	0.007752821	0.138313279	0.524109674	0.951386589
2.45	0.048887704	0.013771074	0.004006873	0.007144424	0.192192778	0.419098446	0.951104152
2.5	0.041410834	0.01723244	0.007057941	0.00749197	0.246159881	0.311995851	0.950701985

Recalculated values

Depth	5T	4T	3T	2T	1T	0T
0	0.000000	0.000000	0.000000	0.000000	0.000000	1.000000
0.05	0.000407	0.000002	0.000994	0.000001	0.008515	0.980162
0.1	0.001637	0.000027	0.003887	0.000016	0.033293	0.922279
0.15	0.003477	0.000089	0.008369	0.000054	0.072264	0.831495
0.2	0.005604	0.000212	0.014022	0.000133	0.122259	0.715538
0.25	0.008266	0.000476	0.020573	0.000309	0.179039	0.582675
0.3	0.011985	0.000905	0.027685	0.000598	0.237782	0.442091
0.35	0.016460	0.001406	0.034663	0.000938	0.293821	0.305425
0.4	0.020724	0.001998	0.040723	0.001361	0.342594	0.185200
0.45	0.024481	0.002906	0.045417	0.002031	0.379692	0.090946
0.5	0.028184	0.004176	0.048556	0.002992	0.401899	0.028384
0.55	0.031958	0.005475	0.049979	0.004035	0.407769	0.001567
0.6	0.035333	0.006507	0.049574	0.004958	0.397037	0.013183
0.65	0.038149	0.007308	0.047358	0.005771	0.370210	0.062409
0.7	0.040526	0.007927	0.043455	0.006520	0.329364	0.144418
0.75	0.042190	0.008337	0.038183	0.007230	0.278261	0.251595
0.8	0.042865	0.008650	0.032002	0.007966	0.221213	0.374608
0.85	0.042649	0.008880	0.025278	0.008662	0.162580	0.503902

0.9	0.041409	0.008704	0.018400	0.009029	0.107168	0.630579
0.95	0.038715	0.007870	0.012017	0.008852	0.059895	0.745301
1	0.034887	0.006673	0.006801	0.008276	0.024773	0.837181
1.05	0.031200	0.005650	0.003046	0.007627	0.004496	0.895963
1.1	0.028007	0.004980	0.000788	0.007048	0.000630	0.917092
1.15	0.024175	0.004582	0.000144	0.006504	0.013555	0.902082
1.2	0.019071	0.004494	0.001240	0.006004	0.042315	0.853754
1.25	0.013678	0.004938	0.004009	0.005681	0.084581	0.774225
1.3	0.009133	0.006178	0.008174	0.005688	0.136612	0.668430
1.35	0.005616	0.008314	0.013242	0.006106	0.193716	0.546016
1.4	0.003036	0.011154	0.018621	0.006963	0.251266	0.417918
1.45	0.001462	0.014439	0.024018	0.008265	0.305085	0.293464
1.5	0.000848	0.018171	0.029451	0.009988	0.350844	0.181395
1.55	0.001324	0.022279	0.034653	0.012068	0.384223	0.090907
1.6	0.003433	0.026167	0.038911	0.014401	0.402222	0.029734
1.65	0.007312	0.029272	0.041669	0.016917	0.403695	0.002270
1.7	0.012201	0.031919	0.042824	0.019633	0.388629	0.009588
1.75	0.017504	0.034666	0.042405	0.022485	0.358018	0.049843
1.8	0.023534	0.037031	0.040446	0.025087	0.314386	0.119031
1.85	0.030582	0.037782	0.037175	0.026854	0.261648	0.211919
1.9	0.038030	0.036429	0.033041	0.027447	0.204306	0.321492
1.95	0.045126	0.033639	0.028426	0.027041	0.146949	0.437636
2	0.051659	0.030255	0.023557	0.026069	0.094187	0.548546
2.05	0.057527	0.026785	0.018594	0.024803	0.050251	0.644081
2.1	0.062425	0.023373	0.013675	0.023205	0.018691	0.717263
2.15	0.065813	0.019940	0.009084	0.021095	0.002218	0.763702
2.2	0.067122	0.016543	0.005268	0.018420	0.002303	0.780685
2.25	0.066153	0.013549	0.002619	0.015367	0.018806	0.767012
2.3	0.063594	0.011526	0.001258	0.012326	0.050079	0.722434
2.35	0.060584	0.010944	0.001108	0.009796	0.093405	0.648329
2.4	0.056964	0.011966	0.002095	0.008149	0.145381	0.550890
2.45	0.051401	0.014479	0.004213	0.007512	0.202073	0.440644
2.5	0.043558	0.018126	0.007424	0.007880	0.258924	0.328174

3. Red laser or He-Ne laser for Period 10 μ m.

Depth	5T	4T	3T	2T	1T	0T	Sum T
0	0	0	0	0	0	0.948812863	0.948812863
0.05	0.000344698	2.37E-06	0.000910976	1.68E-06	0.008057874	0.931302576	0.94993778
0.1	0.00139581	2.78E-05	0.003582749	1.97E-05	0.031567737	0.878471126	0.951658597
0.15	0.003008162	9.36E-05	0.007755183	6.63E-05	0.068530943	0.792665038	0.951573244
0.2	0.004965707	0.000217424	0.013049141	0.000155498	0.11583362	0.681756833	0.950199613
0.25	0.007471715	0.000454889	0.019198055	0.000328511	0.169662303	0.555433366	0.94966431
0.3	0.010835729	0.000827234	0.025883187	0.000598842	0.225660937	0.422643748	0.950255606
0.35	0.014719919	0.00131207	0.032464963	0.000949833	0.279069202	0.293640391	0.950672365
0.4	0.018509199	0.001996331	0.038264396	0.001448692	0.325319381	0.179690106	0.950766101
0.45	0.022186601	0.002977643	0.042930053	0.002170189	0.360650709	0.089329799	0.951160189
0.5	0.025976555	0.004090017	0.046251675	0.002994559	0.382241515	0.028241191	0.951349833
0.55	0.029630724	0.005069813	0.047947921	0.003728828	0.38828032	0.001190073	0.950505285
0.6	0.03291422	0.00593096	0.047890686	0.004378543	0.378272531	0.010750848	0.949524729
0.65	0.036137448	0.006770766	0.046196137	0.005014873	0.353117073	0.055609399	0.950081992
0.7	0.039237099	0.007459176	0.042950367	0.005558287	0.314852754	0.131573124	0.951688489
0.75	0.041365105	0.007862641	0.038241361	0.005916433	0.266554457	0.232206391	0.952086384
0.8	0.042130264	0.007996272	0.032436894	0.006073906	0.212251158	0.348969664	0.950746653
0.85	0.042079043	0.007722857	0.026087345	0.005913084	0.156503939	0.473022556	0.949635091
0.9	0.041447429	0.006821234	0.019661615	0.005287325	0.103912026	0.595723269	0.949982527
0.95	0.039867817	0.005454364	0.013592418	0.004317183	0.058804393	0.706722088	0.950794437
1	0.037510005	0.004057988	0.008340831	0.003297538	0.024893613	0.79488087	0.951080819
1.05	0.034865983	0.002762289	0.004228352	0.002323779	0.004893708	0.853030291	0.951178512
1.1	0.031514141	0.001505947	0.001432319	0.001362724	0.0003829	0.87876724	0.951163306
1.15	0.026850639	0.0004855	0.000139562	0.000540842	0.01173802	0.870918453	0.95042758
1.2	0.021503551	1.24E-05	0.000460257	7.90E-05	0.037975158	0.829236193	0.949296986
1.25	0.01660884	0.00027249	0.002280059	0.00013896	0.076789263	0.757299633	0.949478858

1.3	0.012342789	0.001490739	0.005345591	0.000883261	0.124856203	0.661465725	0.951302891
1.35	0.008382957	0.003800373	0.009377144	0.002399881	0.178148068	0.548232581	0.952449428
1.4	0.004905453	0.006988733	0.014064713	0.004588643	0.232259311	0.425539208	0.951152914
1.45	0.002297423	0.010937856	0.01908376	0.007406288	0.282769277	0.304153317	0.949142524
1.5	0.000749945	0.015876563	0.024094817	0.010980333	0.325500974	0.194646064	0.949051327
1.55	0.000620644	0.0216969	0.028643196	0.0152444	0.356765229	0.104762957	0.950703695
1.6	0.002199365	0.027761928	0.032196874	0.01983616	0.373801848	0.040284194	0.951876546
1.65	0.005126694	0.033713903	0.034440235	0.024477717	0.375237815	0.005623079	0.951615806
1.7	0.00908611	0.039419761	0.035410999	0.028932448	0.361161714	0.002804695	0.95082676
1.75	0.014486789	0.044159915	0.03523536	0.032674531	0.332875792	0.031422272	0.950287048
1.8	0.021533001	0.047122875	0.033927112	0.035230088	0.29271778	0.088866065	0.949927777
1.85	0.029610425	0.048519028	0.031505502	0.036733207	0.243954063	0.169422855	0.950067306
1.9	0.038215717	0.048895835	0.028105836	0.03749512	0.190554652	0.264701283	0.951235603
1.95	0.047077371	0.047872968	0.023947766	0.037237691	0.136909918	0.3663226	0.952414026
2	0.055406476	0.044769528	0.019341914	0.035401812	0.087503819	0.467059344	0.951906439
2.05	0.06247854	0.039771582	0.014696008	0.031958103	0.046480337	0.559295179	0.950064319
2.1	0.068660453	0.033493572	0.010414048	0.027340668	0.017214375	0.634941328	0.94918756
2.15	0.074334394	0.026322247	0.006783457	0.021974509	0.002022928	0.687434508	0.950309579
2.2	0.078626569	0.018936653	0.00396284	0.016377903	0.002013442	0.712077836	0.951912649
2.25	0.080533973	0.012288149	0.00203583	0.011164756	0.017073413	0.705998023	0.952190264
2.3	0.080096232	0.006772877	0.001060495	0.006641552	0.045925363	0.670263391	0.95125643
2.35	0.077382095	0.002540279	0.001059549	0.002956738	0.086127775	0.610163787	0.950296658
2.4	0.072090634	0.000225121	0.00196508	0.000575292	0.134184068	0.531774347	0.949854737
2.45	0.06486289	0.000475937	0.003597889	7.94E-05	0.185903913	0.44012557	0.949965683
2.5	0.057189738	0.003414088	0.005710127	0.001707165	0.236838244	0.341197181	0.950915904

Recalculated values

Depth	5T	4T	3T	2T	1T	0T
0	0.000000	0.000000	0.000000	0.000000	0.000000	1.000000
0.05	0.000363	0.000002	0.000959	0.000002	0.008483	0.980383
0.1	0.001467	0.000029	0.003765	0.000021	0.033171	0.923095
0.15	0.003161	0.000098	0.008150	0.000070	0.072019	0.833005
0.2	0.005226	0.000229	0.013733	0.000164	0.121905	0.717488
0.25	0.007868	0.000479	0.020216	0.000346	0.178655	0.584873
0.3	0.011403	0.000871	0.027238	0.000630	0.237474	0.444768
0.35	0.015484	0.001380	0.034149	0.000999	0.293549	0.308877
0.4	0.019468	0.002100	0.040246	0.001524	0.342166	0.188995
0.45	0.023326	0.003131	0.045134	0.002282	0.379169	0.093917
0.5	0.027305	0.004299	0.048617	0.003148	0.401789	0.029685
0.55	0.031174	0.005334	0.050445	0.003923	0.408499	0.001252
0.6	0.034664	0.006246	0.050436	0.004611	0.398381	0.011322
0.65	0.038036	0.007127	0.048623	0.005278	0.371670	0.058531
0.7	0.041229	0.007838	0.045131	0.005840	0.330836	0.138252
0.75	0.043447	0.008258	0.040166	0.006214	0.279969	0.243892
0.8	0.044313	0.008411	0.034117	0.006389	0.223247	0.367048
0.85	0.044311	0.008132	0.027471	0.006227	0.164804	0.498110
0.9	0.043630	0.007180	0.020697	0.005566	0.109383	0.627089
0.95	0.041931	0.005737	0.014296	0.004541	0.061848	0.743296
1	0.039439	0.004267	0.008770	0.003467	0.026174	0.835766
1.05	0.036656	0.002904	0.004445	0.002443	0.005145	0.896814
1.1	0.033132	0.001583	0.001506	0.001433	0.000403	0.923887
1.15	0.028251	0.000511	0.000147	0.000569	0.012350	0.916344
1.2	0.022652	0.000013	0.000485	0.000083	0.040003	0.873527
1.25	0.017493	0.000287	0.002401	0.000146	0.080875	0.797595
1.3	0.012975	0.001567	0.005619	0.000928	0.131248	0.695326
1.35	0.008801	0.003990	0.009845	0.002520	0.187042	0.575603
1.4	0.005157	0.007348	0.014787	0.004824	0.244187	0.447393
1.45	0.002421	0.011524	0.020106	0.007803	0.297921	0.320451
1.5	0.000790	0.016729	0.025388	0.011570	0.342975	0.205095
1.55	0.000653	0.022822	0.030128	0.016035	0.375264	0.110195
1.6	0.002311	0.029165	0.033825	0.020839	0.392700	0.042321
1.65	0.005387	0.035428	0.036191	0.025722	0.394317	0.005909

1.7	0.009556	0.041458	0.037242	0.030429	0.379840	0.002950
1.75	0.015245	0.046470	0.037079	0.034384	0.350290	0.033066
1.8	0.022668	0.049607	0.035715	0.037087	0.308147	0.093550
1.85	0.031167	0.051069	0.033161	0.038664	0.256776	0.178327
1.9	0.040175	0.051402	0.029547	0.039417	0.200323	0.278271
1.95	0.049430	0.050265	0.025144	0.039098	0.143750	0.384625
2	0.058206	0.047031	0.020319	0.037190	0.091925	0.490657
2.05	0.065762	0.041862	0.015468	0.033638	0.048923	0.588692
2.1	0.072336	0.035287	0.010972	0.028804	0.018136	0.668931
2.15	0.078221	0.027699	0.007138	0.023124	0.002129	0.723380
2.2	0.082599	0.019893	0.004163	0.017205	0.002115	0.748050
2.25	0.084578	0.012905	0.002138	0.011725	0.017931	0.741446
2.3	0.084200	0.007120	0.001115	0.006982	0.048279	0.704609
2.35	0.081429	0.002673	0.001115	0.003111	0.090633	0.642077
2.4	0.075896	0.000237	0.002069	0.000606	0.141268	0.559848
2.45	0.068279	0.000501	0.003787	0.000084	0.195695	0.463307
2.5	0.060142	0.003590	0.006005	0.001795	0.249063	0.358809

4. Blue laser or Helium-Cadmium laser for period 4µm

Depth	5T	4T	3T	2T	1T	0T	Sum T
0	0	0	0	0	0	0.948812863	0.948812863
0.05	0.000796056	8.47E-06	0.00192733	5.19E-06	0.016535895	0.912070149	0.950616014
0.1	0.003038458	7.57E-05	0.007323437	4.61E-05	0.06325855	0.803603652	0.951088279
0.15	0.005983993	0.000261915	0.015113605	0.000167748	0.132064582	0.642156822	0.949340509
0.2	0.010345544	0.000742206	0.024519093	0.000491723	0.211623697	0.455034967	0.950479493
0.25	0.016348354	0.001422639	0.034044423	0.000956047	0.288338893	0.269105089	0.951325802
0.3	0.021842901	0.002391173	0.041584024	0.001656484	0.348739652	0.118071277	0.950499744
0.35	0.026939047	0.004040068	0.046289492	0.002894705	0.382829231	0.025051923	0.951037009
0.4	0.032008424	0.005680532	0.047624375	0.004234138	0.384932326	0.00212753	0.951087118
0.45	0.036111348	0.006827955	0.045367393	0.005331	0.354716663	0.054036999	0.950745717
0.5	0.039372662	0.007619716	0.039851737	0.006297793	0.297235921	0.170802756	0.951558413
0.55	0.040931294	0.008054289	0.031902348	0.007205621	0.222260556	0.330430132	0.951138347
0.6	0.040612882	0.008255454	0.022730954	0.008001587	0.142452299	0.506472509	0.950578862
0.65	0.038127424	0.007487265	0.013577034	0.008021145	0.071291593	0.67404239	0.951051311
0.7	0.033187962	0.005815979	0.006217975	0.007181243	0.021186168	0.803281107	0.950459761
0.75	0.02852702	0.004507464	0.001659079	0.006264604	0.000345388	0.868008361	0.950615471
0.8	0.023526355	0.003793253	0.000122423	0.005478813	0.012110139	0.861190181	0.951252146
0.85	0.016266456	0.003772272	0.001943217	0.004849627	0.054669695	0.786719614	0.94972215
0.9	0.009533752	0.005087745	0.00680989	0.004788978	0.120743531	0.655665205	0.949592998
0.95	0.004758822	0.008175875	0.013610387	0.005594785	0.198655534	0.48993185	0.951522656
1	0.00181518	0.012527359	0.020882328	0.007307185	0.274912474	0.315958157	0.950847208
1.05	0.000797225	0.017776504	0.028237486	0.009891442	0.337633323	0.160889765	0.949561723
1.1	0.002205581	0.023641527	0.034943619	0.0131915	0.376119053	0.050474437	0.950676996
1.15	0.007100909	0.028459074	0.039125616	0.01689085	0.382989177	0.002224113	0.951355363
1.2	0.013957736	0.032518817	0.040162095	0.020912011	0.35730697	0.021352222	0.951067481
1.25	0.021988357	0.036249557	0.038204417	0.024718961	0.303543687	0.101715397	0.951125354
1.3	0.031954134	0.036795206	0.03375283	0.026771274	0.231126104	0.230121914	0.95092101
1.35	0.042228753	0.033614187	0.02790878	0.026541045	0.152581032	0.385270329	0.951017924
1.4	0.051615261	0.028914204	0.021396683	0.025051548	0.080769687	0.53622652	0.951721286
1.45	0.059434017	0.023899408	0.014653244	0.022861578	0.027419419	0.65504215	0.951577482
1.5	0.064434334	0.018670641	0.008339139	0.019609311	0.001665285	0.725450895	0.950888315
1.55	0.065404265	0.013533029	0.003618614	0.015278833	0.008039449	0.739133751	0.95088213
1.6	0.062657529	0.009890176	0.001273811	0.010771138	0.044907787	0.692284471	0.951285351
1.65	0.058608312	0.00917591	0.001235287	0.007473402	0.105639429	0.587258872	0.951523552
1.7	0.051845062	0.011721633	0.003368604	0.006205417	0.180475535	0.443877121	0.951109623
1.75	0.040643902	0.016924607	0.00757979	0.007109242	0.257159219	0.291635726	0.950469244
1.8	0.029159021	0.024026828	0.013200181	0.010095548	0.32178804	0.154274034	0.95081327
1.85	0.019808059	0.03288248	0.018853454	0.015000597	0.362555084	0.053421804	0.951621153
1.9	0.011684763	0.042287991	0.023898306	0.021213335	0.373756966	0.00551828	0.951201001
1.95	0.005690762	0.050109944	0.028662403	0.027106466	0.354313126	0.01861875	0.95038415
2	0.00334605	0.054966669	0.032492021	0.031787961	0.306961306	0.091723681	0.950831697
2.05	0.005518134	0.055977303	0.034548039	0.035435298	0.239545699	0.209577539	0.951626486

2.1	0.011240644	0.054148566	0.034552422	0.037055198	0.163029164	0.351241008	0.951292993
2.15	0.019564145	0.050404606	0.031916119	0.035608674	0.090348481	0.49502568	0.950709729
2.2	0.031390634	0.043126905	0.027137294	0.031203432	0.034428009	0.6164334	0.951005947
2.25	0.044437074	0.032971759	0.021847656	0.024218533	0.004326966	0.695930485	0.951534459
2.3	0.056037616	0.0235736	0.016563917	0.016519105	0.004370142	0.717448479	0.95157724
2.35	0.06696918	0.016383057	0.010978042	0.009946677	0.03459631	0.673476951	0.951223484
2.4	0.075476554	0.011183678	0.005660368	0.004639934	0.090195302	0.576786095	0.95109777
2.45	0.079099048	0.008741559	0.001914884	0.00134267	0.161022903	0.447342926	0.951585053
2.5	0.078937752	0.00961926	0.000573608	0.001176757	0.234128874	0.303141017	0.952013518

Recalculated Values for Period 4 μ m

Depth	5T	4T	3T	2T	1T	0T
0	0	0	0	0	0	1
0.05	0.00083741	8.9071E-06	0.002027453	5.45456E-06	0.017394926	0.959451698
0.1	0.003194717	7.96152E-05	0.00770006	4.85204E-05	0.066511754	0.844930665
0.15	0.006303316	0.000275891	0.01592011	0.0001767	0.139111921	0.676424124
0.2	0.010884553	0.000780875	0.025796552	0.000517342	0.222649409	0.47874254
0.25	0.017184811	0.001495428	0.035786292	0.001004962	0.303091635	0.282873742
0.3	0.022980439	0.002515701	0.043749642	0.00174275	0.366901363	0.124220209
0.35	0.028325971	0.004248066	0.04867265	0.003043736	0.402538731	0.026341691
0.4	0.033654565	0.005972672	0.05007362	0.004451893	0.404728777	0.002236945
0.45	0.037982131	0.007181684	0.047717693	0.005607177	0.373093096	0.056836437
0.5	0.041377031	0.008007618	0.041880495	0.006618398	0.312367498	0.17949792
0.55	0.043034006	0.008468052	0.033541227	0.007575786	0.233678472	0.34740491
0.6	0.042724369	0.00868466	0.023912749	0.008417594	0.149858475	0.532804304
0.65	0.040089766	0.007872619	0.014275817	0.008433977	0.074960827	0.70873399
0.7	0.034917798	0.006119122	0.00654207	0.007555547	0.022290441	0.845150042
0.75	0.030009	0.004741627	0.001745268	0.006590051	0.000363331	0.913101446
0.8	0.024731986	0.003987642	0.000128697	0.00575958	0.012730735	0.905322721
0.85	0.017127595	0.003971975	0.00204609	0.005106364	0.057563884	0.828368185
0.9	0.01003983	0.005357816	0.007171378	0.00504319	0.127152929	0.690469713
0.95	0.005001271	0.008592412	0.014303797	0.005879823	0.208776462	0.514892469
1	0.001909013	0.013174944	0.021961813	0.00768492	0.289123712	0.332291197
1.05	0.000839571	0.018720746	0.029737388	0.01041685	0.355567537	0.169435816
1.1	0.00232001	0.024868096	0.036756563	0.013875901	0.395632854	0.053093151
1.15	0.007463992	0.029914241	0.041126185	0.017754511	0.402572153	0.002337836
1.2	0.014675863	0.034191914	0.042228439	0.021987936	0.37569045	0.022450796
1.25	0.023118254	0.038112281	0.040167594	0.025989173	0.319141621	0.106942157
1.3	0.033603353	0.038694283	0.035494882	0.028152994	0.243054998	0.241998979
1.35	0.044403741	0.035345482	0.029346218	0.027908039	0.160439702	0.405113636
1.4	0.054233589	0.030380958	0.02248209	0.026322358	0.084866954	0.563428104
1.45	0.062458411	0.025115567	0.015398897	0.024024925	0.0288147	0.688375001
1.5	0.067762252	0.019634946	0.008769841	0.020622097	0.001751294	0.762919139
1.55	0.068782726	0.014232078	0.003805533	0.016068062	0.008454727	0.777313747
1.6	0.065866177	0.010396644	0.001339042	0.01132272	0.047207482	0.727735868
1.65	0.061594179	0.009643387	0.00129822	0.007854142	0.11102135	0.617177442
1.7	0.05451008	0.012324166	0.003541762	0.006524397	0.189752612	0.466693965
1.75	0.042761933	0.01780658	0.007974787	0.007479718	0.270560274	0.306833417
1.8	0.030667452	0.025269765	0.013883043	0.010617803	0.338434528	0.162254818
1.85	0.020815068	0.034554171	0.019811932	0.015763203	0.380986785	0.05613768
1.9	0.01228422	0.044457471	0.025124349	0.022301633	0.392931637	0.005801381
1.95	0.005987854	0.052725989	0.030158755	0.028521589	0.372810432	0.019590762
2	0.003519077	0.057809042	0.034172211	0.033431743	0.322834532	0.096466789
2.05	0.005798635	0.058822767	0.036304201	0.037236561	0.251722396	0.220230881
2.1	0.011816174	0.056921018	0.036321535	0.038952455	0.171376395	0.369224845
2.15	0.020578463	0.053017871	0.033570834	0.037454833	0.095032667	0.520690664
2.2	0.033007821	0.045348722	0.028535357	0.032810975	0.036201676	0.648190899
2.25	0.046700436	0.034651145	0.022960446	0.025452082	0.004547356	0.73137707
2.3	0.058889193	0.024773186	0.017406803	0.01735971	0.004592525	0.753957166
2.35	0.070403203	0.017223142	0.011540971	0.01045672	0.036370328	0.708011274
2.4	0.079357303	0.011758705	0.005951405	0.004878504	0.09483284	0.606442485
2.45	0.083123466	0.009186314	0.00201231	0.001410982	0.169215461	0.470102935

2.5	0.082916629	0.010104121	0.000602521	0.001236072	0.245930199	0.318420917
-----	-------------	-------------	-------------	-------------	-------------	-------------

5. Blue laser or Helium-Cadmium Laser For period 5.6µm

Depth	5T	4T	3T	2T	1T	0T	Sum T
0	0	0	0	0	0	0.948812863	0.948812863
0.05	0.0007362	8.87E-06	0.00188302	6.06E-06	0.0164961	0.9124855	0.950746005
0.1	0.002841371	8.11E-05	0.00719163	5.52E-05	0.06314011	0.804920396	0.951539304
0.15	0.005737725	0.000272932	0.01492	0.000189978	0.131877043	0.643747201	0.949742557
0.2	0.010018276	0.000725765	0.024239632	0.00051239	0.211342649	0.456506499	0.950183922
0.25	0.015672342	0.00141026	0.03369881	0.000998009	0.2880133	0.271253529	0.950838973
0.3	0.021061561	0.002515942	0.041357587	0.001797293	0.348520736	0.120322683	0.950828919
0.35	0.026421404	0.004112586	0.046359405	0.002974072	0.382865989	0.025823694	0.951290605
0.4	0.031557332	0.005490752	0.048034579	0.004023162	0.385304498	0.001430176	0.950250822
0.45	0.036068265	0.006620369	0.046172005	0.004910091	0.35546093	0.051648855	0.950112175
0.5	0.040154677	0.007463851	0.041074181	0.005645285	0.298356551	0.166518753	0.951907843
0.55	0.042063562	0.007788205	0.033304518	0.006069619	0.22356027	0.325630686	0.951203033
0.6	0.041893974	0.007437156	0.024186435	0.005972027	0.143826861	0.503244123	0.949877027
0.65	0.040074268	0.00586374	0.015109832	0.004961563	0.072647367	0.673266795	0.950580334
0.7	0.036405322	0.003801679	0.007513041	0.003524541	0.022099326	0.804196749	0.950884568
0.75	0.032322768	0.002030915	0.002363544	0.002200578	0.000479132	0.872433559	0.951227434
0.8	0.026332629	0.000633751	0.000134882	0.001049623	0.011303727	0.871842971	0.950752194
0.85	0.018587217	0.000301977	0.001197541	0.000521277	0.052700715	0.802478224	0.949095677
0.9	0.012008678	0.001651068	0.005154664	0.001115917	0.117330062	0.675980903	0.950501681
0.95	0.006638444	0.005137247	0.011094969	0.003148825	0.193920162	0.512496937	0.95237623
1	0.002625928	0.010279868	0.018069417	0.006483999	0.269555453	0.336043143	0.950072475
1.05	0.000655996	0.017018522	0.025305001	0.011121781	0.331783267	0.177311244	0.949080376
1.1	0.001723149	0.025095548	0.03148609	0.016921997	0.369596531	0.06154559	0.951192219
1.15	0.006168936	0.032994776	0.035130874	0.023126849	0.376181449	0.004533032	0.951738798
1.2	0.012637157	0.040398689	0.035999301	0.029085076	0.350867352	0.012970385	0.950945532
1.25	0.021894607	0.045215645	0.034486964	0.03324267	0.298327974	0.083907513	0.950243235
1.3	0.033591638	0.045963772	0.030895529	0.034785837	0.227525031	0.204633999	0.950157611
1.35	0.046096403	0.044277739	0.025579762	0.034633064	0.15015849	0.350429333	0.95192025
1.4	0.057994357	0.039821936	0.019115673	0.032442477	0.079162854	0.495174581	0.952249175
1.45	0.067113879	0.032242641	0.012555413	0.027407968	0.026698416	0.617987358	0.950023992
1.5	0.073938602	0.022631701	0.007018002	0.020238192	0.001607576	0.699100209	0.949968357
1.55	0.078005163	0.012811039	0.00321163	0.01252511	0.007718669	0.723253291	0.951796512
1.6	0.077999656	0.00537729	0.001324859	0.006115945	0.043569912	0.683222308	0.951997632
1.65	0.073614142	0.001222603	0.001355744	0.001805081	0.103109514	0.588569395	0.950783564
1.7	0.063646151	0.001384398	0.003162889	0.000379223	0.175975596	0.460640533	0.949737048
1.75	0.051398138	0.006662683	0.006178712	0.002920557	0.249157739	0.317886706	0.950522364
1.8	0.039725857	0.016982205	0.009619891	0.009561522	0.309755018	0.181202559	0.952491544
1.85	0.026991784	0.031272054	0.013105251	0.019647941	0.348064507	0.073241528	0.951404601
1.9	0.015081217	0.04730611	0.016537387	0.031825777	0.358264095	0.011113378	0.949142551
1.95	0.006818637	0.064190686	0.019195487	0.045309652	0.337852862	0.003776476	0.950511124
2	0.003674723	0.079255252	0.02035254	0.058856599	0.28994054	0.048389101	0.952548408
2.05	0.005617796	0.089739167	0.020072628	0.069379838	0.223194137	0.1354804	0.951487533
2.1	0.012098426	0.094871827	0.018788202	0.074938412	0.149365472	0.249965013	0.95008969
2.15	0.024594473	0.092352436	0.017015875	0.074934744	0.081131636	0.37040108	0.950459407
2.2	0.041137879	0.083266984	0.01500589	0.069921006	0.029588541	0.473964459	0.951805059
2.25	0.058669445	0.070406472	0.012610784	0.061244426	0.003111398	0.540334404	0.952419454
2.3	0.076247592	0.053490672	0.009967462	0.048416248	0.006250521	0.562194764	0.950939754
2.35	0.092045235	0.034745	0.007504699	0.032816471	0.038129801	0.539435287	0.949917698
2.4	0.105021321	0.018136204	0.005544163	0.018311461	0.092594077	0.472448567	0.951663019
2.45	0.112807253	0.006308582	0.00423017	0.007526842	0.160074303	0.370869861	0.952764162
2.5	0.113353819	0.000841612	0.00345176	0.001672777	0.229457181	0.253601792	0.951156089

Recalculated values

Depth	5T	4T	3T	2T	1T	0T
0	0	0	0	0	0	1

0.05	0.00077434	9.33364E-06	0.001980571	6.37179E-06	0.017350691	0.959757385
0.1	0.002986079	8.52559E-05	0.007557891	5.80296E-05	0.066355756	0.845913976
0.15	0.006041348	0.000287375	0.015709521	0.000200031	0.138855569	0.677812315
0.2	0.010543512	0.000763815	0.025510464	0.000539253	0.222422885	0.480440143
0.25	0.016482646	0.001483175	0.035441133	0.001049609	0.302904391	0.285278093
0.3	0.022150736	0.002646052	0.043496349	0.001890238	0.366544106	0.126545039
0.35	0.027774272	0.004323165	0.048733168	0.003126355	0.402470062	0.027145957
0.4	0.033209476	0.005778213	0.050549369	0.004233789	0.405476627	0.001505051
0.45	0.037962112	0.006967986	0.048596372	0.005167907	0.374125224	0.054360797
0.5	0.042183366	0.007840939	0.043149325	0.005930496	0.31343008	0.174931591
0.55	0.044221434	0.008187742	0.035013048	0.006380992	0.235028971	0.342335626
0.6	0.044104629	0.007829599	0.025462701	0.006287158	0.151416296	0.529799236
0.65	0.042157687	0.006168589	0.015895376	0.00521951	0.076424226	0.708269223
0.7	0.038285743	0.003998044	0.007901108	0.003706592	0.023240809	0.845735409
0.75	0.033980063	0.002135046	0.002484731	0.002313409	0.000503699	0.917166103
0.8	0.027696627	0.000666578	0.000141868	0.001103992	0.011889246	0.917003375
0.85	0.019584134	0.000318173	0.001261771	0.000549236	0.055527294	0.845518875
0.9	0.012634042	0.001737049	0.005423098	0.00117403	0.123440142	0.71118328
0.95	0.006970401	0.005394136	0.011649775	0.003306283	0.20361718	0.538124452
1	0.002763924	0.010820089	0.019018988	0.006824742	0.283720937	0.35370264
1.05	0.000691192	0.017931592	0.026662653	0.011718481	0.34958395	0.186824265
1.1	0.001811567	0.026383256	0.033101711	0.017790302	0.388561348	0.06470363
1.15	0.006481753	0.03466789	0.036912306	0.024299575	0.395257028	0.004762895
1.2	0.013289044	0.042482653	0.037856322	0.030585427	0.368966823	0.013639461
1.25	0.023041056	0.047583232	0.036292775	0.034983327	0.313949064	0.08830109
1.3	0.035353753	0.048374892	0.032516215	0.036610596	0.239460305	0.215368478
1.35	0.048424648	0.046514127	0.026871749	0.036382317	0.157742721	0.368128877
1.4	0.060902501	0.041818819	0.020074235	0.034069315	0.083132499	0.520005261
1.45	0.070644404	0.033938765	0.013215891	0.028849764	0.028102886	0.65049658
1.5	0.0778327	0.023823637	0.007387617	0.02130407	0.001692241	0.735919469
1.55	0.081955714	0.013459851	0.003374282	0.013159441	0.008109578	0.759882267
1.6	0.081932615	0.005648428	0.001391662	0.006424328	0.045766828	0.717672277
1.65	0.07742471	0.00128589	0.001425923	0.00189852	0.108446883	0.619036148
1.7	0.067014497	0.001457664	0.003330279	0.000399293	0.185288756	0.485019021
1.75	0.054073571	0.007009497	0.006500333	0.003072581	0.262127172	0.334433695
1.8	0.041707306	0.017829245	0.010099713	0.010038432	0.325205006	0.190240596
1.85	0.028370458	0.032869353	0.013774635	0.020651509	0.365842783	0.076982524
1.9	0.015889306	0.049840891	0.017423502	0.033531083	0.377460788	0.011708861
1.95	0.007173653	0.067532809	0.020194911	0.047668723	0.355443354	0.0039731
2	0.003857781	0.083203385	0.02136641	0.061788565	0.304384048	0.050799624
2.05	0.005904225	0.094314601	0.02109605	0.072917232	0.234573895	0.142387993
2.1	0.012733983	0.099855653	0.019775188	0.078875092	0.15721197	0.263096227
2.15	0.025876406	0.097166102	0.01790279	0.078840552	0.085360442	0.389707417
2.2	0.043220908	0.087483233	0.015765718	0.073461477	0.031086766	0.497963795
2.25	0.061600427	0.073923807	0.013240787	0.064304048	0.003266836	0.567328189
2.3	0.080181306	0.056250327	0.010481697	0.050914106	0.006572994	0.591199139
2.35	0.096898115	0.036576853	0.007900367	0.034546646	0.04014011	0.567875815
2.4	0.110355576	0.01905738	0.005825762	0.019241539	0.097297127	0.496445231
2.45	0.118399975	0.006621347	0.004439892	0.007900006	0.168010416	0.389256729
2.5	0.119174781	0.00088483	0.003629016	0.001758677	0.241240301	0.266624789

6. Blue laser or Helium-Cadmium laser For period 10µm

Depth	5T	4T	3T	2T	1T	0T	Sum T
0	0	0	0	0	0	0.948812863	0.948812863
0.05	0.000700767	9.06E-06	0.001853224	6.65E-06	0.016467912	0.912761393	0.950836613
0.1	0.002723377	8.37E-05	0.007102872	6.14E-05	0.063057125	0.80579255	0.95184947
0.15	0.005578148	0.000277097	0.014786288	0.000204704	0.131746542	0.644815889	0.950001447
0.2	0.0097644	0.000714891	0.024033689	0.000530029	0.211141385	0.457591385	0.94996017
0.25	0.015153265	0.001420496	0.033430416	0.001052496	0.287773987	0.272903411	0.950564731
0.3	0.020456694	0.002611918	0.041180574	0.001938436	0.348382153	0.121977379	0.951116928
0.35	0.025876199	0.004169031	0.046373942	0.003101462	0.382918735	0.026473167	0.951351907
0.4	0.03090372	0.005522505	0.048203399	0.004116489	0.38552814	0.001070822	0.949619328

0.45	0.035608098	0.006846439	0.046570127	0.005107031	0.355904096	0.049815573	0.949887154
0.5	0.039999132	0.007877184	0.041750354	0.005892187	0.299056026	0.163051686	0.952201451
0.55	0.041878127	0.008305776	0.03407754	0.006237736	0.224349259	0.321222786	0.950919663
0.6	0.04195118	0.007903025	0.025022511	0.005944872	0.144642565	0.498424989	0.949353297
0.65	0.040805324	0.006318901	0.015994617	0.00477599	0.073407495	0.668014925	0.95061958
0.7	0.037872957	0.004435567	0.00821328	0.003368213	0.022564246	0.798332808	0.951241335
0.75	0.033840629	0.002563623	0.002738536	0.001948309	0.00054825	0.867818973	0.951097668
0.8	0.027568053	0.000871378	0.000179439	0.000649019	0.010940332	0.869818105	0.950234545
0.85	0.020267011	0.000230732	0.000894047	0.000107094	0.051853798	0.802594753	0.949300116
0.9	0.013954968	0.001254831	0.004502185	0.00080395	0.116014079	0.67829339	0.951353416
0.95	0.008053113	0.004425918	0.01030186	0.003084697	0.192449818	0.515441457	0.952072268
1	0.003324306	0.009343191	0.017347905	0.006714844	0.268168914	0.339456192	0.949254512
1.05	0.000673686	0.016368811	0.024524432	0.011954817	0.330299138	0.181929536	0.949571304
1.1	0.000929871	0.025074907	0.030591981	0.018503667	0.368115182	0.065408801	0.951840018
1.15	0.004107318	0.033922923	0.034304474	0.025272308	0.37500385	0.006017483	0.951239228
1.2	0.009861385	0.042081388	0.035524028	0.031511233	0.350243537	0.011723191	0.950166334
1.25	0.01899628	0.047694735	0.034309079	0.03593165	0.298190878	0.079673232	0.949918474
1.3	0.030236776	0.050821764	0.030574681	0.038573678	0.227457072	0.195316579	0.950644522
1.35	0.042544744	0.05126318	0.024931312	0.039195042	0.150042339	0.336228935	0.952182167
1.4	0.054309575	0.047024163	0.018270973	0.03627178	0.07911638	0.480722142	0.950707883
1.45	0.064462467	0.039322555	0.011745756	0.030563544	0.026739353	0.603315535	0.948982884
1.5	0.073906848	0.029476432	0.006353356	0.023199437	0.001583021	0.682129511	0.9511677
1.55	0.079602332	0.019084875	0.002574781	0.015348108	0.007584059	0.703783969	0.952172279
1.6	0.080122311	0.009921149	0.000793866	0.008235974	0.043544427	0.665063141	0.950298596
1.65	0.076427318	0.002950662	0.001131475	0.002673178	0.103072273	0.577328182	0.949837996
1.7	0.068461863	0.000528998	0.003258372	0.000468844	0.17564616	0.453767243	0.950495717
1.75	0.05853908	0.003539818	0.006534501	0.002439179	0.248598066	0.31225056	0.951551849
1.8	0.045915749	0.012107958	0.010383418	0.008637379	0.30959075	0.178245681	0.951516192
1.85	0.031191901	0.025604935	0.014184936	0.018743978	0.348337284	0.073253066	0.949379132
1.9	0.018423358	0.043027692	0.017019857	0.032073668	0.357839586	0.013052774	0.949821095
1.95	0.008602045	0.062939791	0.018372146	0.047541781	0.336404236	0.004670371	0.952390369
2	0.002769938	0.081018402	0.018232981	0.061944046	0.288078966	0.047048149	0.951136815
2.05	0.00177503	0.095739598	0.016803437	0.073725696	0.221309329	0.130636481	0.949342661
2.1	0.006685273	0.105759038	0.014430422	0.082137214	0.147482343	0.237587308	0.950575887
2.15	0.017303665	0.108694317	0.011354259	0.085407397	0.079013109	0.347973993	0.951519485
2.2	0.031476092	0.104708652	0.00806801	0.083102525	0.027601854	0.441395168	0.951309434
2.25	0.049140414	0.092606685	0.005299861	0.074351102	0.002095126	0.503436463	0.950422838
2.3	0.068258137	0.07462046	0.003417251	0.060728942	0.006573804	0.522502989	0.949700178
2.35	0.086819204	0.054780279	0.00255153	0.045441557	0.039984539	0.492280922	0.951435142
2.4	0.102186841	0.034396088	0.002692886	0.029535772	0.096435299	0.421637982	0.952131751
2.45	0.111093853	0.01660916	0.003604959	0.015202674	0.166134272	0.324550361	0.949840196
2.5	0.115184855	0.00449687	0.004875234	0.005085133	0.236667256	0.217260429	0.949879123

Recalculated values

Depth	5T	4T	3T	2T	1T	0T	5T
0	0	0	0	0	0	1	0
0.05	0.000737001	9.52417E-06	0.001949046	6.99455E-06	0.017319392	0.959956086	0.000737001
0.1	0.002861143	8.7922E-05	0.00746218	6.45034E-05	0.066246951	0.846554603	0.002861143
0.15	0.005871726	0.00029168	0.01556449	0.000215478	0.138680359	0.678752534	0.005871726
0.2	0.010278747	0.000752548	0.02529968	0.000557948	0.222263408	0.481695338	0.010278747
0.25	0.015941329	0.001494371	0.035169005	0.001107233	0.302740021	0.287096083	0.015941329
0.3	0.021508074	0.002746159	0.043297067	0.002038063	0.366287407	0.12824646	0.021508074
0.35	0.027199398	0.004382218	0.048745308	0.003260058	0.402499572	0.027826892	0.027199398
0.4	0.032543272	0.005815493	0.050760761	0.004334883	0.405981775	0.001127633	0.032543272
0.45	0.037486661	0.007207634	0.04902701	0.00537646	0.374680397	0.052443674	0.037486661
0.5	0.042007006	0.008272603	0.043846135	0.006187962	0.314068022	0.171236544	0.042007006
0.55	0.044039605	0.008734467	0.035836403	0.006559687	0.23592872	0.337802233	0.044039605
0.6	0.044189218	0.00832464	0.026357428	0.006262023	0.152359048	0.525015282	0.044189218
0.65	0.042924978	0.00664714	0.016825465	0.005024081	0.077220685	0.702715302	0.042924978
0.7	0.039814247	0.004662925	0.008634276	0.003540861	0.023720843	0.839253698	0.039814247
0.75	0.035580603	0.002695436	0.002879342	0.002048485	0.000576439	0.912439387	0.035580603
0.8	0.02901184	0.000917013	0.000188837	0.000683009	0.011513296	0.91537201	0.02901184

0.85	0.021349424	0.000243055	0.000941796	0.000112814	0.054623187	0.845459449	0.021349424
0.9	0.014668542	0.001318996	0.0047324	0.000845059	0.121946352	0.7129773	0.014668542
0.95	0.008458511	0.004648721	0.01082046	0.003239981	0.202137826	0.541389004	0.008458511
1	0.003502018	0.009842662	0.018275293	0.007073808	0.282504756	0.357602927	0.003502018
1.05	0.000709463	0.017238107	0.025826847	0.012589699	0.347840269	0.191591232	0.000709463
1.1	0.00097692	0.026343615	0.032139834	0.019439892	0.386740602	0.068718272	0.00097692
1.15	0.00431786	0.035661821	0.03606293	0.026567773	0.394226646	0.00632594	0.00431786
1.2	0.010378588	0.044288444	0.037387168	0.033163912	0.368612868	0.012338041	0.010378588
1.25	0.0199978	0.050209292	0.03611792	0.037826035	0.313912074	0.083873758	0.0199978
1.3	0.031806607	0.053460323	0.032162055	0.040576343	0.239266168	0.205457008	0.031806607
1.35	0.044681307	0.053837576	0.026183343	0.041163386	0.157577346	0.353114085	0.044681307
1.4	0.057125407	0.049462262	0.019218283	0.038152392	0.083218391	0.50564653	0.057125407
1.45	0.067927955	0.041436527	0.012377205	0.032206633	0.028176855	0.635749649	0.067927955
1.5	0.077701175	0.030989732	0.006679533	0.02439048	0.001664293	0.717149574	0.077701175
1.55	0.083600766	0.020043511	0.002704112	0.016119045	0.007965007	0.739135117	0.083600766
1.6	0.084312774	0.010440033	0.000835386	0.008666722	0.045821837	0.699846494	0.084312774
1.65	0.08046353	0.00310649	0.00119123	0.002814352	0.108515635	0.607817527	0.08046353
1.7	0.072027534	0.00055655	0.003428076	0.000493263	0.184794268	0.477400618	0.072027534
1.75	0.06151959	0.003720048	0.006867204	0.00256337	0.261255407	0.328148761	0.06151959
1.8	0.048255352	0.01272491	0.010912498	0.00907749	0.325365719	0.187328059	0.048255352
1.85	0.032855053	0.026970189	0.014941277	0.019743406	0.366910618	0.077158917	0.032855053
1.9	0.019396661	0.045300838	0.017919013	0.033768115	0.376744197	0.01374235	0.019396661
1.95	0.009032058	0.066086127	0.019290562	0.049918376	0.353220955	0.004903841	0.009032058
2	0.002912239	0.085180597	0.019169672	0.065126326	0.302878578	0.049465175	0.002912239
2.05	0.001869746	0.100848305	0.017700076	0.077659731	0.233118491	0.137607301	0.001869746
2.1	0.007032866	0.111257859	0.015180715	0.086407845	0.15515052	0.24994039	0.007032866
2.15	0.018185297	0.114232361	0.011932765	0.089758957	0.083038876	0.365703486	0.018185297
2.2	0.033087123	0.110067921	0.008480952	0.087355935	0.029014591	0.463986955	0.033087123
2.25	0.051703739	0.097437352	0.005576319	0.078229498	0.002204414	0.529697355	0.051703739
2.3	0.071873354	0.07857265	0.003598241	0.063945384	0.006921978	0.550176783	0.071873354
2.35	0.091250786	0.057576472	0.00268177	0.047761066	0.042025502	0.517408807	0.091250786
2.4	0.107324266	0.036125345	0.00282827	0.031020677	0.101283566	0.442835754	0.107324266
2.45	0.116960572	0.017486268	0.003795332	0.016005507	0.174907603	0.341689436	0.116960572
2.5	0.121262645	0.004734149	0.005132478	0.005353453	0.24915513	0.228724291	0.121262645

7. Green laser or semiconductor laser for period 4μm

Depth	5T	4T	3T	2T	1T	0T	Sum T
0	0	0	0	0	0	0.948812863	0.948812863
0.05	0.000521754	4.41E-06	0.00131286	2.87E-06	0.011399223	0.923755063	0.950237301
0.1	0.002073482	4.58E-05	0.005095469	2.96E-05	0.044244114	0.848627244	0.951604193
0.15	0.004263307	0.000147365	0.010787626	9.65E-05	0.094562779	0.730660211	0.950375378
0.2	0.007000268	0.000381345	0.017832466	0.000257968	0.156517409	0.585505824	0.949484734
0.25	0.010970164	0.000822575	0.025793329	0.000563568	0.223089392	0.428077837	0.950555894
0.3	0.015848363	0.001391168	0.033635543	0.000958396	0.286306231	0.274784437	0.951063838
0.35	0.020421673	0.002194628	0.040171188	0.001532907	0.338510605	0.145001357	0.950663358
0.4	0.024730182	0.003446892	0.044891061	0.002450153	0.373747629	0.052450522	0.950982357
0.45	0.029163214	0.004816587	0.047487358	0.003488899	0.388022768	0.005203327	0.951160979
0.5	0.033164173	0.005884755	0.047631601	0.004355562	0.379643189	0.009011004	0.950369562
0.55	0.03667002	0.006744533	0.045367174	0.005103785	0.349622495	0.063479372	0.950495383
0.6	0.039769897	0.00737977	0.040892543	0.005757188	0.301407643	0.161253178	0.951667262
0.65	0.04155414	0.007701351	0.034606204	0.006278121	0.240624689	0.29001288	0.95154189
0.7	0.041782631	0.007756288	0.027227787	0.00662288	0.174418745	0.434816576	0.950433237
0.75	0.040832776	0.007186957	0.019488182	0.006482061	0.110476653	0.581456172	0.950389431
0.8	0.038290293	0.005772809	0.012237686	0.005687198	0.056360011	0.714101298	0.950797291
0.85	0.034598239	0.004140626	0.006380019	0.004621364	0.018445876	0.814242437	0.950614683
0.9	0.031086902	0.002820681	0.002339469	0.003653702	0.00093469	0.869299572	0.950970461
0.95	0.026853775	0.001818341	0.000295467	0.002803354	0.005785528	0.876177916	0.951290847
1	0.020800531	0.001355829	0.000511251	0.00217395	0.032502038	0.835361499	0.950048696
1.05	0.014517653	0.001816041	0.002947877	0.002048346	0.077868715	0.75066151	0.949058772
1.1	0.009446777	0.00352837	0.007171324	0.002666809	0.136386221	0.632183018	0.95058202
1.15	0.005429033	0.006621283	0.012503902	0.004133424	0.200928933	0.492895197	0.952128346
1.2	0.002516261	0.010704161	0.018321179	0.006388187	0.264002859	0.347000614	0.95086591

1.25	0.000930893	0.015609167	0.024377063	0.009390081	0.318736865	0.211135387	0.949223524
1.3	0.001017025	0.021396261	0.030178786	0.013108641	0.358659002	0.101227015	0.949946444
1.35	0.003593155	0.027213827	0.034665737	0.017269087	0.378534558	0.028814153	0.951366888
1.4	0.008327341	0.032447519	0.03712162	0.021612748	0.375993384	0.000549862	0.951555085
1.45	0.014104724	0.037491682	0.037542992	0.025939481	0.351606434	0.017819691	0.951190318
1.5	0.021282486	0.041379996	0.03615769	0.029423764	0.308401175	0.07754793	0.950838154
1.55	0.030239181	0.042291087	0.033288681	0.031096797	0.251628251	0.173290012	0.950378007
1.6	0.039916562	0.040524313	0.029322876	0.031051349	0.187923416	0.293176407	0.950653439
1.65	0.049573052	0.037347214	0.024499848	0.030000033	0.12445095	0.420149702	0.951891897
1.7	0.058477383	0.033035436	0.019094704	0.028068909	0.068458416	0.5379922	0.952261894
1.75	0.065471017	0.027541655	0.013578093	0.024849999	0.026509413	0.635161102	0.951061454
1.8	0.070239159	0.021068103	0.008564911	0.02025297	0.003598202	0.702699565	0.950146253
1.85	0.072791977	0.014228846	0.004659759	0.014818883	0.00230809	0.733059253	0.95067436
1.9	0.07283614	0.008354265	0.00219052	0.009531681	0.022404778	0.720981441	0.951616207
1.95	0.071022247	0.004644334	0.001137543	0.005402463	0.061309405	0.664918724	0.951950708
2	0.067054666	0.003473378	0.00143462	0.00290529	0.114633911	0.572404893	0.951408623
2.05	0.059270363	0.005095763	0.003052097	0.00226132	0.17625249	0.458490529	0.950354598
2.1	0.048680977	0.009558144	0.005787517	0.003801003	0.238701139	0.336839836	0.949897397
2.15	0.038494264	0.016669093	0.009169502	0.007652163	0.29408776	0.21883335	0.950978913
2.2	0.029428525	0.026251811	0.012603515	0.01365555	0.335605588	0.11720157	0.952291545
2.25	0.020545132	0.037353736	0.015884952	0.021320272	0.359089991	0.043337178	0.951725343
2.3	0.012481127	0.048515381	0.019225918	0.029649588	0.362543961	0.005213981	0.950045931
2.35	0.00662719	0.058979195	0.022457811	0.037854772	0.345239013	0.007502151	0.949818115
2.4	0.004024174	0.067808735	0.024958293	0.045795057	0.308699481	0.048707692	0.95127917
2.45	0.005234588	0.073740199	0.026339678	0.052883743	0.257183722	0.121516239	0.952280099
2.5	0.009392085	0.076827818	0.026527625	0.05773139	0.196770857	0.217198371	0.951697923

Recalculated Values

Depth	5T	4T	3T	2T	1T	0T
0	0	0	0	0	0	1
0.05	0.000549078	4.64386E-06	0.001381612	3.01948E-06	0.011996186	0.972130921
0.1	0.002178933	4.81652E-05	0.00535461	3.10799E-05	0.04649424	0.891785944
0.15	0.004485919	0.00015506	0.011350911	0.000101545	0.099500451	0.768812227
0.2	0.007372702	0.000401634	0.018781203	0.000271692	0.164844577	0.616656385
0.25	0.011540788	0.000865362	0.027134994	0.000592882	0.234693608	0.45034473
0.3	0.016663827	0.00146275	0.03536623	0.001007709	0.301037869	0.288923231
0.35	0.021481498	0.002308522	0.042255955	0.00161246	0.356078313	0.152526502
0.4	0.02600488	0.003624559	0.047204936	0.002576444	0.393012159	0.055154043
0.45	0.03066065	0.005063903	0.049925679	0.003668043	0.407946474	0.005470501
0.5	0.034896081	0.006192071	0.05011903	0.004583019	0.399469011	0.009481579
0.55	0.038579903	0.007095808	0.047730031	0.005369605	0.367831871	0.066785565
0.6	0.041789708	0.00775457	0.042969371	0.006049581	0.316715364	0.169442813
0.65	0.043670321	0.008093549	0.036368555	0.00659784	0.252878714	0.304782042
0.7	0.043961668	0.008160792	0.028647764	0.006968275	0.183514989	0.457493024
0.75	0.042964257	0.007562118	0.02050547	0.006820426	0.116243562	0.611808331
0.8	0.040271773	0.006071545	0.012870973	0.005981504	0.059276579	0.751055251
0.85	0.03639565	0.004355735	0.006711467	0.004861448	0.019404156	0.856543089
0.9	0.032689661	0.002966108	0.002460086	0.003842077	0.00098288	0.914118374
0.95	0.028228774	0.001911446	0.000310596	0.002946895	0.006081766	0.921041045
1	0.021894174	0.001427115	0.000538131	0.002288251	0.034210918	0.879282823
1.05	0.015296895	0.001913518	0.003106105	0.002158292	0.082048359	0.790953661
1.1	0.009937887	0.0037118	0.00754414	0.002805449	0.143476542	0.665048365
1.15	0.005701997	0.006954192	0.01313258	0.004341247	0.211031353	0.517677264
1.2	0.002646284	0.011257277	0.019267889	0.006718284	0.277644678	0.364931175
1.25	0.000980689	0.016444143	0.025681056	0.009892381	0.335786943	0.222429577
1.3	0.001070613	0.02252365	0.031768934	0.013799347	0.377557076	0.10656076
1.35	0.003776834	0.028604976	0.036437822	0.018151869	0.397884944	0.03028711
1.4	0.008751297	0.034099465	0.03901153	0.022713081	0.395135699	0.000577857
1.45	0.014828499	0.039415542	0.039469484	0.027270548	0.369648878	0.018734097
1.5	0.02238287	0.043519495	0.038027176	0.030945082	0.324346655	0.081557445
1.55	0.031818056	0.044499228	0.035026779	0.032720451	0.264766492	0.182337986
1.6	0.041988553	0.042627851	0.030844969	0.032663163	0.197678153	0.308394621

1.65	0.052078447	0.039234722	0.025738058	0.031516219	0.130740634	0.441383841
1.7	0.061408929	0.034691544	0.020051946	0.029476039	0.071890324	0.564962437
1.75	0.068839944	0.028958859	0.014276778	0.026128699	0.027873501	0.667844438
1.8	0.073924576	0.022173537	0.009014308	0.021315634	0.003786998	0.739569895
1.85	0.076568781	0.014967108	0.00490153	0.015587759	0.002427845	0.771093956
1.9	0.076539406	0.008779027	0.002301894	0.010016308	0.023543922	0.757638884
1.95	0.074607064	0.004878754	0.00119496	0.00567515	0.06440397	0.698480203
2	0.070479355	0.003650774	0.00150789	0.003053672	0.120488619	0.601639379
2.05	0.062366577	0.00536196	0.003211535	0.002379449	0.185459712	0.482441533
2.1	0.051248669	0.010062291	0.006092782	0.004001488	0.251291497	0.354606547
2.15	0.040478567	0.017528352	0.009642172	0.008046616	0.309247404	0.230113778
2.2	0.030902852	0.02756699	0.013234933	0.014339673	0.352418952	0.123073202
2.25	0.021587249	0.039248441	0.01669069	0.022401706	0.377304223	0.045535383
2.3	0.013137393	0.051066353	0.02023683	0.031208584	0.381606772	0.005488136
2.35	0.006977326	0.062095252	0.023644328	0.039854759	0.363479078	0.007898514
2.4	0.004230276	0.071281635	0.026236559	0.048140502	0.324509871	0.051202311
2.45	0.0054969	0.077435409	0.027659591	0.055533811	0.270071508	0.127605564
2.5	0.009868767	0.080727105	0.027873997	0.060661464	0.206757683	0.228221966

8. Green laser or Semiconductor laser For period 5.6µm

Depth	5T	4T	3T	2T	1T	0T	Sum T
0	0	0	0	0	0	0.948812863	0.948812863
0.05	0.000521754	4.41E-06	0.00131286	2.87E-06	0.011399223	0.923755063	0.950237301
0.1	0.002073482	4.58E-05	0.005095469	2.96E-05	0.044244114	0.848627244	0.951604193
0.15	0.004263307	0.000147365	0.010787626	9.65E-05	0.094562779	0.730660211	0.950375378
0.2	0.007000268	0.000381345	0.017832466	0.000257968	0.156517409	0.585505824	0.949484734
0.25	0.010970164	0.000822575	0.025793329	0.000563568	0.223089392	0.428077837	0.950555894
0.3	0.015848363	0.001391168	0.033635543	0.000958396	0.286306231	0.274784437	0.951063838
0.35	0.020421673	0.002194628	0.040171188	0.001532907	0.338510605	0.145001357	0.950663358
0.4	0.024730182	0.003446892	0.044891061	0.002450153	0.373747629	0.052450522	0.950982357
0.45	0.029163214	0.004816587	0.047487358	0.003488899	0.388022768	0.005203327	0.951160979
0.5	0.033164173	0.005884755	0.047631601	0.004355562	0.379643189	0.009011004	0.950369562
0.55	0.03667002	0.006744533	0.045367174	0.005103785	0.349622495	0.063479372	0.950495383
0.6	0.039769897	0.00737977	0.040892543	0.005757188	0.301407643	0.161253178	0.951667262
0.65	0.04155414	0.007701351	0.034606204	0.006278121	0.240624689	0.29001288	0.95154189
0.7	0.041782631	0.007756288	0.027227787	0.00662288	0.174418745	0.434816576	0.950433237
0.75	0.040832776	0.007186957	0.019488182	0.006482061	0.110476653	0.581456172	0.950389431
0.8	0.038290293	0.005772809	0.012237686	0.005687198	0.056360011	0.714101298	0.950797291
0.85	0.034598239	0.004140626	0.006380019	0.004621364	0.018445876	0.814242437	0.950614683
0.9	0.031086902	0.002820681	0.002339469	0.003653702	0.00093469	0.869299572	0.950970461
0.95	0.026853775	0.001818341	0.000295467	0.002803354	0.005785528	0.876177916	0.951290847
1	0.020800531	0.001355829	0.000511251	0.00217395	0.032502038	0.835361499	0.950048696
1.05	0.014517653	0.001816041	0.002947877	0.002048346	0.077868715	0.75066151	0.949058772
1.1	0.009446777	0.00352837	0.007171324	0.002666809	0.136386221	0.632183018	0.95058202
1.15	0.005429033	0.006621283	0.012503902	0.004133424	0.200928933	0.492895197	0.952128346
1.2	0.002516261	0.010704161	0.018321179	0.006388187	0.264002859	0.347000614	0.95086591
1.25	0.000930893	0.015609167	0.024377063	0.009390081	0.318736865	0.211135387	0.949223524
1.3	0.001017025	0.021396261	0.030178786	0.013108641	0.358659002	0.101227015	0.949946444
1.35	0.003593155	0.027213827	0.034665737	0.017269087	0.378534558	0.028814153	0.95136688
1.4	0.008327341	0.032447519	0.03712162	0.021612748	0.375993384	0.000549862	0.951555085
1.45	0.014104724	0.037491682	0.037542992	0.025939481	0.351606434	0.017819691	0.951190318
1.5	0.021282486	0.041379996	0.03615769	0.029423764	0.308401175	0.07754793	0.950838154
1.55	0.030239181	0.042291087	0.033288681	0.031096797	0.251628251	0.173290012	0.950378007
1.6	0.039916562	0.040524313	0.029322876	0.031051349	0.187923416	0.293176407	0.950653439
1.65	0.049573052	0.037347214	0.024499848	0.030000033	0.12445095	0.420149702	0.951891897
1.7	0.058477383	0.033035436	0.019094704	0.028068909	0.068458416	0.5379922	0.952261894
1.75	0.065471017	0.027541655	0.013578093	0.024849999	0.026509413	0.635161102	0.951061454
1.8	0.070239159	0.021068103	0.008564911	0.02025297	0.003598202	0.702699565	0.950146253
1.85	0.072791977	0.014228846	0.004659759	0.014818883	0.00230809	0.733059253	0.95067436
1.9	0.07283614	0.008354265	0.00219052	0.009531681	0.022404778	0.720981441	0.951616207
1.95	0.071022247	0.004644334	0.001137543	0.005402463	0.061309405	0.664918724	0.951950708
2	0.067054666	0.003473378	0.00143462	0.00290529	0.114633911	0.572404893	0.951408623

2.05	0.059270363	0.005095763	0.003052097	0.00226132	0.17625249	0.458490529	0.950354598
2.1	0.048680977	0.009558144	0.005787517	0.003801003	0.238701139	0.336839836	0.949897397
2.15	0.038494264	0.016669093	0.009169502	0.007652163	0.29408776	0.21883335	0.950978913
2.2	0.029428525	0.026251811	0.012603515	0.01365555	0.335605588	0.11720157	0.952291545
2.25	0.020545132	0.037353736	0.015884952	0.021320272	0.359089991	0.043337178	0.951725343
2.3	0.012481127	0.048515381	0.019225918	0.029649588	0.362543961	0.005213981	0.950045931
2.35	0.00662719	0.058979195	0.022457811	0.037854772	0.345239013	0.007502151	0.949818115
2.4	0.004024174	0.067808735	0.024958293	0.045795057	0.308699481	0.048707692	0.95127917
2.45	0.005234588	0.073740199	0.026339678	0.052883743	0.257183722	0.121516239	0.952280099
2.5	0.009392085	0.076827818	0.026527625	0.05773139	0.196770857	0.217198371	0.951697923

Recalculated values

Depth	5T	4T	3T	2T	1T	0T
0	0	0	0	0	0	1
0.05	0.000549078	4.64386E-06	0.001381612	3.01948E-06	0.011996186	0.972130921
0.1	0.002178933	4.81652E-05	0.00535461	3.10799E-05	0.04649424	0.891785944
0.15	0.004485919	0.00015506	0.011350911	0.000101545	0.099500451	0.768812227
0.2	0.007372702	0.000401634	0.018781203	0.000271692	0.164844577	0.616656385
0.25	0.011540788	0.000865362	0.027134994	0.000592882	0.234693608	0.45034473
0.3	0.016663827	0.00146275	0.03536623	0.001007709	0.301037869	0.288923231
0.35	0.021481498	0.002308522	0.042255955	0.00161246	0.356078313	0.152526502
0.4	0.02600488	0.003624559	0.047204936	0.002576444	0.393012159	0.055154043
0.45	0.03066065	0.005063903	0.049925679	0.003668043	0.407946474	0.005470501
0.5	0.034896081	0.006192071	0.05011903	0.004583019	0.399469011	0.009481579
0.55	0.038579903	0.007095808	0.047730031	0.005369605	0.367831871	0.066785565
0.6	0.041789708	0.00775457	0.042969371	0.006049581	0.316715364	0.169442813
0.65	0.043670321	0.008093549	0.036368555	0.00659784	0.252878714	0.304782042
0.7	0.043961668	0.008160792	0.028647764	0.006968275	0.183514989	0.457493024
0.75	0.042964257	0.007562118	0.02050547	0.006820426	0.116243562	0.611808331
0.8	0.040271773	0.006071545	0.012870973	0.005981504	0.059276579	0.751055251
0.85	0.03639565	0.004355735	0.006711467	0.004861448	0.019404156	0.856543089
0.9	0.032689661	0.002966108	0.002460086	0.003842077	0.00098288	0.914118374
0.95	0.028228774	0.001911446	0.000310596	0.002946895	0.006081766	0.921041045
1	0.021894174	0.001427115	0.000538131	0.002288251	0.034210918	0.879282823
1.05	0.015296895	0.001913518	0.003106105	0.002158292	0.082048359	0.790953661
1.1	0.009937887	0.0037118	0.00754414	0.002805449	0.143476542	0.665048365
1.15	0.005701997	0.006954192	0.01313258	0.004341247	0.211031353	0.517677264
1.2	0.002646284	0.011257277	0.019267889	0.006718284	0.277644678	0.364931175
1.25	0.000980689	0.016444143	0.025681056	0.009892381	0.335786943	0.222429577
1.3	0.001070613	0.02252365	0.031768934	0.013799347	0.377557076	0.10656076
1.35	0.003776834	0.028604976	0.036437822	0.018151869	0.397884944	0.03028711
1.4	0.008751297	0.034099465	0.03901153	0.022713081	0.395135699	0.000577857
1.45	0.014828499	0.039415542	0.039469484	0.027270548	0.369648878	0.018734097
1.5	0.02238287	0.043519495	0.038027176	0.030945082	0.324346655	0.081557445
1.55	0.031818056	0.044499228	0.035026779	0.032720451	0.264766492	0.182337986
1.6	0.041988553	0.042627851	0.030844969	0.032663163	0.197678153	0.308394621
1.65	0.052078447	0.039234722	0.025738058	0.031516219	0.130740634	0.441383841
1.7	0.061408929	0.034691544	0.020051946	0.029476039	0.071890324	0.564962437
1.75	0.068839944	0.028958859	0.014276778	0.026128699	0.027873501	0.667844438
1.8	0.073924576	0.022173537	0.009014308	0.021315634	0.003786998	0.739569895
1.85	0.076568781	0.014967108	0.00490153	0.015587759	0.002427845	0.771093956
1.9	0.076539406	0.008779027	0.002301894	0.010016308	0.023543922	0.757638884
1.95	0.074607064	0.004878754	0.00119496	0.00567515	0.06440397	0.698480203
2	0.070479355	0.003650774	0.00150789	0.003053672	0.120488619	0.601639379
2.05	0.062366577	0.00536196	0.003211535	0.002379449	0.185459712	0.482441533
2.1	0.051248669	0.010062291	0.006092782	0.004001488	0.251291497	0.354606547
2.15	0.040478567	0.017528352	0.009642172	0.008046616	0.309247404	0.230113778
2.2	0.030902852	0.02756699	0.013234933	0.014339673	0.352418952	0.123073202
2.25	0.021587249	0.039248441	0.01669069	0.022401706	0.377304223	0.045535383
2.3	0.013137393	0.051066353	0.02023683	0.031208584	0.381606772	0.005488136
2.35	0.006977326	0.062095252	0.023644328	0.039854759	0.363479078	0.007898514
2.4	0.004230276	0.071281635	0.026236559	0.048140502	0.324509871	0.051202311

2.45	0.0054969	0.077435409	0.027659591	0.055533811	0.270071508	0.127605564
2.5	0.009868767	0.080727105	0.027873997	0.060661464	0.206757683	0.228221966

9. Green laser or Semiconductor laser For Period 10µm

Depth	5T	4T	3T	2T	1T	0T	Sum T
0	0	0	0	0	0	0.948812863	0.948812863
0.05	0.000700767	9.06E-06	0.001853224	6.65E-06	0.016467912	0.912761393	0.950836613
0.1	0.002723377	8.37E-05	0.007102872	6.14E-05	0.063057125	0.80579255	0.95184947
0.15	0.005578148	0.000277097	0.014786288	0.000204704	0.131746542	0.644815889	0.950001447
0.2	0.0097644	0.000714891	0.024033689	0.000530029	0.211141385	0.457591385	0.94996017
0.25	0.015153265	0.001420496	0.033430416	0.001052496	0.287773987	0.272903411	0.950564731
0.3	0.020456694	0.002611918	0.041180574	0.001938436	0.348382153	0.121977379	0.951116928
0.35	0.025876199	0.004169031	0.046373942	0.003101462	0.382918735	0.026473167	0.951351907
0.4	0.03090372	0.005522505	0.048203399	0.004116489	0.38552814	0.001070822	0.949619328
0.45	0.035608098	0.006846439	0.046570127	0.005107031	0.355904096	0.049815573	0.949887154
0.5	0.03999132	0.007877184	0.041750354	0.005892187	0.299056026	0.163051686	0.952201451
0.55	0.041878127	0.008305776	0.03407754	0.006237736	0.224349259	0.321222786	0.950919663
0.6	0.04195118	0.007903025	0.025022511	0.005944872	0.144642565	0.498424989	0.949353297
0.65	0.040805324	0.006318901	0.015994617	0.00477599	0.073407495	0.668014925	0.95061958
0.7	0.037872957	0.004435567	0.00821328	0.003368213	0.022564246	0.798332808	0.951241335
0.75	0.033840629	0.002563623	0.002738536	0.001948309	0.00054825	0.867818973	0.951097668
0.8	0.027568053	0.000871378	0.000179439	0.000649019	0.010940332	0.869818105	0.950234545
0.85	0.020267011	0.000230732	0.000894047	0.000107094	0.051853798	0.802594753	0.949300116
0.9	0.013954968	0.001254831	0.004502185	0.00080395	0.116014079	0.67829339	0.951353416
0.95	0.008053113	0.004425918	0.01030186	0.003084697	0.192449818	0.515441457	0.952072268
1	0.003324306	0.009343191	0.017347905	0.006714844	0.268168914	0.339456192	0.949254512
1.05	0.000673686	0.016368811	0.024524432	0.011954817	0.330299138	0.181929536	0.949571304
1.1	0.000929871	0.025074907	0.030591981	0.018503667	0.368115182	0.065408801	0.951840018
1.15	0.004107318	0.033922923	0.034304474	0.025272308	0.37500385	0.006017483	0.951239228
1.2	0.009861385	0.042081388	0.035524028	0.031511233	0.350243537	0.011723191	0.950166334
1.25	0.01899628	0.047694735	0.034309079	0.03593165	0.298190878	0.079673232	0.949918474
1.3	0.030236776	0.050821764	0.030574681	0.038573678	0.227457072	0.195316579	0.950644522
1.35	0.042544744	0.05126318	0.024931312	0.039195042	0.150042339	0.336228935	0.952182167
1.4	0.054309575	0.047024163	0.018270973	0.03627178	0.07911638	0.480722142	0.950707883
1.45	0.064462467	0.039322555	0.011745756	0.030563544	0.026739353	0.603315535	0.948982884
1.5	0.073906848	0.029476432	0.006353356	0.023199437	0.001583021	0.682129511	0.9511677
1.55	0.079602332	0.019084875	0.002574781	0.015348108	0.007584059	0.703783969	0.952172279
1.6	0.080122311	0.009921149	0.000793866	0.008235974	0.043544427	0.665063141	0.950298596
1.65	0.076427318	0.002950662	0.001131475	0.002673178	0.103072273	0.577328182	0.949837996
1.7	0.068461863	0.000528998	0.003258372	0.000468844	0.17564616	0.453767243	0.950495717
1.75	0.05853908	0.003539818	0.006534501	0.002439179	0.248598066	0.31225056	0.951551849
1.8	0.045915749	0.012107958	0.010383418	0.008637379	0.30959075	0.178245681	0.951516192
1.85	0.031191901	0.025604935	0.014184936	0.018743978	0.348337284	0.073253066	0.949379132
1.9	0.018423358	0.043027692	0.017019857	0.032073668	0.357839586	0.013052774	0.949821095
1.95	0.008602045	0.062939791	0.018372146	0.047541781	0.336404236	0.004670371	0.952390369
2	0.002769938	0.081018402	0.018232981	0.061944046	0.288078966	0.047048149	0.951136815
2.05	0.00177503	0.095739598	0.016803437	0.073725696	0.221309329	0.130636481	0.949342661
2.1	0.006685273	0.105759038	0.014430422	0.082137214	0.147482343	0.237587308	0.950575887
2.15	0.017303665	0.108694317	0.011354259	0.085407397	0.079013109	0.347973993	0.951519485
2.2	0.031476092	0.104708652	0.00806801	0.083102525	0.027601854	0.441395168	0.951309434
2.25	0.049140414	0.092606685	0.005299861	0.074351102	0.002095126	0.503436463	0.950422838
2.3	0.068258137	0.07462046	0.003417251	0.060728942	0.006573804	0.522502989	0.949700178
2.35	0.086819204	0.054780279	0.00255153	0.045441557	0.039984539	0.492280922	0.951435142
2.4	0.102186841	0.034396088	0.002692886	0.029535772	0.096435299	0.421637982	0.952131751
2.45	0.111093853	0.01660916	0.003604959	0.015202674	0.166134272	0.324550361	0.949840196
2.5	0.115184855	0.00449687	0.004875234	0.005085133	0.236667256	0.217260429	0.949879123

Recalculated Values

Depth	5T	4T	3T	2T	1T	0T
-------	----	----	----	----	----	----

0	0	0	0	0	0	1
0.05	0.000737001	9.52417E-06	0.001949046	6.99455E-06	0.017319392	0.959956086
0.1	0.002861143	8.7922E-05	0.00746218	6.45034E-05	0.066246951	0.846554603
0.15	0.005871726	0.00029168	0.01556449	0.000215478	0.138680359	0.678752534
0.2	0.010278747	0.000752548	0.02529968	0.000557948	0.222263408	0.481695338
0.25	0.015941329	0.001494371	0.035169005	0.001107233	0.302740021	0.287096083
0.3	0.021508074	0.002746159	0.043297067	0.002038063	0.366287407	0.12824646
0.35	0.027199398	0.004382218	0.048745308	0.003260058	0.402499572	0.027826892
0.4	0.032543272	0.005815493	0.050760761	0.004334883	0.405981775	0.001127633
0.45	0.037486661	0.007207634	0.04902701	0.00537646	0.374680397	0.052443674
0.5	0.042007006	0.008272603	0.043846135	0.006187962	0.314068022	0.171236544
0.55	0.044039605	0.008734467	0.035836403	0.006559687	0.23592872	0.337802233
0.6	0.044189218	0.00832464	0.026357428	0.006262023	0.152359048	0.525015282
0.65	0.042924978	0.00664714	0.016825465	0.005024081	0.077220685	0.702715302
0.7	0.039814247	0.004662925	0.008634276	0.003540861	0.023720843	0.839253698
0.75	0.035580603	0.002695436	0.002879342	0.002048485	0.000576439	0.912439387
0.8	0.02901184	0.000917013	0.000188837	0.000683009	0.011513296	0.91537201
0.85	0.021349424	0.000243055	0.000941796	0.000112814	0.054623187	0.845459449
0.9	0.014668542	0.001318996	0.0047324	0.000845059	0.121946352	0.7129773
0.95	0.008458511	0.004648721	0.01082046	0.003239981	0.202137826	0.541389004
1	0.003502018	0.009842662	0.018275293	0.007073808	0.282504756	0.357602927
1.05	0.000709463	0.017238107	0.025826847	0.012589699	0.347840269	0.191591232
1.1	0.00097692	0.026343615	0.032139834	0.019439892	0.386740602	0.068718272
1.15	0.00431786	0.035661821	0.03606293	0.026567773	0.394226646	0.00632594
1.2	0.010378588	0.044288444	0.037387168	0.033163912	0.368612868	0.012338041
1.25	0.0199978	0.050209292	0.03611792	0.037826035	0.313912074	0.083873758
1.3	0.031806607	0.053460323	0.032162055	0.040576343	0.239266168	0.205457008
1.35	0.044681307	0.053837576	0.026183343	0.041163386	0.157577346	0.353114085
1.4	0.057125407	0.049462262	0.019218283	0.038152392	0.083218391	0.50564653
1.45	0.067927955	0.041436527	0.012377205	0.032206633	0.028176855	0.635749649
1.5	0.077701175	0.030989732	0.006679533	0.02439048	0.001664293	0.717149574
1.55	0.083600766	0.020043511	0.002704112	0.016119045	0.007965007	0.739135117
1.6	0.084312774	0.010440033	0.000835386	0.008666722	0.045821837	0.699846494
1.65	0.08046353	0.00310649	0.00119123	0.002814352	0.108515635	0.607817527
1.7	0.072027534	0.00055655	0.003428076	0.000493263	0.184794268	0.477400618
1.75	0.06151959	0.003720048	0.006867204	0.00256337	0.261255407	0.328148761
1.8	0.048255352	0.01272491	0.010912498	0.00907749	0.325365719	0.187328059
1.85	0.032855053	0.026970189	0.014941277	0.019743406	0.366910618	0.077158917
1.9	0.019396661	0.045300838	0.017919013	0.033768115	0.376744197	0.01374235
1.95	0.009032058	0.066086127	0.019290562	0.049918376	0.353220955	0.004903841
2	0.002912239	0.085180597	0.019169672	0.065126326	0.302878578	0.049465175
2.05	0.001869746	0.100848305	0.017700076	0.077659731	0.233118491	0.137607301
2.1	0.007032866	0.111257859	0.015180715	0.086407845	0.15515052	0.24994039
2.15	0.018185297	0.114232361	0.011932765	0.089758957	0.083038876	0.365703486
2.2	0.033087123	0.110067921	0.008480952	0.087355935	0.029014591	0.463986955
2.25	0.051703739	0.097437352	0.005576319	0.078229498	0.002204414	0.529697355
2.3	0.071873354	0.07857265	0.003598241	0.063945384	0.006921978	0.550176783
2.35	0.091250786	0.057576472	0.00268177	0.047761066	0.042025502	0.517408807
2.4	0.107324266	0.036125345	0.00282827	0.031020677	0.101283566	0.442835754
2.45	0.116960572	0.017486268	0.003795332	0.016005507	0.174907603	0.341689436
2.5	0.121262645	0.004734149	0.005132478	0.005353453	0.24915513	0.228724291